Electronic Supplementary Material (ESI) for Energy & Environmental Science.
This journal is © The Royal Society of Chemistry 2023

Supporting Information for:

Identification of Potential Solid-State Li-Ion Conductors with Semi-Supervised Learning

Forrest A. L. Laskowski‡ [a], Daniel B. McHaffie‡ [b], Kimberly A. See* [a]

[a]Division of Chemistry and Chemical Engineering

[b]Department of Applied Physics and Materials Science

California Institute of Technology, Pasadena, California 91125, United States

*Corresponding Author: ksee@caltech.edu

‡Co-authors with equal contribution

Contents

I. Digitized labels for lithium-ion conductors: RT conductivity, activation energy, and corresponding ICSD Identifier

Data labels for the semi-supervised learning approach were ultimately digitized from over 300 literature publications. Many more publications were initially examined. The stepwise decision chart below was used as a guide for deciding what data to digitize. Room temperature conductivity data was only digitized if it originated from an equivalent circuit fit (where a blocking feature was clearly present) or if calculated from NMR. DC techniques were categorically discounted because they cannot differentiate between electronic and ionic conductivity.

Step	Question	Outcome
1	Does the paper have any conductivity data present?	**Yes:** proceed to step 2.
		No: find a new paper.
2	Are room-temperature conductivity data values explicitly reported in the text, either from an equivalent circuit fit or NMR?	**Yes:** record the data.
		No: proceed to step 3.
3	Are room-temperature conductivity data present in a figure, either from an equivalent circuit fit or NMR?	**Yes:** digitize the data and record it.
		No: proceed to step 4.
4	Is the presented data an Arrhenius plot with a linear fit?	**Yes:** proceed to step 5.
		No: find a new paper.
5	Digitize the available data. Can a room-temperature conductivity be interpolated from the digitized datapoints?	**Yes:** record the digitized interpolation.
		No: proceed to step 6.
6	Does extrapolation of the Arrhenius plot to room temperature result in a value < 1E-10 S cm^{-1}?	**Yes:** record the data as "<1E-10 S cm^{-1}"
		No: find a new paper.

All of the digitized data is presented in the subsequent table. Activation energies were also digitized when available. The activation energies were not used in the manuscript but are still presented here to aid future machine learning endeavors. The digitized data was manually matched with the appropriate ICSD ID, so that the crystallographic information file (.cif) can be downloaded. Rows without an associated ICSD ID are highlighted.

Compound	$\sigma_{25°C}$ (S cm^{-1})	E_a (eV)	Space Group	Space Group #	Other names	ICSD	Citation
$LiAlSi_3O_8$	1.30E-10		$C\bar{1}$	2		81980	[1]
$LiSn_2(PO_4)_3$	2.04E-9		$P\bar{1}$	2		83832	[2]
Li_7BiO_6	8.80E-07	0.58	$P\bar{1}$	2		155950	[3]
Li_7SbO_6	6.70E-08	0.7	$P\bar{1}$	2		413370	[3]
$Li_7P_3S_{11}$	1.70E-02	0.17	$P\bar{1}$	2		157654	[4]

$Li_7P_3S_{11}$	3.2E-3	0.124	$P\bar{1}$	2		157654	[5]
$LiV(PO_4)F$	8.1E-7	0.23	$P\bar{1}$	2		183876	[6]
$Li_2B_3PO_8$	5.80E-15	0.76	$P\bar{1}$	2		248343	[7]
$Li_3BP_2O_8$	9.60E-12	0.62	$P\bar{1}$	2		248343	[7]
$Li_2NaBP_2O_8$	4.40E-18	1.21	$P\bar{1}$	2		291512	[7]
$Li_4P_2O_7$	<1E-10	1.617	$P\bar{1}$	2		248414	[8]
$LiMgSO_4F$	5.40E-08	0.54	$P\bar{1}$	2		281119	[9]
$Li_6CuB_4O_{10}$	1.00E-13	0.92	$P\bar{1}$	2	β-$Li_6CuB_4O_{10}$	4819	[10]
$Li_{0.91}Hf_{2.022}(PO_4)_3$	<1E-10	0.47	$C\bar{1}$	2			[11]
$Li_7P_3S_{11}$	8.6E-3	0.29	$P\bar{1}$	2			[12]
Li_2ZnGeO_4	1.00E-07	0.4	Pc	7		34362	[13]
$Li_{3.8}Ge_{0.8}P_{0.2}S_4$	1.78E-6	0.47	$P2_1/m$	11			[14]
$Li_{3.6}Ge_{0.6}P_{0.4}S_4$	1.75E-4	0.34	$P2_1/m$	11			[14]
$Li_{3.4}Ge_{0.4}P_{0.6}S_4$	6.54E-4	0.28	$P2_1/m$	11			[14]
$Li_{3.35}Ge_{0.35}P_{0.65}S_4$	1.54E-3	0.23	$P2_1/m$	11			[14]
$Li_{3.3}Ge_{0.3}P_{0.7}S_4$	1.74E-3	0.22	$P2_1/m$	11			[14]
$Li_{3.25}Ge_{0.25}P_{0.75}S_4$	2.2E-03	0.207	$P2_1/m$	11			[14]
$Li_{3.2}Ge_{0.2}P_{0.8}S_4$	5.55E-4	0.27	$P2_1/m$	11			[14]
Li_4SiS_4	5.00E-08	0.56	$P2_1/m$	11		59708	[15]
$Li_{7.22}Si_{1.5}P_{0.5}O_8$	1.64E-7	0.48	$P2_1/m$	11		238602	[16]
Li_4SiO_4	5.00E-10	0.55	$P2_1/m$	11		238603	[17]
Li_4SiS_4	1.59E-8	0.56	$P2_1/m$	11			[18]
$Li_{3.8}Si_{0.8}P_{0.2}S_4$	8.11E-7	0.37	$P2_1/m$	11			[18]
$Li_{3.6}Si_{0.6}P_{0.4}S_4$	7.19E-5	0.34	$P2_1/m$	11			[18]

$Li_{3.5}Si_{0.5}P_{05}S_4$	1.66E-4	0.34	$P2_1/m$	11			[18]
$Li_{3.4}Si_{0.4}P_{0.6}S_4$	6.62E-4	0.29	$P2_1/m$	11			[18]
$Li_{3.3}Si_{0.3}P_{0.7}S_4$	1.02E-5	0.36	$P2_1/m$	11			[18]
$Li_{3.2}Si_{0.2}P_{0.8}S_4$	3.20E-6	0.37	$P2_1/m$	11			[18]
Li_4SiS_4	1.62E-8	0.56	$P2_1/m$	11			[18]
$Li_{3.8}Si_{0.8}P_{0.2}S_4$	8.07E-7	0.37	$P2_1/m$	11			[18]
$Li_{3.6}Si_{0.6}P_{0.4}S_4$	7.11E-5	0.34	$P2_1/m$	11			[18]
$Li_{3.5}Si_{0.5}P_{0.5}S_4$	1.61E-4	0.34	$P2_1/m$	11			[18]
$Li_{3.4}Si_{0.4}P_{0.6}S_4$	6.49E-4	0.29	$P2_1/m$	11			[18]
$Li_{3.3}Si_{0.3}P_{0.7}S_4$	9.84E-6	0.36	$P2_1/m$	11			[18]
$Li_{3.2}Si_{0.2}P_{0.8}S_4$	3.05E-6	0.37	$P2_1/m$	11			[18]
$Li_{3.1}P_{0.9}Si_{0.1}O_4$	7.47E-8		P21/m	11			[19]
$Li_{3.5}P_{0.5}Si_{0.5}O_4$	2.89E-6		P21/m	11			[19]
$Li_{3.9}P_{0.1}Si_{0.9}O_4$	1.99E-8		$P2_1/m$	11			[19]
$Li_{3.7}P_{0.3}Si_{0.7}O_4$	3.84E-7		$P2_1/m$	11		35168	[19]
Li3InCl6	2.04E-3	0.35	C2/m	12		89617	[20]
$Li_2P_2S_6$	7.80E-11	0.48	C2/m	12		253894	[21]
$Li_{0.6}[Li_{0.2}Sn_{0.8}S_2]$	1.2E−4	0.17	C2/m	12			[22]
$Li_3(Mo_8S_8O_8(OH)_8(HWO_5(H_2O)))*(H_2O)_{18}$	3.8E-7	0.62	C2/m	12		412011	[23]
$Li_{17}Sb_{13}S_{28}$	1.05E-9	0.4	C2/m	12		429902	[24]
Li_3InBr_6	9.04E-4		C2/m	12			[25]
Li_3YBr_6	1.92E-3	0.37	C2/m	12			[26]
$Li_{0.84}Sn_{0.79}S_2$	1.2E-4	0.17	C2/m	12			[27]
$LiAlSi_4O_{10}$	1.01E-10		P2/c	13		194284	[1]
$LiPO_3$	1.00E-09		P2/c	13		51630	[28]

LiGaBr4	7.00E-6	0.54	$P2_1/c$	14		61337	[25]
Li_2SO_4	1.40E-14	1.1	$P2_1/c$	14		2512	[29]
Li_3BO_3	7.40E-11	0.63	$P2_1/c$	14		9105	[30]
$Li_6Ge_2O_7$	8.50E-07	0.43	$P2_1/c$	14		31050	[31]
$LiAlCl_4$	1.00E-06	0.47	$P2_1/c$	14		35275	[32]
$LiYO_2$	1.80E-08	0.72	$P2_1/c$	14		45511	[33]
$LiBO_2$	1.00E-08	0.71	$P2_1/c$	14		200891	[34]
$LiClC_3H_7NO$	1.6E-4	0.881	$P2_1/c$	14		238683	[35]
$LaLiO_2$	<1E-10	0.92	$P2_1/c$	14		239278	[36]
$(La_{0.9}Sr_{0.1})LiO_2$	6.29E-10	0.62	$P2_1/c$	14		239279	[36]
$La(Li_{0.76}Mg_{0.08})O_2$	7.27E-10	0.66	$P2_1/c$	14		239280	[36]
$Li_{2.5}V_2(PO_4)_3$	1.9E-7		$P2_1/c$	14		240269	[37]
$Li_4Zn(PO_4)_2$	<1E-10	1.3	$P2_1/c$	14	α-$Li_4Zn(PO_4)_2$	255464	[38]
$LiSbO_2$	<1E-10	0.88	$P2_1/c$	14		262075	[39]
$Li_2Sr_2Al(PO_4)_3$	<1E-10	1.02	$P2_1/c$	14		431319	[40]
Li_2ZrO_3	6.10E-10	0.78	C2/c	15		94894	[33]
$Li_6Zr_2O_7$	5.20E-10	0.68	C2/c	15		73835	[41]
Li_3AlF_6	5.00E-07	0.54	C2/c	15		85171	[42]
Li_2SnS_3	1.50E-05	0.59	C2/c	15		251656	[43]
$LiTa_2PO_8$	1.6E-3	0.32	C2/c	15		267438	[44]
$LiBaP_2O_7$	1.00E-10		C2/c	15		280927	[45]
$Li_3Na_5(TiS_4)_2$	8.80E-06	0.4	C2/c	15		391258	[46]
$LiGd(PO_3)_4$	<1E-10	1.7	C2/c	15		416442	[47]
LiVO3	2.048E-9		C2/c	15		51443	[48]

Li_2CrCl_4	<1E-10	1.22	C2/c	15		202627	[49]
Li_3ErI_6	9.92E-5	0.37	C2/c	15			[50]
$Li_{3.7}Zn_{0.7}Ga_{0.3}(PO_4)_2$	<1E-10	0.91	$P2_12_12_1$	19	β'-$Li_{3.7}Zn_{0.7}Ga_{0.3}(PO_4)_2$	255466	[38]
Li_3SbS_4	1.5E-6	0.518	$Pmn2_1$	31		8407	[51]
Li_3PS_4	2.60E-07	0.49	$Pmn2_1$	31	γ-Li_3PS_4	180318	[52]
$LiGaO_2$	2.40E-14	0.86	$Pna2_1$	33		18152	[53]
LiB_6O_9F	5.40E-24	1.38	$Pna2_1$	33		420286	[54]
Li_3SbS_3	1.00E-07	0.4	$Pna2_1$	33		424834	[55]
$LiSi_2N_3$	6.17E-08	0.64	$Cmc2_1$	36		34118	[56]
$Li_2(PO_2N)$	<1E-10	0.57	$Cmc2_1$	36		188493	[57]
$LiGa_2GeS_6$	3.80E-08	0.47	Fdd2	43		254406	[58]
$La_{0.64}Li_{0.08}TiO_3$	3.35E-4		Pmmm	47		92228	[59]
$La_{0.62}Li_{0.14}TiO_3$	4.42E-4		Pmmm	47		92231	[59]
$La_{0.595}Li_{0.215}TiO_3$	8.53E-4		Pmmm	47		92234	[59]
$Li_{0.4}Na_{0.1}La_{0.5}Nb_2O_6$	9.92E-6		Pmmm	47		180629	[60]
$Li_{0.3}Na_{0.2}La_{0.5}Nb_2O_6$	1.11E-5		Pmmm	47		180630	[60]
$Li_{0.2}Na_{0.3}La_{0.5}Nb_2O_6$	1.18E-5		Pmmm	47		180631	[60]
$Li_{0.1}Na_{0.4}La_{0.5}Nb_2O_6$	1.21E-5		Pmmm	47		180632	[60]
$Li_{0.07}Na_{0.43}La_{0.5}Nb_2O_6$	1.23E-5		Pmmm	47		180633	[60]
$Li_{0.04}Na_{0.46}La_{0.5}Nb_2O_6$	5.91E-6		Pmmm	47		180634	[60]
$Li_{0.02}Na_{0.48}La_{0.5}Nb_2O_6$	3.99E-6		Pmmm	47		180635	[60]
$(Ag_{0.33}Li_{0.67})_{0.27}La_{0.57}TiO_3$	1E-4	0.30	Pmmm	47			[61]
$(Ag_{0.5}Li_{0.5})_{0.27}La_{0.57}TiO_3$	2.3E-5	0.28	Pmmm	47			[61]

$(Ag_{0.67}Li_{0.33})_{0.27}La_{0.57}TiO_3$	2E-7	0.37	Pmmm	47			[61]
$Pr_{0.56}Li_{0.34}TiO_{3.01}$	1E-6	0.47	Pmmm	47			[62]
$Nd_{0.55}Li_{0.34}TiO_3$	8E-7	0.53	Pmmm	47			[62]
$Li_{0.09}La_{0.77}TiO_3$	1.23E-4		Pmmm	47			[63]
$Li_{0.15}La_{0.72}TiO_3$	4.14E-4		Pmmm	47			[63]
$Li_{0.24}La_{0.65}TiO_3$	5.77E-4		Pmmm	47			[63]
$Li_{0.12}La_{0.75}TiO_3$	2.38E-4		Pmmm	47			[63]
$Li_{0.16}La_{0.7}TiO_3$	5.21E-4		Pmmm	47			[63]
$Li_{0.23}La_{0.7}TiO_3$	5.26E-4		Pmmm	47			[63]
Li_5AlO_4	5.00E-10	0.99	Pmmn	59		16229	[64]
$Li_{14}Nd_5(Si_{11}N_{19}O_5)O_2F_2$	1.7E-10	0.69	Pmmn	59		262923	[65]
Li_5GaO_4	5.00E-09	0.71	Pbca	61	α-Li_5GaO_4	9082	[64]
Li_2SiN_2	1.60E-07		Pbca	61		420126	[66]
$Li_{6.5}O_8P_{1.5}Si_{0.5}$	4.49E-07	0.44	Pnma	62		238600	[16]
$Li_{3.4}Si_{0.7}S_{0.3}O_4$	4.21E-7		Pnma	62		47145	[67]
$Li_{3.2}Si_{0.6}S_{0.4}O_4$	1.32E-6		Pnma	62			[67]
$Li_{3.1}Si_{0.55}S_{0.45}O_4$	3.14E-7		Pnma	62			[67]
$Li_{6.6}SiPO_8$	1.48E-7	0.49	Pnma	62		238601	[16]
$Li_{4.2}Si_{0.8}Al_{0.2}S_4$	2.40E-8	0.53	Pnma	62			[18]
$Li_{4.4}Si_{0.6}Al_{0.4}S_4$	3.04E-8	0.52	Pnma	62			[18]
$Li_{4.6}Si_{0.4}Al_{0.6}S_4$	1.45E-8	0.52	Pnma	62			[18]
$Li_{4.8}Si_{0.2}Al_{0.8}S_4$	2.25E-7	0.52	Pnma	62			[18]
$Li_{3.8}Si_{0.8}Al_{0.2}S_4$	2.38E-8	0.53	Pnma	62			[18]
$Li_{3.6}Si_{0.6}Al_{0.4}S_4$	3.06E-8	0.52	Pnma	62			[18]

$Li_{3.4}Si_{0.4}Al_{0.6}S_4$	1.45E-8	0.52	Pnma	62			[18]
$Li_{3.2}Si_{0.2}Al_{0.8}S_4$	2.28E-7	0.52	Pnma	62			[18]
$Li_4Zn(PO_4)_2$	<1E-10	1.1	Pnma	62	β-$Li_4Zn(PO_4)_2$	255465	[38]
$Li_{3.5}Zn_{0.5}Ga_{0.5}(PO_4)_2$	<1E-10	1.02	Pnma	62	β-$Li_{3.5}Zn_{0.5}Ga_{0.5}(PO_4)_2$	255468	[38]
Li_3PS_4	1.60E-04	0.36	Pnma	62	β-Li_3PS_4	180319	[52]
Li_3PO_4	<1E-10	1.14	Pnma	62	γ-Li_3PO_4	20208	[68]
Li_3PS_4	3.00E-7		Pnma	62	γ-Li_3PS_4	35018	[69]
$Li_{2.88}PO_{3.73}N_{0.14}$	1.4E-13	0.97	Pnma	62		79426	[70]
Li_3PO_4	4.2E-18	1.24	Pnma	62	γ-Li_3PO_4	79427	[70]
Li_4GeS_4	2E-7	0.53	Pnma	62		92200	[71]
$Li_{14}Zn(GeO_4)_4$	1.00E-06	0.24	Pnma	62		100169	[72]
$Li_{3.75}Ge_{0.75}V_{0.25}O_4$	5.66E-6		Pnma	62		150918	[73]
$Li_{3.70}Ge_{0.85}W_{0.15}O_4$	3.80E-5		Pnma	62		150920	[73]
$Li_{0.2}Ca_{0.4}TaO_3$	3.53E-9	0.54	Pnma	62		151936	[74]
$Li_{0.2}(Ca_{0.36}Sr_{0.04})TaO_3$	9.2E-9		Pnma	62		151937	[74]
$Li_2Mg_2(MoO_4)_3$	<1E-10	0.71	Pnma	62		170956	[75]
Li_4SnSe_4	2E-5	0.45	Pnma	62		193768	[76]
$Li(BH_4)$	1E-8		Pnma	62		239763	[77]
$LiZnSO_4F$	2.80E-05	0.2455	Pnma	62		261343	[78]
Li_4GeS_4	2.00E-07	0.53	Pnma	62		290831	[79]
Li_4SnS_4	7.0E-5	0.29	Pnma	62		290832	[80]
Li_2ZnI_4	4.00E-08	0.58	Pnma	62		402062	[81]

$Pr_{0.53}Li_{0.41}TiO_3$	0.84E-7	0.462	Pnma	62			[82]
$Pr_{0.54}Li_{0.38}TiO_3$	1.18E-6	0.452	Pnma	62			[82]
$Pr_{0.55}Li_{0.35}TiO_3$	1.51E-6	0.441	Pnma	62			[82]
$Pr_{0.56}Li_{0.32}TiO_3$	1.91E-6	0.437	Pnma	62			[82]
$Pr_{0.57}Li_{0.29}TiO_3$	2.86E-6	0.429	Pnma	62			[82]
$Pr_{0.58}Li_{0.26}TiO_3$	3.87E-6	0.421	Pnma	62			[82]
$Pr_{0.59}Li_{0.23}TiO_3$	3.40E-6	0.425	Pnma	62			[82]
$Li_{2.5}Y_{0.5}Zr_{0.5}Cl_6$	1.4E-3	0.33	Pnma	62			[83]
$Li_{2.633}Er_{0.633}Zr_{0.367}Cl_6$	1.1E-3	0.35	Pnma	62			[83]
$Li_{3.33}Ge_{0.33}V_{0.67}O_4$	6.94E-6		Pnma	62			[84]
$Li_{3.6}Ge_{0.6}V_{0.4}O_4$	1.97E-5	0.44	Pnma	62			[84]
$Li_{3.75}Ge_{0.75}V_{0.25}O_4$	1.08E-5		Pnma	62			[84]
$Li_{3.5}Ge_{0.5}V_{0.5}O_4$	1.77E-5		Pnma	62		66576	[84]
$Li_{3.87}Sn_{0.87}As_{0.13}S_4$	1.48E-5	0.39	Pnma	62			[85]
$Li_{3.855}Sn_{0.855}As_{0.145}S_4$	1.31E-4	0.35	Pnma	62			[85]
$Li_{3.85}Sn_{0.85}As_{0.15}S_4$	2.08E-4	0.31	Pnma	62			[85]
$Li_{3.84}Sn_{0.84}As_{0.16}S_4$	5.85E-4	0.29	Pnma	62			[85]
$Li_{3.83}Sn_{0.83}As_{0.17}S_4$	1.39E-3	0.21	Pnma	62			[85]
$Li_{3.825}Sn_{0.825}As_{0.175}S_4$	5.18E-4	0.27	Pnma	62			[85]
$Li_{3.82}Sn_{0.82}As_{0.18}S_4$	2.83E-4	0.35	Pnma	62			[85]
$Li_{3.8}Sn_{0.8}As_{0.2}S_4$	1.06E-4	0.4	Pnma	62			[85]
$Li_{3.75}Sn_{0.75}As_{0.25}S_4$	3.69E-6	0.48	Pnma	62			[85]
$Nd_{0.54}Li_{0.36}TiO_3$	3.42E-8	0.50	Pnma	62		81047	[86]
$Pr_{0.51}Li_{0.39}TiO_{2.96}$	5.34E-7	0.44	Pnma	62		81048	[86]
$Sm_{0.52}Li_{0.38}TiO_{2.97}$	2E-7	0.64	Pnma	62			[62]

Li_4GeO_4	2.80E-10	0.73	Cmcm	63		18096	[87]
$LiCl*H_2O$	1E-8	0.777	Cmcm	63		281198	[88]
Li_2MgBr_4	7.80E-10	0.77	Cmmm	65		73276	[89]
$Li_{0.22}La_{0.60}TiO_3$	4.8E-4	0.391	Cmmm	65			[90]
$Li_{0.18}La_{0.61}TiO_3$	2.0E-4	0.432	Cmmm	65		99398	[90]
$LiBiO_2$	3.80E-08	0.1	Ibam	72		46022	[30]
$Li_{2.5}Zn_{0.25}PS_4$	8.40E-4		$I\bar{4}$	82			[69]
$LiZnPS_4$	5.4E-8		$I\bar{4}$	82		95785	[69]
$Li_2Zn_{0.5}PS_4$	1.30E-4	0.22	$I\bar{4}$	82		264462	[69]
$(Li_{1.69}Zn_{0.66})PS_4$	1.30E-4	0.181	$I\bar{4}$	82		264462	[69]
$Li_{1.5}Zn_{0.75}PS_4$	1.65E-5	0.25	$I\bar{4}$	82		264463	[69]
$(Li_{1.19}Zn_{0.9})PS_4$	0.65E-5	0.25	$I\bar{4}$	82		264463	[69]
$(Li_{0.5}Ce_{0.5})(MoO_4)$	1.3E-8	0.4	$I4_1/a$	88		186450	[91]
$(Li_{0.5}Ce_{0.25}Pr_{0.25})(MoO_4)$	1E-9	0.5	$I4_1/a$	88		186451	[91]
$(Li_{0.5}Ce_{0.25}Sm_{0.25})(MoO_4)$	1.8E-10	0.5	$I4_1/a$	88		186452	[91]
Li_2TeO_4	<1E-10	1.129	$P4_122$	91		1485	[92]
Li_3BN_2	1.60E-10	0.67	$P4_22_12$	94	α-Li_3BN_2	655673	[93]
$Li_2B_4O_7$	1.00E-10		$I4_1cd$	110		65930	[94]
$LiY(BH_4)_4$	1.26E-6		$P\bar{4}2c$	112		239762	[77]
$LiPN_2$	1.6E-7	0.40	$I\bar{4}2d$	122		66007	[95]
$La_{0.565}Li_{0.305}TiO_3$	9.57E-4		P4/mmm	123		92235	[59]
$La_{0.5}Li_{0.5}TiO_3$	9.25E-4	0.39	P4/mmm	123		92236	[59]
$Li_{0.33}La_{0.5}TiO_3$	1E-3	0.15	P4/mmm	123		82671	[96]
$Li_{0.27}La_{0.57}TiO_3$	3.4E-4	0.38	P4/mmm	123			[61]
$La_{0.61}Li_{0.18}TiO3$	4.12e-4		P4/mmm	123			[97]

$La_{0.55}Li_{0.36}TiO3$	6.88E-4	0.35	P4/mmm	123			[97]
$La_{0.54}Li_{0.39}TiO3$	6.51E-4		P4/mmm	123			[97]
$La_{0.52}Li_{0.45}TiO3$	5.01E-4		P4/mmm	123		50434	[97]
$La_{0.58}Li_{0.27}TiO3$	5.99E-4		P4/mmm	123		82672	[97]
$La_{0.56}Li_{0.33}TiO3$	6.68E-4		P4/mmm	123		504435	[97]
$Li_{0.31}La_{0.63}TiO_3$	4.11E-4		P4/mmm	123			[63]
$Li_{0.39}La_{0.59}TiO_3$	8.83E-4		P4/mmm	123			[63]
$Li_{0.49}La_{0.55}TiO_3$	9.39E-4		P4/mmm	123			[63]
$Li_{0.68}La_{0.49}TiO_3$	1.03E-3		P4/mmm	123			[63]
$Li_{0.24}La_{0.65}TiO_3$	9.57E-4		P4/mmm	123			[63]
$Li_{0.33}La_{0.58}TiO_3$	8.93E-4		P4/mmm	123			[63]
$Li_{0.36}La_{0.55}TiO_3$	9.34E-4		P4/mmm	123			[63]
$Li_{0.42}La_{0.52}TiO_3$	8.47E-4		P4/mmm	123			[63]
$Li_{0.29}La_{0.57}TiO_3$	4.4E-5	0.453	P4/mmm	123			[90]
$La_{0.56}Li_{0.33}TiO_3$	1.65E-4	0.41	P4/mmm	123			[98]
$La_{0.56}Li_{0.33}TiO_3$-5wt% Al_2O_3	1.66E-4	0.24	P4/mmm	123			[98]
$La_{0.56}Li_{0.33}TiO_3$-10wt% Al_2O_3	9.33E-4	0.17	P4/mmm	123			[98]
$La_{0.56}Li_{0.33}TiO_3$-15wt% Al_2O_3	9.56E-5	0.50	P4/mmm	123			[98]
$Li(LaTiO_4)$	<1E-10	0.83	P4/nmmZ	129		91843	[99]
$Li(NdTiO_4)$	<1E-10	0.87	P4/nmmZ	129		91844	[99]
$La_{0.65}Li_{0.05}(Mg_{0.5}W_{0.5})O_3$	1.8E-7	0.46	P4/nmm	129		151900	[100]
$La_{0.63}Li_{0.11}(Mg_{0.5}W_{0.5})O_3$	6.8E-6	0.38	P4/nmm	129		151901	[100]
$La_{0.62}$ $Li_{0.14}(Mg_{0.5}W_{0.5})O_3$	1.2E-5	0.37	P4/nmm	129		151902	[100]

Li_4PS_4I	1.2E-4	0.37	P4/nmmZ	129		432169	[101]
$Li_{9.75}Sn_{0.75}P_{2.25}S_{12}$	3.57E-3		$P4_2$/nmcS	137			
Li_6ZnO_4	9.40E-09	0.61	$P4_2$/nmc	137		62137	[64]
$Li_{9.42}Si_{1.02}P_{2.1}S_{9.96}O_{2.04}$	1.1E-4	0.238	$P4_2$/nmc	137			[102]
$Li_{9.54}Si_{1.74}P_{1.44}S_{11.7}Cl_{0.3}$	2.53E-2	0.238	$P4_2$/nmc	137			[102]
$Li_{10}GeP_2S_{11.7}O_{0.3}$	1.15E-2	0.155	$P4_2$/nmc	137			[102]
$Li_{10}(Si_{0.5}Sn_{0.5})P_2S_{12}$	4.28E-3	0.29	$P4_2$/nmc	137			[102]
$Li_9P_3S_9O_3$	4.27E-5	0.311	$P4_2$/nmc	137			[103]
$Li_{10.05}Ge_{1.05}P_{1.95}S_{12}$	1.22E-2	0.28	$P4_2$/nmc4	137			[104]
$Li_{10.2}Ge_{1.2}P_{1.8}S_{12}$	1.32E-2		$P4_2$/nmc4	137			[104]
$Li_{10.5}Ge_{1.5}P_{1.5}S_{12}$	1.10E-2		$P4_2$/nmc 4	137			[104]
$Li_{10}GePS_{12}$	1.21E-2		$P4_2$/nmc	137		188887	[104]
$Li_{10.35}Ge_{1.35}P_{1.65}S_{12}$	1.44E-2	0.269	$P4_2$/nmc S	137		193947	[104]
$Li_{3.475}Si_{0.475}P_{0.525}S_4$	5.27E-3		$P4_2$/nmc	137			[105]
$Li_{3.45}Si_{0.45}P_{0.55}S_4$	6.73E-3	0.27	$P4_2$/nmc	137			[105]
$Li_{3.425}Si_{0.425}P_{0.575}S_4$	5.65E-3		$P4_2$/nmc	137			[105]
$Li_{3.4}Si_{0.4}P_{0.6}S_4$	4.21E-3		$P4_2$/nmc	137			[105]
$Li_{3.335}Sn_{0.33}P_{0.67}S_4$	3.73E-3		$P4_2$/nmc	137			[105]
$Li_{3.3}Sn_{0.3}P_{0.7}S_4$	3.65E-3		$P4_2$/nmc	137			[105]
$Li_{3.285}Sn_{0.28}P_{0.72}S_4$	4.36E-3		$P4_2$/nmc	137			[105]
$Li_{3.27}Sn_{0.27}P_{0.73}S_4$	4.96E-3		$P4_2$/nmc	137			[105]
$Li_{3.26}Sn_{0.26}P_{0.74}S_4$	4.53E-3		$P4_2$/nmc	137			[105]
$Li_{3.25}Sn_{0.25}P_{0.75}S_4$	3.6E-3		$P4_2$/nmc	137			[105]
$Li_{10}SiP_2S_{12}$	2.3E-3	0.196	P42/nmc	137			[106]
$Li_{10}SnP_2S_{12}$	7E-3	0.27	$P4_2$/nmc C	137		193755	[107]

$Li_{10}GeP_2S_{12}$	2.46E-2	0.274	$P4_2/nmc$	137		241439	[108]
$Li_{10}(Ge_{0.776}Sn_{0.224})P_2S_{12}$	1.41E-2	0.276	$P4_2/nmc$	137		255748	[108]
$Li_{10}SnP_2S_{12}$	3.98E-3	0.305	$P4_2/nmc$	137		255750	[108]
$Li_{10}(Ge_{0.416}Sn_{0.584})P_2S_{12}$	7.43E-3	0.285	$P4_2/nmc$	137		255757	[108]
$Li_{10.35}Si_{1.35}P_{1.65}S_{12}$	6.5E-3		$P4_2/nmcS$	137		252037	[109]
$Li_{9.81}Sn_{0.81}P_{2.19}S_{12}$	5.5E-3		$P4_2/nmc$	137		252040	[109]
$Li_{10}GeP_2S_{12}$	1.20E-02	0.25	$P4_2/nmc$	137		255749	[110]
$Li_{10.2}Si_{1.2}P_{1.8}S_{12}$	4.16E-3		$P4_2/nmcS$	137			[111]
$Li_{10.275}Si_{1.275}P_{1.725}S_{12}$	5.61E-3		$P4_2/nmcS$	137			[111]
$Li_{10.35}Si_{1.35}P_{1.65}S_{12}$	6.68E-3		$P4_2/nmcS$	137			[111]
$Li_{10.425}Si_{1.425}P_{1.575}S_{12}$	5.22E-3		$P4_2/nmcS$	137			[111]
$Li10GeP_2S_{12}$	1.21E-2		$P4_2/nmcS$	137			[111]
$Li_{10.05}Ge_{1.05}P_{1.95}S_{12}$	1.25E-2		$P4_2/nmcS$	137			[111]
$Li_{10.2}Ge_{1.2}P_{1.8}S_{12}$	1.36E-2		$P4_2/nmcS$	137			[111]
$Li_{10.35}Ge_{1.35}P_{1.65}S_{12}$	1.41E-2		$P4_2/nmcS$	137			[111]
$Li_{10.5}Ge_{1.5}P_{1.5}S_{12}$	1.09E-2		$P4_2/nmcS$	137			[111]
$Li_{9.79}Sn_{0.79}P_{2.21}S_{12}$	4.56E-3		$P4_2/nmcS$	137			[111]
$Li_{9.81}Sn_{0.81}P_{2.19}S_{12}$	4.98E-3		$P4_2/nmcS$	137			[111]
$Li_{9.87}Sn_{0.87}P_{2.13}S_{12}$	4.32E-3		$P4_2/nmcS$	137			[111]
$Li_{9.9}Sn_{0.9}P_{2.1}S_{12}$	3.66E-3		$P4_2/nmcS$	137			[111]
$Li_{10}SnP_2S_{12}$	3.65E-3		$P4_2/nmcS$	137			[111]
$Li_{10.2}(Sn_{0.2}Si_{0.8})1.2P_{1.8}S_{12}$	7.82E-3		$P4_2/nmcS$	137		5667	[111]
$Li_{10.5}(Sn_{0.2}Si_{0.8})_{1.5}P_{1.5}S_{12}$	8.79E-3		$P4_2/nmcS$	137		5668	[111]
$Li_{10.35}(Sn_{0.2}Si_{0.8})_{1.35}P_{1.65}S_{12}$	1.08E-2		$P4_2/nmcS$	137		5669	[111]

$Li_{10.35}(Sn_{0.27}Si_{1.08})P_{1.65}S_{12}$	1.1E-3	0.197	$P4_2/nmcS$	137		257946	[111]
$Li_{10.2}(Sn_{0.2}Si_{0.8})_{1.2}P_{1.8}S_{12}$	2.69E-3		$P4_2/nmcS$	137		257948	[111]
$Li_{10}GeP_2S_{12}$	1.43E-3	0.24	$P4_2/nmcS$	137			[112]
$Li_{9.8}Ba_{0.1}GeP_2S_{12}$	5.61E-4		$P4_2/nmcS$	137			[112]
$Li_{9.6}Ba_{0.2}GeP_2S_{12}$	5.72E-4		$P4_2/nmcS$	137			[112]
$Li_{9.4}Ba_{0.3}GeP_2S_{12}$	7.07E-4	0.29	$P4_2/nmcS$	137			[112]
$Li_{9.2}Ba_{0.4}GeP_2S_{12}$	3.16E-4		$P4_2/nmcS$	137			[112]
$Li_9Ba_{0.5}GeP_2S_{12}$	9.98E-5		$P4_2/nmcS$	137			[112]
$Li_{10}GeP_2S_{12}$	5.0E-3	0.35	$P4_2/nmc$	137			[113]
$LiLaNb_2O_7$	<1E-8		I4/mmm	139		72566	[114]
$Li_4Sr_3Nb_{5.77}Fe_{0.23}O_{19.77}$	<1E-10		I4/mmm	139		87823	[115]
$Li_4Sr_3Nb_6O_{20}$	<1E-10		I4/mmm	139		87824	[115]
$Li_4Sr_{3.056}Nb_6O_{20}$	<1E-10	0.74	I4/mmm	139		109168	[115]
$LiScO_2$	1.00E-12	0.87	$I4_1/amd$	141		36124	[33]
r-$LiAlO_2$	1.10E-12	0.97	$I4_1/amd$	141		99517	[33]
Li_3BN_2	8.70E-08	0.55	$I4_1/amd$	141	β-Li_3BN_2	155126	[93]
Li_4SrN_2	2.30E-13	0.9	$I4_1/amd$	141		87413	[116]
$LiScO_2$	<1E-10	1.047	$I4_1/amd$	141		257819	[117]
$Li_{0.9}Sc_{0.9}Zr_{0.1}O_2$	<1E-10	0.912	$I4_1/amd$	141		257820	[117]
$Li_7La_3HfO_{12}$	9.85E-7	0.53	$I4_1/acdZ$	142	“tetragonal-LLHO”	174202	[118]
$Li_7La_3Zr_2O_{12}$	1.63E-6	0.54	$I4_1/acdZ$	142	“tetragonol-LLZO”	183684	[119]
$Li_7La_3Zr_2O_{12}$	5E-7	0.59	I41/acdZ	142			[120]
$Li_7La_3Zr_2O_{12}$	9.9E-6	0.43	$I4_1/acdZ$	142		238687	[121]

$LiGaSiO_4$	3.00E-16	0.9	R3H	146		65125	[122]
$LiGa_{0.5}Al_{0.5}GeO_4$	<1E-10	1.06	R3H	146		257740	[123]
$LiAlGeO_4$	<1E-10	0.97	R3H	146		257741	[123]
$LiGaGeO_4$	<1E-10	1.12	$R\bar{3}$	148		257739	[123]
$LiTi_2(PO_4)_3$	1.61E-4	0.21	$R\bar{3}$	148			[124]
$Li_{1.2}Ti_{1.8}Al_{0.2}(PO_4)_3$	4.82E-3	0.18	$R\bar{3}$	148			[124]
$LiNaSO_4$	8.80E-10		P31c	159		14364	[125]
$Li_{3.333}Mg_{0.333}P_2S_6$	8.20E-8	0.517	$P\bar{3}1m$	162		95606	[126]
$Li_{2.667}Mg_{0.667}P_2S_6$	4.00E-06	0.46	$P\bar{3}1m$	162		95607	[126]
$Li_4P_2S_6$	2.38E-07	0.29	$P\bar{3}1m$	162		242170	[127]
$Li_4P_2S_6$	1.6E-10	0.48	$P\bar{3}1m$	162			[128]
Li_3YCl_6	5.39E-4	0.40	$P\bar{3}m1$	164			[26]
Li_3ErCl_6	3.3E-4	0.41	$P\bar{3}m1$	164		50151	[129]
$Li_{4.4}Al_{0.4}Ge_{0.6}S_4$	4.33E-5	0.38	$P\bar{3}m1$	164		235201	[130]
$Li_{4.4}Al_{0.4}Sn_{0.6}S_4$	3.6E-6	0.15	$P\bar{3}m1$	164		235207	[130]
Li_5NCl_2	1.20E-06	0.5	$R\bar{3}m$	166		84763	[131]
$LiHf_2(PO_4)_3$	2.833E-7		$R\bar{3}cH$	167			[2]
$LiZr_2(PO_4)_3$	2.96E-10		$R\bar{3}cH$	167		201935	[2]
$LiGe_2(PO_4)_3$	3.33E-7		$R\bar{3}cH$	167		263767	[2]
$Li_{1.1}Ti_{1.9}Sc_{0.1}(PO_4)_3$	3.89E-4	0.3	$R\bar{3}cH$	167			[132]
$Li_{1.2}Ti_{1.8}Sc_{0.2}(PO_4)_3$	2.51E-3	0.25	$R\bar{3}cH$	167			[132]
$Li_{1.3}Ti_{1.7}Sc_{0.3}(PO_4)_3$	7.91E-4	0.28	$R\bar{3}cH$	167			[132]
$Li_{1.4}Ti_{1.6}Sc_{0.4}(PO_4)_3$	1.99E-4	0.31	$R\bar{3}cH$	167			[132]
$Li_{1.5}Ti_{1.5}Sc_{0.5}(PO_4)_3$	9.74E-5	0.32	$R\bar{3}cH$	167			[132]
$LiTi_2(PO_4)_3$	7.61E-6	0.38	$R\bar{3}cH$	167		95979	[132]

$LiGe_2(PO_4)_3$	4.83E-9	0.654	$R\bar{3}cH$	167		69763	[133]
$Li_{1.2}Al_{0.2}Ge_{1.8}(PO_4)_3$	4.83E-5	0.387	$R\bar{3}cH$	167		263760	[133]
$Li_{1.4}Al_{0.4}Ge_{1.6}(PO_4)_3$	1.88E-4	0.407	$R\bar{3}cH$	167		263762	[133]
$Li_{1.5}Al_{0.5}Ge_{1.5}(PO_4)_3$	3.36E-4	0.426	$R\bar{3}cH$	167		263763	[133]
$Li_{1.7}Al_{0.7}Ge_{1.3}(PO_4)_3$	2.64E-4	0.450	$R\bar{3}cH$	167		263765	[133]
$Li_{1.8}Al_{0.8}Ge_{1.2}(PO_4)_3$	1.37E-4	0.429	$R\bar{3}cH$	167		263766	[133]
$LiTi_2(PO_4)_3$	1.0E-4		$R\bar{3}cH$	167			[134]
$Li_{1.2}Ti_2Si_{0.2}P_{2.8}O_{12}$	8.6E-5		$R\bar{3}cH$	167			[134]
$Li_{1.3}Ti_2Si_{0.3}P_{2.7}O_{12}$	3.2E-4		$R\bar{3}cH$	167			[134]
$Li_{1.4}Ti_2Si_{0.4}P_{2.6}O_{12}$	1.5E-4		$R\bar{3}cH$	167			[134]
$Li_{1.5}Ti_2Si_{0.5}P_{2.5}O_{12}$	9.6E-5		$R\bar{3}cH$	167			[134]
$Li_{1.3}Al_{0.3}Ti_{1.7}(PO_4)_3$	3E-3		$R\bar{3}cH$	167			[134]
$Li_{1.4}Al_{0.4}Ti_{1.6}(PO_4)_3$	3.88E-4		$R\bar{3}cH$	167			[134]
$Li_{1.5}Al_{0.5}Ti_{1.5}(PO_4)_3$	2.48E-4		$R\bar{3}cH$	167			[134]
$Li_{1.2}Cr_{0.2}Ti_{1.8}(PO_4)_3$	1.82E-5		$R\bar{3}cH$	167			[134]
$Li_{1.3}Cr_{0.3}Ti_{1.7}(PO_4)_3$	3.51E-5		$R\bar{3}cH$	167			[134]
$Li_{1.4}Cr_{0.4}Ti_{1.6}(PO_4)_3$	1.49E-4		$R\bar{3}cH$	167			[134]
$Li_{1.5}Cr_{0.5}Ti_{1.5}(PO_4)_3$	3.86E-4		$R\bar{3}cH$	167			[134]
$Li_{1.6}Cr_{0.6}Ti_{1.4}(PO_4)_3$	1.26E-4		$R\bar{3}cH$	167			[134]
$Li_{1.7}Cr_{0.7}Ti_{1.3}(PO_4)_3$	8.05E-6		$R\bar{3}cH$	167			[134]
$Li_{1.2}Ga_{0.2}Ti_{1.8}(PO_4)_3$	1.62E-4		$R\bar{3}cH$	167			[134]
$Li_{1.3}Ga_{0.3}Ti_{1.7}(PO_4)_3$	2.61E-4		$R\bar{3}cH$	167			[134]
$Li_{1.4}Ga_{0.4}Ti_{1.6}(PO_4)_3$	1.28E-4		$R\bar{3}cH$	167			[134]
$Li_{1.5}Ga_{0.5}Ti_{1.5}(PO_4)_3$	1.22E-4		$R\bar{3}cH$	167			[134]
$Li_{1.2}Fe_{0.2}Ti_{1.8}(PO_4)_3$	1.80E-4		$R\bar{3}cH$	167			[134]

$Li_{1.3}Fe_{0.3}Ti_{1.7}(PO_4)_3$	2.46E-4		$R\bar{3}cH$	167			[134]
$Li_{1.4}Fe_{0.4}Ti_{1.6}(PO_4)_3$	3.92E-4		$R\bar{3}cH$	167			[134]
$Li_{1.2}Sc_{0.2}Ti_{1.8}(PO_4)_3$	6.90E-4		$R\bar{3}cH$	167			[134]
$Li_{1.3}Sc_{0.3}Ti_{1.7}(PO_4)_3$	7.03E-4		$R\bar{3}cH$	167			[134]
$Li_{1.4}Sc_{0.4}Ti_{1.6}(PO_4)_3$	5.15E-4		$R\bar{3}cH$	167			[134]
$Li_{1.5}Sc_{0.5}Ti_{1.5}(PO_4)_3$	2.53E-4		$R\bar{3}cH$	167			[134]
$Li_{1.2}In_{0.2}Ti_{1.8}(PO_4)_3$	3.90E-4		$R\bar{3}cH$	167			[134]
$Li_{1.3}In_{0.3}Ti_{1.7}(PO_4)_3$	3.93E-4		$R\bar{3}cH$	167			[134]
$Li_{1.4}In_{0.4}Ti_{1.6}(PO_4)_3$	3.02E-4		$R\bar{3}cH$	167			[134]
$Li_{1.5}In_{0.5}Ti_{1.5}(PO_4)_3$	2.04E-4		$R\bar{3}cH$	167			[134]
$Li_{1.2}La_{0.2}Ti_{1.8}(PO_4)_3$	8.00E-5		$R\bar{3}cH$	167			[134]
$Li_{1.3}La_{0.3}Ti_{1.7}(PO_4)_3$	5.23E-4		$R\bar{3}cH$	167			[134]
$Li_{1.4}La_{0.4}Ti_{1.6}(PO_4)_3$	4.98E-4		$R\bar{3}cH$	167			[134]
$Li_{1.5}La_{0.5}Ti_{1.5}(PO_4)_3$	2.81E-4		$R\bar{3}cH$	167			[134]
$Li_{1.5}Fe_{0.5}Ti_{1.5}(PO_4)_3$	1.74E-4		$R\bar{3}cH$	167		55751	[134]
$Li_{0.87}Hf_{2.032}P_3O_{12}$	1.29E-05	0.33	$R\bar{3}cH$	167		83501	[134]
$Li_{1.2}Al_{0.2}Ti_{1.8}(PO_4)_3$	5.95E-4		$R\bar{3}cH$	167		427621	[134]
$Li(Ti_{1.4}Sn_{0.6})(PO_4)_3$	2.28E-5	0.32	$R\bar{3}cH$	167		183672	[135]
$Li(Ti_{0.6}Sn_{1.4})(PO_4)_3$	9.42E-6		$R\bar{3}cH$	167		183676	[135]
$Li(Ti_{0.4}Sn_{1.6})(PO_4)_3$	3.15E-6		$R\bar{3}cH$	167		183677	[135]
$Li_{1.15}Y_{0.15}Zr_{1.85}(PO_4)_3$	1.4E-4	0.39	$R\bar{3}cH$	167		191891	[136]
LiZr2(PO4)3	1E-9	0.76	$R\bar{3}cH$	167		201935	[137]
$Li_{1.3}(Al_{0.3}Ti_{1.7})(PO_4)_3$	8.02E-7		$R\bar{3}cH$	167		253240	[138]
$Li_{1.3}(Al_{0.23}Ga_{0.07}Ti_{1.7})(PO_4)_3$	4.46E-6		$R\bar{3}cH$	167		253241	[138]

$Li_{1.3}(Al_{0.23}Sc_{0.07}Ti_{1.7})(PO_4)_3$	1.94E-7		$R\bar{3}cH$	167		253242	[138]
$Li_{1.3}(Al_{0.23}Y_{0.07}Ti_{1.7})(PO_4)_3$	3.84E-8		$R\bar{3}cH$	167		253243	[138]
$Li_{1.3}Al_{0.3}Ti_{1.7}(PO_4)_3$	7E-4		$R\bar{3}cH$	167		257190	[139]
$LiZr_2(PO_4)_3$	8.5E-5		$R\bar{3}cH$	167			[140]
$Li_{1.025}Y_{0.025}Zr_{1.975}(PO_4)_3$	1.28E-4		$R\bar{3}cH$	167			[140]
$Li_{1.05}Y_{0.05}Zr_{1.95}(PO_4)_3$	1.3E-4		$R\bar{3}cH$	167			[140]
$Li_{1.1}Y_{0.1}Zr_{1.9}(PO_4)_3$	1.0E-4		$R\bar{3}cH$	167			[140]
$Li_{1.1}Al_{0.1}Ge1_{.9}(PO_4)_3$	1.29E-5		$R\bar{3}cH$	167			[140]
$Li_{1.2}Al_{0.2}Ge1_{.8}(PO_4)_3$	1.89E-5	0.46	$R\bar{3}cH$	167			[140]
$Li_{1.3}Al_{0.3}Ge1_{.7}(PO_4)_3$	1.91E-4		$R\bar{3}cH$	167			[140]
$Li_{1.4}Al_{0.4}Ge1_{.6}(PO_4)_3$	3.17E-4	0.37	$R\bar{3}cH$	167			[140]
$Li_{1.5}Al_{0.5}Ge1_{.5}(PO_4)_3$	3.45E-4		$R\bar{3}cH$	167			[140]
$Li_{1.6}Al_{0.6}Ge1_{.4}(PO_4)_3$	3.94E-4	0.37	$R\bar{3}cH$	167			[140]
$Li_{1.7}Al_{0.7}Ge1_{.3}(PO_4)_3$	2.75E-4		$R\bar{3}cH$	167			[140]
$Li_{1.8}Al_{0.8}Ge1_{.2}(PO_4)_3$	1.23E-4	0.43	$R\bar{3}cH$	167			[140]
$LiGe_2(PO_4)_3$	3.12E-9	0.60	$R\bar{3}cH$	167			[141]
$Li_{0.86}Hf_{2.035}(PO_4)_3$	9.2E-8	0.48	$R\bar{3}cH$	167			[11]
$Li_{1.7}Al_{0.3}Ti_{1.6}(PO_4)_3$	5E-5		$R\bar{3}cH$	167			[142]
$Li_{1.2}In_{0.2}Ti_{1.8}(PO_4)_3$	8.22E-5	0.32	$R\bar{3}cH$	167			[143]
$Li_{1.3}Al_{0.2}Sc_{0.1}Ti_{1.7}(PO_4)_3$	9.72E-4	0.25	$R\bar{3}cH$	167			[144]
$Li_{1.3}Al_{0.15}Sc_{0.15}Ti_{1.7}(PO_4)_3$	1.24E-3	0.23	$R\bar{3}cH$	167			[144]
$Li_{1.3}Al_{0.1}Sc_{0.2}Ti_{1.7}(PO_4)_3$	4.29E-4	0.26	$R\bar{3}cH$	167			[144]
$Li_{1.3}Sc_{0.3}Ti_{1.7}(PO_4)_3$	4.52E-4	0.25	$R\bar{3}cH$	167			[144]

$Li_{1.3}Al_{0.3}Ti_{1.7}(PO_4)_3$	1.13E-3	0.23	$R\bar{3}cH$	167		257190	[144]
$LiTi(PO_4)_3$	6E-5	0.33	$R\bar{3}c$	167			[145]
$Li_{1.05}Al_{0.05}Ti_{0.95}(PO_4)_3$	1.1E-3	0.31	$R\bar{3}c$	167			[145]
$Li_{1.1}Al_{0.1}Ti_{0.9}(PO_4)_3$	6.7E-4	0.32	$R\bar{3}c$	167			[145]
$Li_{1.2}Al_{0.2}Ti_{0.8}(PO_4)_3$	4.0E-3	0.31	$R\bar{3}c$	167			[145]
$Li_{1.3}Al_{0.3}Ti_{0.7}(PO_4)_3$	6.2E-3	0.30	$R\bar{3}c$	167			[145]
$Li_{1.4}Al_{0.4}Ti_{0.6}(PO_4)_3$	3.3E-3	0.29	$R\bar{3}c$	167			[145]
$Li_{1.05}Cr_{0.05}Ti_{0.95}(PO_4)_3$	1.8E-4	0.33	$R\bar{3}c$	167			[145]
$Li_{1.1}Cr_{0.1}Ti_{0.9}(PO_4)_3$	2.6E-4	0.32	$R\bar{3}c$	167			[145]
$Li_{1.2}Cr_{0.2}Ti_{0.8}(PO_4)_3$	4.3E-4	0.31	$R\bar{3}c$	167			[145]
$Li_{1.3}Cr_{0.3}Ti_{0.7}(PO_4)_3$	2.9E-4	0.32	$R\bar{3}c$	167			[145]
$Li_{1.05}Fe_{0.05}Ti_{0.95}(PO_4)_3$	1.3E-4	0.34	$R\bar{3}c$	167			[145]
$Li_{1.1}Fe_{0.1}Ti_{0.9}(PO_4)_3$	6.3E-4	0.34	$R\bar{3}c$	167			[145]
$Li_{1.2}Fe_{0.2}Ti_{0.8}(PO_4)_3$	1.4E-3	0.32	$R\bar{3}c$	167			[145]
$Li_{1.3}Fe_{0.3}Ti_{0.7}(PO_4)_3$	2.3E-3	0.31	$R\bar{3}c$	167			[145]
$Li_{1.5}Fe_{0.5}Ti_{0.5}(PO_4)_3$	2.7E-4	0.32	$R\bar{3}c$	167			[145]
$LiGe_2(PO_4)_3$	3.37E-7	0.38	$R\bar{3}c$	167			[146]
$Li_{1.3}Al_{0.3}Ge_{1.7}(PO_4)_3$	1.42E-4	0.37	$R\bar{3}c$	167			[146]
$Li_{1.7}Al_{0.7}Ge_{1.3}(PO_4)_3$	2.04E-4		$R\bar{3}c$	167			[146]
$Li_{1.3}Cr_{0.3}Ge_{1.7}(PO_4)_3$	8.87E-5	0.39	$R\bar{3}c$	167			[146]
$Li_{1.5}Cr_{0.5}Ge_{1.5}(PO_4)_3$	1.21E-4	0.37	$R\bar{3}c$	167			[146]
$Li_{1.7}Cr_{0.7}Ge_{1.3}(PO_4)_3$	2.46E-5		$R\bar{3}c$	167			[146]
$Li_{1.3}Ga_{0.3}Ge_{1.7}(PO_4)_3$	4.47E-5	0.38	$R\bar{3}c$	167			[146]
$Li_{1.5}Ga_{0.5}Ge_{1.5}(PO_4)_3$	2.01E-5		$R\bar{3}c$	167			[146]
$Li_{1.3}Fe_{0.3}Ge_{1.7}(PO_4)_3$	2.99E-5	0.39	$R\bar{3}c$	167			[146]

$Li_{1.5}Fe_{0.5}Ge_{1.5}(PO_4)_3$	2.56E-5		$R\bar{3}c$	167			[146]
$Li_{1.3}Sc_{0.3}Ge_{1.7}(PO_4)_3$	5.59E-5		$R\bar{3}c$	167			[146]
$Li_{1.3}In_{0.3}Ge_{1.7}(PO_4)_3$	9.22E-6		$R\bar{3}c$	167			[146]
$Li_{1.5}In_{0.5}Ge_{1.5}(PO_4)_3$	5.81E-6		$R\bar{3}c$	167			[146]
$Li_{1.5}Al_{0.5}Ge_{1.5}(PO_4)_3$	2.86E-4	0.38	$R\bar{3}c$	167		263764	[146]
$LiIO_3$	1.90E-07		$P6_3$	173		35473	[147]
$Li_9Mg_3(PO_4)_4F_3$	<1E-10	0.835	$P6_3$	173		426103	[148]
$Pb_{6.12}Ca_{1.9}Li_{1.96}(PO_4)_6$	<1E-10	1.05	$P6_3/m$	176		59615	[149]
$LiNdSiO_4$	<1E-10		$P6_3/m$	176			[150]
$LiDySiO_4$	<1E-10		$P6_3/m$	176			[150]
$Li_2La_8Si_6O_{25}$	<1E-10		$P6_3/m$	176			[150]
$Li_3La_7Si_6O_{24}$	<1E-10		$P6_3/m$	176			[150]
$Li_{0.284}Sm_{4.512}Si_3O_{12.91}$	<1E-10		$P6_3/m$	176		83279	[150]
$LiLa_9Si_6O_{26}$	<1E-10		$P6_3/m$	176		291218	[150]
$LiEu_9Si_6O_{26}$	<1E-10		$P6_3/m$	176		291220	[150]
$LiAlSiO_4$	2.00E-09	0.68	$P6_422$	181		55665	[151]
$Li_3(NH_2)_2I$	1E-5	0.58	$P6_3mc$	186		167528	[152]
$Ba_3LiTa_5ZrSi_4O_{26}$	<1E-10	0.79	$P\bar{6}2m$	189		239277	[153]
Li_3N	1.2E-3	0.25	P6/mmm	191		26540	[154]
Li_3N	3.00E-04	0.26	P6/mmm	191		156894	[155]
$Fe_2Na_2K(Li_3Si_{12}O_{30})$	<1E-10	1.22	P6/mcc	192		235750	[156]
Li_3P	7.03E-4	0.18	$P6_3/mmc$	194		642223	[157]
$Li_{5.5}K_{0.25}La_{2.75}Nb_2O_{12}$	3.19E-3	0.49	$I2_13$	199			[158]
$Li_{5.5}La_3Nb_{1.75}In_{0.25}O_{12}$	8.07E-3	0.49	$I2_13$	199			[158]
$Li_6BaLa_2Nb_2O_{12}$	6E-6	0.44	$I2_13$	199			[159]

$Li_5La_3Nb_2O_{12}$	8E-6	0.43	$I2_13$	199		54865	[159]
$(K_{0.1}Li_{0.9})(SbO_3)$	1.36E-8		$Pn\bar{3}Z$	201		200984	[160]
Li_8GeP_4	1.8E-5	0.435	$Pa\bar{3}$	205	α-Li_8GeP_4	235184	[161]
Li_8SiP_4	4.5E-5	0.404	$Pa\bar{3}$	205		235186	[161]
Li_3AlN_2	5.00E-08	0.45	$Ia\bar{3}$	206		257464	[162]
$Li_2MgTi_3O_8$	<1E-10	0.71	$P4_332$	212		86165	[163]
$Li_2CoTi_3O_8$	<1E-10	1.33	$P4_332$	212		86166	[163]
$Li_2CoGe_3O_8$	<1E-10	1.49	$P4_332$	212		86167	[163]
$Li_2ZnGe_3O_8$	<1E-10	2.14	$P4_332$	212		86169	[163]
$(Li_{0.61}Mg_{0.39})(Li_{0.46}Mg_{0.005}Ti_{0.035})Ti_{1.5}O_4$	6.56E-10	0.685	$P4_332$	212		168144	[164]
$(Li_{0.55}Mg_{0.45})(Li_{0.445}Mg_{0.055})Ti_{1.5}O_4$	1.53E-11	0.786	$P4_332$	212		168145	[164]
Li_5NI_2	4.00E-6		$F\bar{4}3m$	216		16800	[165]
Li_2VCl_4	6.95E-6		$F\bar{4}3m$	216		74959	[166]
$Li_6PS_5C_{l0.25}Br_{0.75}$	1.86E-3	0.328	$F\bar{4}3m$	216			[167]
Li_6PS_5Cl	2.05E-3	0.452	$F\bar{4}3m$	216		259200	[167]
$Li_6PS_5Cl_{0.5}Br_{0.5}$	3.33E-3	0.367	$F\bar{4}3m$	216		259201	[167]
Li_6PS_5Br	1.15E-3	0.303	$F\bar{4}3m$	216		259202	[167]
$Li_6PS_5Br_{0.5}I_{0.5}$	2.62E-5	0.312	$F\bar{4}3m$	216		259203	[167]
Li_6PS_5I	1.3E-6	0.383	$F\bar{4}3m$	216		259204	[167]
$Li_6PS_5Cl_{0.75}Br_{0.25}$	2.26E-3	0.408	$F\bar{4}3m$	216		259206	[167]
$Li_6PS_5Br_{0.75}I_{0.25}$	1.12E-4	0.321	$F\bar{4}3m$	216		259209	[167]
$Li_6PS_5Br_{0.25}I_{0.75}$	4.72E-6	0.351	$F\bar{4}3m$	216		259211	[167]
Li_6PS_5Br	7.01E-4	0.194	$F\bar{4}3m$	216		234584	[168]

$Li_{6.025}P_{0.975}Si_{0.025}S_5Br$	8.78E-4	0.196	$F\bar{4}3m$	216		234585	[168]
$Li_{6.05}P_{0.95}Si_{0.05}S_5Br$	4.37E-4	0.173	$F\bar{4}3m$	216		234586	[168]
$Li_{6.075}P_{0.925}Si_{0.075}S_5Br$	8.73E-4	0.178	$F\bar{4}3m$	216		234587	[168]
$Li_{6.1}P_{0.95}Si_{0.1}S_5Br$	7.99E-4	0.22	$F\bar{4}3m$	216		234588	[168]
$Li_{6.125}P_{0.875}Si_{0.125}S_5Br$	9.02E-4	0.189	$F\bar{4}3m$	216		234589	[168]
$Li_{6.175}P_{0.825}Si_{0.175}S_5Br$	9.31E-4	0.142	$F\bar{4}3m$	216		234591	[168]
$Li_{6.2}P_{0.8}Si_{0.2}S_5Br$	1.69E-3	0.25	$F\bar{4}3m$	216		234592	[168]
$Li_{6.225}P_{0.775}Si_{0.225}S_5Br$	1.08E-3	0.248	$F\bar{4}3m$	216		234593	[168]
$Li_{6.25}P_{0.75}Si_{0.25}S_5Br$	1.41E-3	0.223	$F\bar{4}3m$	216		234594	[168]
$Li_{6.3}P_{0.7}Si_{0.3}S_5Br$	1.65E-3	0.236	$F\bar{4}3m$	216		234595	[168]
$Li_{6.35}P_{0.65}Si_{0.35}S_5Br$	2.34E-3	0.142	$F\bar{4}3m$	216		234596	[168]
$Li_{6.5}P_{0.5}Si_{0.5}S_5Br$	2.19E-3	0.27	$F\bar{4}3m$	216		234597	[168]
$Li_7Ge_3PS_{12}$	1.1E-4	0.259	$F\bar{4}3m$	216		258187	[169]
$Li_6B_{0.9}PH_{3.6}S_{4.9}$	1.8E-3	0.166	$F\bar{4}3m$	216		264526	[170]
Li_6PS_5Cl	1.30E-03	0.33	$F\bar{4}3m$	216			[171]
Li_6PS_5Br	2.77E-3	0.31	$F\bar{4}3m$	216		267193	[172]
$Li_6P(S_{4.9}Se_{0.1})Br$	3.20E-3	0.33	$F\bar{4}3m$	216		267194	[172]
$Li_6P(S_{4.8}Se_{0.2})Br$	3.92E-3	0.34	$F\bar{4}3m$	216		267195	[172]
$Li_6P(S_{4.7}Se_{0.3})Br$	3.62E-3	0.33	$F\bar{4}3m$	216		267196	[172]
$Li_6P(S_{4.6}Se_{0.4})Br$	3.64E-3	0.33	$F\bar{4}3m$	216		267197	[172]
$Li_6P(S_{4.5}Se_{0.5})Br$	2.68E-3	0.34	$F\bar{4}3m$	216		267198	[172]
$Li_6P(S_{4.4}Se_{0.6})Br$	2.78E-3	0.34	$F\bar{4}3m$	216		267199	[172]
$Li_6P(S_{4.3}Se_{0.7})Br$	3.01E-3	0.35	$F\bar{4}3m$	216		267200	[172]
$Li_6P(S_{4.2}Se_{0.8})Br$	3.48E-3	0.34	$F\bar{4}3m$	216		267201	[172]
$Li_6P(S_{4.1}Se_{0.9})Br$	3.82E-3	0.34	$F\bar{4}3m$	216		267202	[172]

$Li_6P(S_4Se)Br$	3.61E-3	0.34	$F\bar{4}3m$	216		267203	[172]
Li_6PO_5Cl	5.54E-10	0.66	$F\bar{4}3m$	216		421479	[173]
Li_6PS_5Br	3.2E-5	0.32	$F\bar{4}3m$	216		234598	[174]
Li_6PS_5Cl	3.3E-5	0.38	$F\bar{4}3m$	216		259205	[174]
Li_6PS_5I	2.2E-4	0.26	$F\bar{4}3m$	216		259212	[174]
Li_6PS_5I	1.26E-6	0.38	$F\bar{4}3m$	216			[175]
$Li_6P_{0.92}Ge_{0.08}S_5I$	9.02E-6	0.39	$F\bar{4}3m$	216			[175]
$Li_6P_{0.85}Ge_{0.15}S_5I$	3.99E-5	0.36	$F\bar{4}3m$	216			[175]
$Li_6P_{0.75}Ge_{0.25}S_5I$	3.26E-5	0.36	$F\bar{4}3m$	216			[175]
$Li_6P_{0.74}Ge_{0.26}S_5I$	1.51E-4	0.30	$F\bar{4}3m$	216			[175]
$Li_6P_{0.64}Ge_{0.36}S_5I$	6.58E-4	0.24	$F\bar{4}3m$	216			[175]
$Li_6P_{0.53}Ge_{0.47}S_5I$	1.52E-3	0.24	$F\bar{4}3m$	216			[175]
$Li_6P_{0.48}Ge_{0.52}S_5I$	1.83E-3	0.23	$F\bar{4}3m$	216			[175]
$Li_6P_{0.31}Ge_{0.69}S_5I$	5.16E-3	0.24	$F\bar{4}3m$	216			[175]
$Li_6P_{0.21}Ge_{0.79}S_5I$	5.41E-3	0.25	$F\bar{4}3m$	216			[175]
Li_6PS_5Cl	1.31E-6	0.38	$F\bar{4}3m$	216			[176]
Li_6PS_5Br	2.41E-5	0.16	$F\bar{4}3m$	216		259208	[176]
Li_6PS_5I	4.1E-7	0.32	$F\bar{4}3m$	216		418489	[176]
Li_6PS_5I	9.24E-5		$F\bar{4}3m$	216			[177]
$Li_{6.1}P_{0.9}Sn_{0.1}S_5I$	1.61E-4		$F\bar{4}3m$	216			[177]
$Li_{6.2}P_{0.8}Sn_{0.2}S_5I$	2.32E-4		$F\bar{4}3m$	216			[177]
$Li_{6.25}P_{0.75}Sn_{0.25}S_5I$	2.92E-4		$F\bar{4}3m$	216			[177]
$Li_{6.3}P_{0.7}Sn_{0.3}S_5I$	3.06E-4		$F\bar{4}3m$	216			[177]
$Li_{6.5}P_{0.5}Sn_{0.5}S_5I$	2.35E-4		$F\bar{4}3m$	216			[177]
$Li_{6.4}P_{0.6}Ge_{0.4}S_5I$	2.51E-4		$F\bar{4}3m$	216			[177]

$Li_{6.45}P_{0.55}Ge_{0.45}S_5I$	3.65E-4		$F\bar{4}3m$	216			[177]
$Li_{6.5}P_{0.5}Ge_{0.5}S_5I$	5.42E-4		$F\bar{4}3m$	216			[177]
$Li_{6.55}P_{0.45}Ge_{0.55}S_5I$	4.11E-4		$F\bar{4}3m$	216			[177]
$Li_{6.6}P_{0.4}Ge_{0.6}S_5I$	2.74E-4		$F\bar{4}3m$	216			[177]
$Li_{6.8}P_{0.2}Ge_{0.8}S_5I$	5.21E-5		$F\bar{4}3m$	216			[177]
$LiCe(BH_4)_3Cl$	1.03E-4		$I\bar{4}3m$	217		185218	[178]
Li_7PN_4	1.60E-07	0.4	$P\bar{4}3n$	218		69017	[95]
β-Li_8GeP_4	8.6E-5	0.394	$P\bar{4}3n$	218	β-Li_8GeP_4	235185	[161]
$Li_4B_7O_{12}Cl$	2.4E-5		$F\bar{4}3c$	219		1125	[179]
$Fe_{0.16}La_{2.95}Li_{5.68}Zr_2O_{12}$	9.35E-4	0.29	$I\bar{4}3d$	220		431391	[180]
$Fe_{0.19}La_{2.95}Li_{5.57}Zr_2O_{12}$	1.38E-3	0.28	$I\bar{4}3d$	220		431392	[180]
Li_3ClO	2.5E-2		$Pm\bar{3}m$	221			[181]
$Li_{2.99}Ba_{0.005}Cl_{0.5}I_{0.5}$	2.5E-3	0.06	$Pm\bar{3}m$	221			[181]
$Li_{0.31}La_{0.63}((Ti_{0.9}Co_{0.1})O_3$	2.60E-4		$Pm\bar{3}m$	221		151533	[182]
$(La_{0.49}Li_{0.461}Sr_{0.049})(TiO_3$)	7.09E-4	0.33	$Pm\bar{3}m$	221		190825	[183]
$(La_{0.46}Li_{0.429}Sr_{0.111})(TiO_3$)	1.97E-4	0.33	$Pm\bar{3}m$	221		190826	[183]
$(La_{0.402}Li_{0.368}Sr_{0.230})(TiO_3$)	2.87E-5	0.36	$Pm\bar{3}m$	221		190827	[183]
$Li_2(OH)_{0.9}F_{0.1}Cl$	3.86E-5	0.52	$Pm\bar{3}m$	221			[184]
$Li_2(OH)Br$	1.20E-6	0.75	$Pm\bar{3}m$	221		200874	[184]
Li_9NS_3	8.30E-07	0.52	$Pm\bar{3}m$	221		240749	[185]
$(La_{0.55}Li_{0.45})(Ti_{0.9}Al_{0.1})O_3$	1.51E-3		$Pm\bar{3}m$	221		254045	[186]
$(La_{0.6}Li_{0.4})(Ti_{0.8}Al_{0.2})O_3$	5.68E-4		$Pm\bar{3}m$	221		254046	[186]
$(La_{0.65}Li_{0.35})(Ti_{0.7}Al_{0.3})O_3$	1.61E-4		$Pm\bar{3}m$	221		254047	[186]

$(La_{0.7}Li_{0.3})(Ti_{0.6}Al_{0.4})O_3$	1.04E-7		$Pm\bar{3}m$	221		254048	186
$(Li_{0.16}Sr_{0.69})(Ga_{0.25}Ta_{0.75})O_3$	3.69E-6	0.359	$Pm\bar{3}m$	221		291520	187
$Li_{0.375}Sr_{0.4375}Zr_{0.25}Ta_{0.75}O_3$	2.0E-4	0.26	$Pm\bar{3}m$	221			188
$Li_{0.25}Sr_{0.625}Ta_{0.5}Zr_{0.5}O_3$	3.34E-7	0.42	$Pm\bar{3}m$	221			188
$Li_{0.375}Sr_{0.4375}Hf_{0.25}Ta_{0.75}O_3$	3.8E-4	0.36	$Pm\bar{3}m$	221			189
$Li_{0.375}Sr_{0.4375}Zr_{0.25}Nb_{0.75}O_3$	2.00E-5	0.26	$Pm\bar{3}m$	221			190
$Li_{0.25}Sr_{0.625}Zr_{0.5}Nb_{0.5}O_3$	2.75E-7	0.36	$Pm\bar{3}m$	221			190
$Li_{2.99}Ba_{0.005}ClO$	2.5E-2	0.13	$Pm\bar{3}m$	221			191
$Li_{2.99}Ba_{0.005}Cl_{0.5}I_{0.5}O$	3.37E-3		$Pm\bar{3}m$	221			191
$Sm_{0.5}Li_{0.42}TiO_{2.96}$	3.93E-10	0.58	$Pm\bar{3}m$	221			86
$La_{0.52}Li_{0.35}TiO_{2.96}$	9.11E-4	0.32	$Pm\bar{3}m$	221			86
$La_{0.61}Li_{0.15}TiO_3$	2.06E-4		$Pm\bar{3}m$	221			192
$La_{0.58}Li_{0.24}TiO_3$	7.22E-4		$Pm\bar{3}m$	221			192
$La_{0.55}Li_{0.33}TiO_3$	1.58E-3		$Pm\bar{3}m$	221			192
$La_{0.54}Li_{0.36}TiO_3$	9.79E-3		$Pm\bar{3}m$	221			192
$La_{0.52}Li_{0.42}TiO_3$	7.21E-4		$Pm\bar{3}m$	221			192
$La_{0.6}Sr_{0.06}Li_{0.06}TiO_3$	1.13E-5	0.37	$Pm\bar{3}m$	221			193
$La_{0.56}Sr_{0.1}Li_{0.1}TiO_3$	1.37E-5	0.37	$Pm\bar{3}m$	221			193
$La_{0.51}Sr_{0.15}Li_{0.15}TiO_3$	5.3E-5	0.38	$Pm\bar{3}m$	221			193
$La_{0.41}Sr_{0.25}Li_{0.25}TiO_3$	7.64E-5	0.35	$Pm\bar{3}m$	221			193
$La_{0.385}Sr_{0.275}Li_{0.275}TiO_3$	6.04E-5	0.37	$Pm\bar{3}m$	221			193
$La_{0.36}Sr_{0.3}Li_{0.3}TiO_3$	1.92E-5	0.35	$Pm\bar{3}m$	221			193
$La_{0.61}Li_{0.18}TiO3$	2.09E-4		$Pm\bar{3}m$	221			97

$La_{0.58}Li_{0.27}TiO3$	8.32E-4		$Pm\bar{3}m$	221			97
$La_{0.56}Li_{0.33}TiO3$	1.30E-3		$Pm\bar{3}m$	221			97
$La_{0.55}Li_{0.36}TiO3$	1.54E-3	0.33	$Pm\bar{3}m$	221			97
$La_{0.54}Li_{0.39}TiO3$	1.25E-3		$Pm\bar{3}m$	221			97
$La_{0.52}Li_{0.45}TiO3$	7.85E-4		$Pm\bar{3}m$	221			97
$La_{0.51}Li_{0.34}TiO_{2.94}$	7E-5	0.36	$Pm\bar{3}m$	221			62
Li_3OBr	1.10E-06	0.74	$Pm\bar{3}m$	221		67265	194,195
$Li_{7.2}N_{1.6}Cl_{2.4}$	8.4E-7	0.49	$Fm\bar{3}m$	225		49646	131
Li_6NI_3	3.70E-06		$Fm\bar{3}m$	225		83380	165
$Li_{0.19}La_{0.67}(Ti_{0.9}Co_{0.1})O_3$	1.08E-4		$Fm\bar{3}m$	225		151535	182
Li_6NBr_3	1.00E-08	0.69	$Fm\bar{3}m$	225		84091	196
LiI	1E-7		$Fm\bar{3}m$	225		414244	197
$Li(Li_{0.34}Ti_{1.66})O_4$	6.03E-8	0.506	$Fd\bar{3}m$	227		168137	164
$(Li_{0.916}Mg_{0.084})(Li_{0.352}Mg_{0.016}Ti_{1.634})O_4$	1.73E-8	0.564	$Fd\bar{3}m$	227		168139	164
$(Li_{0.826}Mg_{0.174})(Li_{0.374}Mg_{0.026}Ti_{1.60})O_4$	4.24E-9	0.615	$Fd\bar{3}m$	227		168141	164
$(Li_{0.74}Mg_{0.26})(Li_{0.40}Mg_{0.04}Ti_{1.56})O_4$	1.51E-9	0.639	$Fd\bar{3}m$	227		168142	164
Li_2MnCl_4	4.79E-6		$Fd\bar{3}m$	227		69678	166
Li_2MgCl_4	6.24E-7		$Fd\bar{3}m$	227		74957	166
$Li_{1.9}Mn_{0.9}Ga_{0.1}Cl_4$	2.37E-7		$Fd\bar{3}m$	227		50305	198
$Li_{1.65}Mn_{0.65}In_{0.35}Cl_4$	9.9E-8		$Fd\bar{3}m$	227		50306	198
$LiCdCl_4$	5.80E-07	0.44	$Fd\bar{3}m$	227		74958	199
$LiSrNb_2O_6F$	<1E-10	0.604	$Fd\bar{3}m$	227		236009	200
$LiSrTa_2O_6F$	<1E-10	0.604	$Fd\bar{3}m$	227		236010	200

$LiSr_{0.9}Nb_2O_6F_{0.8}$	<1E-10	0.709	$Fd\bar{3}m$	227		236011	[200]
$LiSr_{0.9}Ta_2O_6F_{0.8}$	<1E-10	0.76	$Fd\bar{3}m$	227		236012	[200]
$Li_{1.1}SrNb_{1.9}Zr_{0.1}O_6F$	<1E-10	0.622	$Fd\bar{3}m$	227		236013	[200]
$Li_{1.1}SrTa_{1.9}Zr_{0.1}O_6F$	<1E-10	0.693	$Fd\bar{3}m$	227		236014	[200]
$Li_6SrLa_2Nb_2O_{12}$	4.2E-6	0.5	$Ia\bar{3}d$	230		157628	[159]
$Li_6CaLa_2Nb_2O_{12}$	1.6E-6	0.55	$Ia\bar{3}d$	230		161386	[159]
$Li_{5.25}Ba_{0.25}La_{2.75}Ta_2O_{12}$	6.03E-6	0.479	$Ia\bar{3}d$	230			[201]
$Li_{5.5}Ba_{0.5}La_{2.5}Ta_2O_{12}$	1.35E-5	0.455	$Ia\bar{3}d$	230			[201]
$Li_{6.25}Ba_{1.25}La_{1.75}Ta_2O_{12}$	5.05E-5	0.395	$Ia\bar{3}d$	230			[201]
$Li_{6.5}Ba_{1.5}La_{1.5}Ta_2O_{12}$	3.2E-5	0.402	$Ia\bar{3}d$	230			[201]
$Li_{6.75}Ba_{1.75}La_{1.25}Ta_2O_{12}$	1.25E-5	0.418	$Ia\bar{3}d$	230			[201]
$Li_7Ba_2LaTa_2O_{12}$	3.00E-6	0.442	$Ia\bar{3}d$	230			[201]
$Li_5La_3Ta_2O_{12}$	4.33E-6	0.50	$Ia\bar{3}d$	230		154400	[201]
$Li_6BaLa_2Ta_2O_{12}$	3.02E-5	0.419	$Ia\bar{3}d$	230		237201	[201]
$Li_7La_3Zr_{1.89}Al_{0.15}O_{12}$	3.4E-4	0.334	$Ia\bar{3}d$	230			[202]
$Li_{7.06}La_3Y_{0.06}Zr_{1.94}O_{12}$	9.56E-4	0.26	$Ia\bar{3}d$	230			[203]
$Li_{6.25}La_3Zr_2Ga_{0.25}O_{12}$	3.5E-4		$Ia\bar{3}d$	230			[204]
$Li_7La_3Zr_2O_{12}$	1.2E-4		$Ia\bar{3}d$	230			[205]
$Li_{6.8}La_3Zr_{1.8}Ta_{0.2}O_{12}$	2.8E-4		$Ia\bar{3}d$	230			[205]
$Li_{6.6}La_3Zr_{1.6}Ta_{0.4}O_{12}$	7.3E-4		$Ia\bar{3}d$	230			[205]
$Li_{6.5}La_3Zr_{1.5}Ta_{0.5}O_{12}$	9.2E-4		$Ia\bar{3}d$	230			[205]
$Li_{6.4}La_3Zr_{1.4}Ta_{0.6}O_{12}$	1.0E-3	0.35	$Ia\bar{3}d$	230			[205]
$Li_{6.2}La_3Zr_{1.2}Ta_{0.8}O_{12}$	3.2E-4		$Ia\bar{3}d$	230			[205]
$Li_6La_3ZrTaO_{12}$	1.6E-4		$Ia\bar{3}d$	230			[205]
$Li_7La_3Zr_2O_{12}$	1.2E-4		$Ia\bar{3}d$	230			[205]

$Li_{6.8}La_3Zr_{1.8}Ta_{0.2}O_{12}$	2.8E-4		Ia$\bar{3}$d	230			205
$Li_{6.6}La_3Zr_{1.6}Ta_{0.4}O_{12}$	7.3E-4		Ia$\bar{3}$d	230			205
$Li_{6.5}La_3Zr_{1.5}Ta_{0.5}O_{12}$	9.2E-4		Ia$\bar{3}$d	230			205
$Li_{6.4}La_3Zr_{1.4}Ta_{0.6}O_{12}$	1E-3	0.35	Ia$\bar{3}$d	230			205
$Li_{6.2}La_3Zr_{1.2}Ta_{0.8}O_{12}$	3.2E-4		Ia$\bar{3}$d	230			205
$Li_6La_3ZrTaO_{12}$	1.6E-4		Ia$\bar{3}$d	230			205
$Li_{6.8}La_3Zr_{1.8}Ta_{0.2}O_{12}$	7.8E-4		Ia$\bar{3}$d	230			206
$Li_{6.75}La_3Zr_{1.75}Ta_{0.25}O_{12}$	8.8E-4		Ia$\bar{3}$d	230			206
$Li_{6.65}La_3Zr_{1.65}Ta_{0.35}O_{12}$	7.7E-4		Ia$\bar{3}$d	230			206
$Li_{6.6}La_3Zr_{1.6}Ta_{0.4}O_{12}$	7.2E-4		Ia$\bar{3}$d	230			206
$Li_{6.55}La_3Zr_{1.55}Ta_{0.45}O_{12}$	6.9E-4		Ia$\bar{3}$d	230			206
$Li_6La_3ZrTaO_{12}$	4.4E-4		Ia$\bar{3}$d	230			206
$Li_5La_3Ta_2O_{12}$	1.6E-4		Ia$\bar{3}$d	230			206
$Li_{6.7}La_3Zr_{1.7}Ta_{0.3}O_{12}$	9.6E-4	0.37	Ia$\bar{3}$d	230			206
$Li_{6.5}La_3Zr_{1.5}Ta_{0.5}O_{12}$	6.7E-4		Ia$\bar{3}$d	230		183686	206
$Li_{6.05}Ga_{0.25}La_3Zr_2O_{11.8}F_{0.2}$	1.28E-3	0.28	Ia$\bar{3}$d	230			207
$Li_{5.72}Al_{0.26}La_3Zr_{1.5}W_{0.25}O_{12}$	4.9E-4	0.35	Ia$\bar{3}$d	230			208
$Li_{6.8}La_3Zr_{1.9}Mo_{0.1}O_{12}$	8.00E-5	0.46	Ia$\bar{3}$d	230			209
$Li_{6.6}La_3Zr_{1.8}Mo_{0.2}O_{12}$	3.11E-4	0.48	Ia$\bar{3}$d	230			209
$Li_{6.4}La_3Zr_{1.7}Mo_{0.3}O_{12}$	3.69E-4	0.49	Ia$\bar{3}$d	230			209
$Li_{6.2}La_3Zr_{1.6}Mo_{0.4}O_{12}$	3.40E-4	0.48	Ia$\bar{3}$d	230			209
$Li_{6.5}La_3Zr_{1.75}Mo_{0.25}O_{12}$	3.33E-4	0.39	Ia$\bar{3}$d	230		239128	209
$Li_{6.75}La_3Zr_{1.875}Te_{0.125}O_{12}$	3.30E-4	0.41	Ia$\bar{3}$d	230			210
$Li_{6.5}La_3Zr_{1.75}Te_{0.25}O_{12}$	1.02E-3	0.38	Ia$\bar{3}$d	230			210

$Li_{6.375}La_3Zr_{1.375}Nb_{0.625}O_{12}$	1.37E-3	0.25	Ia$\bar{3}$d	230			[211]
$Li_5La_3Ta_2O_{12}$	1.2E-6	0.56	Ia$\bar{3}$d	230		154400	[212]
$Li_5La_3Nb_2O_{12}$	1E-5	0.43	Ia$\bar{3}$d	230		171171	[212]
$Li_5La_3Bi_2O_{12}$	4.00E-05	0.47	Ia$\bar{3}$d	230		158372	[213]
$Li_6La_2SrBi_2O_{12}$	5.20E-05	0.43	Ia$\bar{3}$d	230		158373	[213]
$Li_5Nd_3Sb_2O_{12}$	1.3E-7	0.67	Ia$\bar{3}$d	230		159426	[214]
$Li_4Nd_3TeSbO_{12}$	1.96E-6	0.64	Ia$\bar{3}$d	230		159732	[215]
$Li_5La_3Sb_2O_{12}$	8.2E-6	0.51	Ia$\bar{3}$d	230		161342	[216]
$Li_6SrLa_2Sb_2O_{12}$	6.6E-6	0.54	Ia$\bar{3}$d	230		161343	[216]
$Li_6(La_2Ca)(NbO_6)_2$	1.33E-6		Ia$\bar{3}$d	230		161386	[217]
$Li_6(La_2Sr)(NbO_6)_2$	3.69E-6		Ia$\bar{3}$d	230		161387	[217]
$Li_6CaLa_2Ta_2O_{12}$	2.2E-6	0.5	Ia$\bar{3}$d	230		163860	[218]
$Li_6BaLa_2Ta_2O_{12}$	1.3E-5	0.44	Ia$\bar{3}$d	230		163861	[218]
$Li_{6.15}La_3Zr_{1.75}Ta_{0.25}Ga_{0.2}O_{12}$	4.1E-4	0.27	Ia$\bar{3}$d	230			[219]
$Li_{6.15}La_3Zr_{1.75}Ta_{0.25}Al_{0.2}O_{12}$	3.7E-4	0.30	Ia$\bar{3}$d	230			[219]
$Li_{6.75}La_3Zr_{1.75}Ta_{0.25}O_{12}$	8.7E-4	0.22	Ia$\bar{3}$d	230		183873	[219]
$Li_{6.16}Al_{0.28}La_3Zr_2O_{12}$	6.1E-4	0.34	Ia$\bar{3}$d	230		185539	[220]
$Li_7La_3Zr_2O_{12}$	1.97E-6	0.49	Ia$\bar{3}$d	230			[221]
$Li_7La_3Zr_2O_{12}$-0.5wt% Al	1.58E-4		Ia$\bar{3}$d	230			[221]
$Li_7La_3Zr_2O_{12}$-0.9wt% Al	3.2E-4	0.34	Ia$\bar{3}$d	230			[221]
$Li_{6.06}Al_{0.2}La_3Zr_2O_{12}$	4E-4	0.34	Ia$\bar{3}$d	230		185539	[221]
$Li_6BaLa_2Ta_2O_{12}$	2.45E-5	0.40	Ia$\bar{3}$d	230		185602	[222]
$Nd_3Zr_2Al_{0.5}Li_{5.5}O_{12}$	3.9E-5	0.56	Ia$\bar{3}$d	230		189530	[223]

$(Li_{6.26}Al_{0.24})La_3Zr_2O_{12}$	3.1E-4	0.33	Ia$\bar{3}$d	230		195182	[224]
$Li_6La_3Nb_{1.5}Y_{0.5}O_{12}$	1.88E-4		Ia$\bar{3}$d	230		237141	[225]
$Li_{5.2}La_3Nb_{1.9}Y_{0.1}O_{12}$	6.39E-5		Ia$\bar{3}$d	230		237143	[225]
$Li_{5.4}La_3Nb_{1.8}Y_{0.2}O_{12}$	6.74E-5		Ia$\bar{3}$d	230		237144	[225]
$Li_{5.5}La_3Nb_{1.75}Y_{0.25}O_{12}$	9.18E-5		Ia$\bar{3}$d	230		237145	[225]
$Li_{6.5}La_3Nb_{1.25}Y_{0.75}O_{12}$	3.43E-4		Ia$\bar{3}$d	230		237146	[225]
$Li_6Ba_{0.5}Sr_{0.5}La_2Ta_2O_{12}$	7.1E-6	0.45	Ia$\bar{3}$d	230		237199	[226]
$Li_6SrLa_2Ta_2O_{12}$	5.4E-6	0.45	Ia$\bar{3}$d	230		237200	[226]
$Li_6BaLa_2Ta_2O_{12}$	1.5E-5	0.47	Ia$\bar{3}$d	230		237201	[226]
$Li_6CaLa_2Ta_2O_{12}$	2.2E-6	0.47	Ia$\bar{3}$d	230		237202	[226]
$Li_6BaLa_2Ta_2O_{12}$	4E-5	0.4	Ia$\bar{3}$d	230			[227]
$Li_6SrLa_2Ta_2O_{12}$	7E-6	0.5	Ia$\bar{3}$d	230			[227]
$Li_6SrLa_2Ta_2O_{12}$	7E-6	0.5	Ia$\bar{3}$d	230		237200	[227]
$Li_6BaLa_2Ta_2O_{12}$	4E-5	0.4	Ia$\bar{3}$d	230		237201	[227]
$Li_{5.74}La_3Zr_{1.5}Ta_{0.5}O_{12}$	9.03E-4	0.435	Ia$\bar{3}$d	230		239663	[228]
$La_3Li_{5.08}Ta_{1.51}Zr_{0.39}O_{12}$	1.03E-4	0.536	Ia$\bar{3}$d	230		239664	[228]
$Li_{51.2}Al_{1.6}La_{24}Zr_{16}O_96$	2.54E-4	0.36	Ia$\bar{3}$d	230		241475	[229]
$Li_{49.6}Al_{1.6}La_{24}Zr_{14.4}Ta_{1.6}O_{96}$	6.14E-4	0.29	Ia$\bar{3}$d	230		241476	[229]
$Li_{6.5}La_3Hf_{1.5}Ta_{0.5}O_{12}$	4.0E-4	0.40	Ia$\bar{3}$d	230		258921	[230]
$Li_{6.5}La_3Sn_{1.5}Ta_{0.5}O_{12}$	1.9E-4	0.45	Ia$\bar{3}$d	230		258922	[230]
$Li_5La_3Ta_2O_{12}$	1.59E-5		Ia$\bar{3}$d	230		259164	[231]
$Li_{5.3}La_3Ta_{1.85}Sm_{0.15}O_{12}$	7.11E-6		Ia$\bar{3}$d	230		259165	[231]
$Li_{5.5}La_3Ta_{1.75}Sm_{0.25}O_{12}$	5.17E-6		Ia$\bar{3}$d	230		259166	[231]
$Li_{5.70}La_3Ta_{1.65}Sm_{0.35}O_{12}$	2.15E-5		Ia$\bar{3}$d	230		259167	[231]

$Li_{5.90}La_3Ta_{1.55}Sm_{0.45}O_{12}$	1.18E-5		Ia$\bar{3}$d	230		259168	[231]
$Li_{6.10}La_3Ta_{1.45}Sm_{0.55}O_{12}$	1.40E-5		Ia$\bar{3}$d	230		259169	[231]
$Li_7La_3Zr_2O_{12}$	5.69E-04	0.36	Ia$\bar{3}$d	230	“cubic LLZO”	422259	[232]
$Li_5La_3Nb_2O_{12}$	4.99e-6		Ia$\bar{3}$d	230			[233]
$Li_5La_3Nb_{1.95}Y_{0.05}O_{12}$	1.32E-5		Ia$\bar{3}$d	230			[233]
$Li_5La_3Nb_{1.9}Y_{0.1}O_{12}$	1.43E-5		Ia$\bar{3}$d	230			[233]
$Li_5La_3Nb_{1.85}Y_{0.15}O_{12}$	5.85E-6		Ia$\bar{3}$d	230			[233]
$Li_5La_3Nb_{1.8}Y0_{.2}O_{12}$	9.05E-6		Ia$\bar{3}$d	230			[233]
$Li_5La_3Nb_{1.75}Y_{0.25}O_{12}$	9.42E-6		Ia$\bar{3}$d	230			[233]
$Li_{6.24}La_3Zr_2Al_{0.24}O_{11.98}$	4.0E-4	0.26	Ia$\bar{3}$d	230			[234]
$Li_7La_3Zr_2O_{12}$-0.3Ga	3.8E-5	0.37	Ia$\bar{3}$d	230			[235]
$Li_7La_3Zr_2O_{12}$-0.4Ga	4.4E-5	0.36	Ia$\bar{3}$d	230			[235]
$Li_7La_3Zr_2O_{12}$-0.5Ga	8.9E-5	0.36	Ia$\bar{3}$d	230			[235]
$Li_7La_3Zr_2O_{12}$-Ga	5.4E-4	0.32	Ia$\bar{3}$d	230			[235]
$La_3Zr_2Ga_{0.5}Li_{5.5}O_{12}$	1E-4		Ia$\bar{3}$d	230			[236]
$Li_{6.8}La_3Zr_{1.8}Sb_{0.2}O_{12}$	5.9E-5	0.39	Ia$\bar{3}$d	230			[237]
$Li_{6.6}La_3Zr_{1.6}Sb_{0.4}O_{12}$	7.7E-4	0.34	Ia$\bar{3}$d	230			[237]
$Li_{6.4}La_3Zr_{1.4}Sb_{0.6}O_{12}$	6.6E-4	0.36	Ia$\bar{3}$d	230			[237]
$Li_{6.2}La_3Zr_{1.2}Sb_{0.8}O_{12}$	4.5E-4	0.37	Ia$\bar{3}$d	230			[237]
$Li_6La_3ZrSbO_{12}$	2.6E-4	0.38	Ia$\bar{3}$d	230			[237]
$Li_{6.5}La_3Zr_{1.75}Te_{0.25}O_{12}$-0.07Al	4E-4	0.33	Ia$\bar{3}$d	230			[238]
$Li_{6.65}La_{2.75}Ba_{0.25}Zr_{1.4}Ta_{0.5}Nb_{0.1}O_{12}$	5.27E-4	0.26	Ia$\bar{3}$d	230			[239]
$Li_{6.4}La_3Zr_{1.4}Ta_{0.6}O_{12}$	7.24E-4	0.24	Ia$\bar{3}$d	230			[239]

$Li_{6.4}La_3Zr_{1.4}Ta_{0.5}Nb_{0.1}O_{12}$	4.44E-4	0.27	Ia$\bar{3}$d	230			239
$Li_{6.4}La_3Zr_{1.4}Ta_{0.4}Nb_{0.2}O_{12}$	4.55E-4	0.28	Ia$\bar{3}$d	230			239
$Li_{6.4}La_3Zr_{1.4}Ta_{0.3}Nb_{0.3}O_{12}$	6.06E-4	0.26	Ia$\bar{3}$d	230			239
$Li_7La_3Zr_2O_{12}$	1.74E-4	0.26	Ia$\bar{3}$d	230			239
$Li_3Nd_3Te_2O_{12}$	<1E-10	1.22	Ia$\bar{3}$d	230			240
$Li_{7.131}La_3Zr_2O_{12}Al_{0.244}$	7.73E-5		Ia$\bar{3}$d	230			241
$Li_{6.949}La_3Zr_2O_{12}Al_{0.262}$	2.25E-4		Ia$\bar{3}$d	230			241
$Li_{6.835}La_3Zr_2O_{12}Al_{0.231}$	2.20E-4		Ia$\bar{3}$d	230			241
$Li_{6.660}La_3Zr_2O_{12}Al_{0.258}$	1.51E-4		Ia$\bar{3}$d	230			241
$Li_{6.75}La_3Zr_{1.75}Ta_{0.25}O_{12}$	4.1E-4	0.42	Ia$\bar{3}$d	230			121
$Li_{6.5}La_3Zr_{1.5}Ta_{0.5}O_{12}$	6.1E-4	0.4	Ia$\bar{3}$d	230			121
$Li_6La_3ZrTaO_{12}$	2.1E-4	0.42	Ia$\bar{3}$d	230			121
$Li_3Gd_3Te_2O_{12}$	<1E-10		Ia$\bar{3}$d	230			242
$Li_3Tb_3Te_2O_{12}$	<1E-10		Ia$\bar{3}$d	230			242
$Li_3Er_3Te_2O_{12}$	<1E-10		Ia$\bar{3}$d	230			242
$Li_3Lu_3Te_2O_{12}$	<1E10		Ia$\bar{3}$d	230			242
Li_2S*P_2S_5	3.2E-03						4
$0.7Li_2S$-$0.3P_2S_5$	5.4E-5						4
$Li_{3.8}Ge_{0.8}P_{0.2}S_4$	1.75E-6	0.466					14
$Li_{3.6}Ge_{0.6}P_{0.4}S_4$	1.74E-4	0.339					14
$Li_{3.4}Ge_{0.4}P_{0.6}S_4$	6.53E-4	0.275					14
$Li_{3.35}Ge_{0.35}P_{0.65}S_4$	1.53E-3	0.229					14
$Li_{3.3}Ge_{0.3}P_{0.7}S_4$	1.76E-3	0.221					14

$Li_{3.2}Ge_{0.2}P_{0.8}S_4$	5.57E-4	0.275					14
$Li_{2.9}Ca_{0.05}InBr_6$	2.16E-4						25
$Li_{2.86}Ca_{0.07}InBr_6$	4.04E-4						25
$Li_{2.8}Ca_{0.1}InBr_6$	3.00E-4						25
$Li_{2.7}Ca_{0.15}InBr_6$	6.97E-5						25
$Li_{3.9}Zn_{0.05}GeS_4$	2.72E-7	0.517					71
$Li_{3.8}Zn_{0.1}GeS_4$	9.95E-8	0.545					71
$Li_{3.6}Zn_{0.2}GeS_4$	5.90E-8	0.539					71
Li_2GeS_3	9.7E-9						71
Li_2ZnGeS_4	1.4E-9						71
$Li_{9.6}P_3S_{12}$	1.2E-3	0.259					102
$Li_{1.3}Al_{0.3}Ge_{1.7}(PO_4)_3$	8.24E-5	0.386					133
$Li_{1.6}Al_{0.6}Ge_{1.4}(PO_4)_3$	2.84E-4	0.430					133
$LiTi_2(PO_4)_3$-$0.2Li_2O$	2.4E-4						134
$LiTi_2(PO_4)_3$-$0.3Li_2O$	1.5E-3						134
$LiTi_2(PO_4)_3$-$0.4Li_2O$	1.3E-4						134
$Li_{1.3}Al_{0.3}Ti_{1.7}(PO_4)_3$-$0.3Li_2O$	3.5E-4						134
$LiTi_2(PO_4)_3$-$0.1Li_4P_2O_7$	1.6E-4						134
$Li_{1.4}Al_{0.4}Ti_{1.6}$ $(PO_4)_3$	3.38E-3	0.30			LATP		243
$Li_{1.2}Ge_{0.2}Ti_{1.8}(PO_4)_3$	7.94E-5	0.27			LAGP		243
$Li_{1.5}Ge_{0.5}Ti_{1.5}(PO_4)_3$	1.90E-4	0.33			LAGP		243
$Li_{1.2}Al_{0.2}Ti_{1.8}(PO_4)_3$	3.38E-3	0.28			LATP	427619	243
Li_3ClO	0.85E-3	0.26					194
$Li_3Cl_{0.5}Br_{0.5}O$	1.94E-3	0.18					194
Li_3OCl	1.47E-4	0.26					194

$Li_3OCl_{0.5}Br_{0.5}$	9.49E-4	0.18					194
$Li_{6.6}La_{2.6}Ce_{0.4}Zr_2O_{12}$	1.44E-5	0.48					244
$Li_{1.4}Al_{0.4}Ti_{1.6}(PO_4)_3$	1.1E-03						245
$80Li_2S * 20P_2S_5$	7.2E-04						246
$0.8Li_2S-0.2P_2S_5$	7.2E-4						246
$0.75Li_2S-0.25P_2S_5$	2.8E-4						246
$Li_2S*P_2S_5*P_2S_3$	5.4E-03						247
$Li_2S*P_2S_5*Li_3N$	1.4E-03						248
$Li_5La_3Nb_{1.9}Y_{0.1}O_{12}$	1.44E-5	0.55					233
$Li_7La_3Zr_2O_{12}$	2.35E-4	0.339					249
$Li_{6.88}La_3Zr_{1.88}Nb_{0.12}O_{12}$	5.99E-4	0.319					249
$Li_{6.75}La_3Zr_{1.75}Nb_{0.25}O_{12}$	7.71E-4	0.3					249
$Li_{6.62}La_3Zr_{1.62}Nb_{0.38}O_{12}$	4.41E-4	0.31					249
$Li_{6.5}La_3Zr_{1.5}Nb_{0.5}O_{12}$	2.98E-4	0.319					249
$Li_6La_3ZrNbO_{12}$	1.50E-4	0.42					249
$Li_5La_3Nb_2O_{12}$	3E-5	0.44					249
$Li_7La_3Hf_2O_{12}$	2.4E-4	0.29					250
Li_7GePS_8	7E-3	0.22					251
$Li_{10}(Ge_{0.95}Si_{0.05})P_2S_{12}$	8.63E-3	0.251					252
$Li_{10}(Ge_{0.9}Si_{0.1})P_2S_{12}$	8.07E-3	0.26					252
$Li_{10}(Ge_{0.8}Si_{0.2})P_2S_{12}$	7.28E-3	0.261					252
$Li_{10}(Ge_{0.7}Si_{0.3})P_2S_{12}$	5.82E-3	0.265					252
$Li_{10}(Ge_{0.6}Si_{0.4})P_2S_{12}$	5.24E-3	0.28					252
$Li_{10}(Ge_{0.5}Si_{0.5})P_2S_{12}$	4.2E-3	0.284					252
$Li_{10}(Ge_{0.2}Si_{0.8})P_2S_{12}$	4.81E-3	0.269					252

$Li_{10}(Ge_{0.95}Sn_{0.05})P_2S_{12}$	7.8E-3	0.254					252
$Li_{10}(Ge_{0.9}Sn_{0.1})P_2S_{12}$	7.53E-3	0.256					252
$Li_{10}(Ge_{0.8}Sn_{0.2})P_2S_{12}$	7.06E-3	0.252					252
$Li_{10}(Ge_{0.7}Sn_{0.3})P_2S_{12}$	6.49E-3	0.254					252
$Li_{10}(Ge_{0.5}Sn_{0.5})P_2S_{12}$	6.17E-3	0.249					252
$Li_{10}(Ge_{0.4}Sn_{0.6})P_2S_{12}$	5.76E-3	0.265					252
$Li_{10}(Ge_{0.3}Sn_{0.7})P_2S_{12}$	5.56E-3	0.261					252
$Li_{10}(Ge_{0.2}Sn_{0.8})P_2S_{12}$	4.77E-3	0.269					252
$0.5(Li_2O) * 0.5(P_2O_5)$	1.1E-9	0.71					253
$0.58(Li_2O) * 0.5(P_2O_5)$	2E-8	0.60					253
$0.6(Li_2O) * 0.5(P_2O_5)$	3E-8	0.61					253
$0.63(Li_2O) * 0.5(P_2O_5)$	1.3E-7	0.56					253
$0.66(Li_2O) * 0.5(P_2O_5)$	2.3E-7	0.55					253
$0.7(Li_2O) * 0.5(P_2O_5)$	3E-7	0.57					253
$0.2(Li_2S)\ 0.8(GeS_2)$	1.1E-7	0.52					253
$0.3(Li_2S)\ 0.7(GeS_2)$	9.3E-7	0.48					253
$0.4(Li_2S)\ 0.6(GeS_2)$	2.9E-6	0.42					253
$0.5(Li_2S)\ 0.5(GeS_2)$	3.3E-5	0.35					253
$0.6(Li_2S)\ 0.4(GeS_2)$	9.2E-5	0.32					253
$0.63(Li_2S)\ 0.37(GeS_2)$	1.5E-4	0.34					253
$0.66(Li_2S)\ 0.34(GeS_2)$	1.0E-4	0.37					253
$0.7(Li_2S)\ 0.3(GeS_2)$	1.2E-4	0.34					253
$Li_2O\text{-}P_2O_5$	1.1E-9	0.71					253
$0.58Li_2O\text{-}0.42P_2O_5$	2.0E-8	0.60					253
$0.6Li_2O\text{-}0.4P_2O_5$	3.0E-8	0.61					253

$0.63Li_2O$-$0.37P_2O_5$	1.3E-7	0.56					253
$0.66Li_2O$-$0.34P_2O_5$	2.3E-7	0.55					253
$0.7Li_2O$-$0.3P_2O_5$	3.0E-7	0.57					253
$0.2Li_2S$-$0.8GeS_2$	1.1E-7	0.52					253
$0.3Li_2S$-$0.7GeS_2$	9.3E-7	0.48					253
$0.4Li_2S$-$0.6GeS_2$	2.9E-6	0.42					253
$0.5Li_2S$-$0.5GeS_2$	3.3E-5	0.35					253
$0.6Li_2S$-$0.4GeS_2$	9.2E-5	0.32					253
$0.63Li_2S$-$0.37GeS_2$	1.5E-4	0.34					253
$0.66Li_2S$-$0.34GeS_2$	1.0E-4	0.37					253
$0.7Li_2S$-$0.3GeS_2$	1.2E-4	0.34					253
$Li_{6.55}La_3Zr_2Ga_{0.15}O_{12}$	1.3E-3	0.3					254
$Li_{6.40}La_3Zr_2Ga_{0.2}O_{12}$	9E-4	0.3					254
$Li_{6.10}La_3Zr_2Ga_{0.25}O_{12}$	7E-5	0.3					254
$Li_{6.8}La_3Zr_{1.8}Sb_{0.2}O_{12}$	5.9E-5	0.39					255
$Li_{6.6}La_3Zr_{1.6}Sb_{0.4}O_{12}$	7.7E-4	0.34					255
$Li_{6.4}La_3Zr_{1.4}Sb_{0.6}O_{12}$	6.6E-4	0.36					255
$Li_{6.2}La_3Zr_{1.2}Sb_{0.8}O_{12}$	4.5E-4	0.37					255
$Li_6La_3ZrSbO_{12}$	2.6E-4	0.38					255
$Li(In_{0.62}Li_{1.38})Br_{3.92}$	4.9E-6	0.58					256
Li_3InBr_6	1.77E-4						257
$Li_3InBr_4Cl_2$	7.58E-6						257
$Li_3InBr_3Cl_3$	1.14E-4						257
$Li_3InBr_{2.5}Cl_{3.5}$	3.60E-6						257
$Li_3InBr_2Cl_4$	6.89E-8						257

$Li_{1.8}Mg_{1.1}Cl_4$	1.52E-6						258
$Li_{1.6}Mg_{1.2}Cl_4$	3.07E-6						258
$Li_{1.34}Mg_{1.33}Cl_4$	3.07E-6						258
$Li_{1.9}Mn_{1.05}Cl_4$	4.61E-6						258
$Li_{1.72}Mn_{1.14}Cl_4$	3.62E-6						258
$Li_{1.6}Mn_{1.2}Cl_4$	1.45E-5						258
$Li_{1.52}Mn_{1.24}Cl_4$	1.85E-5						258
$Li_{1.34}Mn_{1.33}Cl_4$	9.57E-6						258
$Li_{1.94}Cl_{1.03}Cl_4$	2.56E-6						258
$Li_{1.90}Cd_{1.05}Cl_4$	3.50E-6						258
Li_2OHBrF	7.10E-7						259
$Li_2OHBr_{0.99}F_{0.01}$	9.16E-7						259
$Li_2OHBr_{0.98}F_{0.02}$	1.11E-6						259
$Li_2OHBr_{0.95}F_{0.05}$	6.75E-7						259
$Li_2OHBr_{0.9}F_{0.1}$	6.80E-7						259
$Li_2OHBr_{0.8}F_{0.2}$	5.44E-7						259
$Li_3(OH)_2Cl$	2.72E-8	0.88					260
$Li_5(OH)_3Cl_2$	2.52E-8	0.75					260
Li_2OHCl	4.28E-8	0.56					260
$Li_5(OH)_2Cl_3$	1.48E-7	0.49					260
Li_3OHCl_2	8.92E-8	0.67					260
$Li_{3.7}Zn_{0.15}GeO_4$	4.63E-7						261
$Li_{3.5}Zn_{0.25}GeO_4$	2.42E-7						261
$Li_{3.1}Zn_{0.45}GeO_4$	9.89E-8						261
$Li_{2.8}Zn_{0.6}GeO_4$	1.27E-7						261

$Li_{2.6}Zn_{0.7}GeO_4$	5.79E-8						[261]
$Li_{2.3}Zn_{0.85}GeO_4$	4.23E-9						[261]
$Li_7La_{2.75}Ca_{0.25}Zr_{1.75}Nb_{0.25}O_{12}$	2.2E-4	0.35					[262]
$Li_{1.5}Cr_{0.5}Ti_{1.5}(PO_4)_3$	1.98E-4	0.29					[263]
$Li_3V_2(PO_4)_3$	2.09E-7						[263]
$Li_3V_{1.8}Al_{0.2}(PO_4)_3$	1.88E-6						[263]
$Li_3V_{1.6}Al_{0.4}(PO_4)_3$	6.21E-6						[263]
$Li_3V_{1.4}Al_{0.6}(PO_4)_3$	9.34E-7						[263]
$Li_7P_{2.9}Mn_{0.1}S_{10.7}I_{0.3}$	5.6E-3	0.22					[264]
0.3 Li_2S * 0.7 SiS_2	1.6E-6	0.46					[265]
0.4 Li_2S * 0.6 SiS_2	2.8E-5	0.38					[265]
0.5 Li_2S * 0.5 SiS_2	1.0E-4	0.32					[265]
0.6 Li_2S * 0.4 SiS_2	5.0E-4	0.25					[265]
$(2Li_2S\text{-}P_2S_5)$	1.12E-4						[266]
$(2Li_2S\text{-}P_2S_5)_{0.85}(LiI)_{0.15}$	2.35E-4						[266]
$(2Li_2S\text{-}P_2S_5)_{0.75}(LiI)_{0.25}$	3.96E-4						[266]
$(2Li_2S\text{-}P_2S_5)_{0.60}(LiI)_{0.40}$	7.60E-4						[266]
$(2Li_2S\text{-}P_2S_5)_{0.55}(LiI)_{0.45}$	1.12E-3						[266]
0.14 SiS_2-0.09 P_2S_5-0.47 Li_2S-0.30 LiI	1.32E-3	0.34					[267]
$0.26B_2S_3$ – $0.3Li_2S$ – 0.44LiI	1.57E-3	0.3					[268]
$0.26B_2S_3$ – $0.31Li_2S$ – 0.43LiI	7.99E-4	0.33					[268]
$0.27B_2S_3$ – $0.32Li_2S$ – 0.41LiI	4.25E-4	0.35					[268]
0.5 SiS_2-0.5 Li_2S	1.5E-4	0.34					[269]

0.1 LiBr-0.45 SiS_2-0.45 Li_2S	1.9E-4	0.30					269
0.2 LiBr-0.4 SiS_2-0.4 Li_2S	2.1E-4	0.33					269
0.25 LiBr-0.38 SiS_2-0.38 Li_2S	2.4E-4	0.31					269
0.3 LiBr-0.3 SiS_2-0.35 Li_2S	3.2E-4	0.33					269
0.35 LiBr-0.33 SiS_2-0.33 Li_2S	2.3E-4	0.38					269
0.4 LiBr-0.3 SiS_2-0.3 Li_2S	1.1E-4	0.42					269
SiS_2-Li_2S	1.20E-4	0.35					270
0.9(SiS_2-Li_2S)-0.1LiCl	1.84E-4	0.34					270
0.8(SiS_2-Li_2S)-0.2LiCl	2.35E-4	0.33					270
0.75(SiS_2-Li_2S)-0.25LiCl	2.66E-4	0.35					270
0.7(SiS_2-Li_2S)-0.3LiCl	2.33E-4	0.35					270
0.65(SiS_2-Li_2S)-0.35LiCl	1.78E-4	0.36					270
0.6(SiS_2-Li_2S)-0.4LiCl	0.93E-4	0.34					270
(0.4SiS_2-0.6Li_2S)	5.3E-4	0.33					271
0.9(0.4SiS_2-0.6Li_2S)-0.1LiI	6.5E-4	0.31					271
0.8(0.4SiS_2-0.6Li_2S)-0.2LiI	7.7E-4	0.30					271
0.7(0.4SiS_2-0.6Li_2S)-0.3LiI	1.15E-3	0.29					271
0.6(0.4SiS_2-0.6Li_2S)-0.4LiI	1.78E-3	0.28					271
0.55(0.4SiS_2-0.6Li_2S)-0.45LiI	1.41E-3	0.29					271

$0.24SiS_2$-$0.36Li_2S$-0.4LiI	1.8E-3	0.28					272
$0.28SiS_2$-$0.42Li_2S$-0.30LiI	1.8E-3	0.31					273
$0.14SiS_2$-$0.09P_2S_5$-$0.47Li_2S$-0.30LiI	2.1E-3	0.34					273
$0.27SiS_2$-$0.03Al_2S_3$-$0.30Li_2S$-0.40LiI	1.2E-3	0.34					273
$0.21SiS_2$-$0.09B_2S_3$-$0.30Li_2S$-0.40LiI	1.7E-3	0.30					273
$0.30Li_2S$-$0.7GeS_2$	4.4E-7	0.63					274
$0.40Li_2S$-$0.60GeS_2$	3.2E-6	0.52					274
$0.50Li_2S$-$0.50GeS_2$	4.0E-5	0.51					274
$0.3Li_2S$-$0.7P_2S_5$	1.7E-2	0.18					275
$0.7Li_2S$-$0.3P_2S_5$	3.2E-3	0.12					276
$0.6Li_2S$-$0.4P_2S_5$	1.5E-4	0.31					277
$0.95(0.6Li_2S$-$0.4SiS_2)$-$0.05Li_4SiO_4$	1.58E-3	0.34					278
$0.9(0.6Li_2S$-$0.4SiS_2)$-$0.1Li_4SiO_4$	4.34E-4	0.37					278
$0.8(0.6Li_2S$-$0.4SiS_2)$-$0.2Li_4SiO_4$	1.59E-4	0.43					278
$0.95(0.6Li_2S$-$0.4SiS_2)$-$0.05Li_3PO_4$	8.68E-4	0.35					278
$0.7(0.6Li_2S$-$0.4SiS_2)$-$0.3Li_3PO_4$	2.08E-5	0.46					278
$0.6(0.6Li_2S$-$0.4SiS_2)$-$0.4Li_3PO_4$	5.33E-6	0.51					278
$0.95(0.6Li_2S$-$0.4SiS_2)$-$0.05Li_4GeO_4$	1.19E-3	0.28					278
$0.9(0.6Li_2S$-$0.4SiS_2)$-$0.1Li_4GeO_4$	3.18E-4	0.35					278

$0.85(0.6Li_2S\text{-}0.4SiS_2)\text{-}0.15Li_4GeO_4$	1.14E-4	0.40					278
$0.95(0.6Li_2S\text{-}0.4SiS_2)\text{-}0.05Li_3BO_3$	1.44E-3	0.33					278
$0.93(0.6Li_2S\text{-}0.4SiS_2)\text{-}0.07Li_3BO_3$	3.84E-4	0.35					278
$0.85(0.6Li_2S\text{-}0.4SiS_2)\text{-}0.15Li_3BO_3$	3.42E-4	0.36					278
$0.75(0.6Li_2S\text{-}0.4SiS_2)\text{-}0.25Li_3BO_3$	7.06E-5	0.38					278
$0.95(0.6Li_2S\text{-}0.4SiS_2)\text{-}0.05Li_3AlO_3$	1.31E-3	0.31					278
$0.94(0.6Li_2S\text{-}0.4SiS_2)\text{-}0.06Li_3AlO_3$	6.83E-4	0.34					278
$0.92(0.6Li_2S\text{-}0.4SiS_2)\text{-}0.08Li_3AlO_3$	4.04E-4	0.34					278
$0.825(0.6Li_2S\text{-}0.4SiS_2)\text{-}0.175Li_3AlO_3$	1.31E-4	0.36					278
$0.975(0.6Li_2S\text{-}0.4SiS_2)\text{-}0.025Li_3GaO_3$	6.82E-4	0.31					278
$0.95(0.6Li_2S\text{-}0.4SiS_2)\text{-}0.05Li_3GaO_3$	3.25E-4	0.32					278
$0.92(0.6Li_2S\text{-}0.4SiS_2)\text{-}0.08Li_3GaO_3$	3.03E-4	0.35					278
$0.89(0.6Li_2S\text{-}0.4SiS_2)\text{-}0.11Li_3GaO_3$	1.13E-4	0.38					278
$0.97(0.6Li_2S\text{-}0.4SiS_2)\text{-}0.03Li_3InO_3$	3.09E-4	0.34					278
$0.95(0.6Li_2S\text{-}0.4SiS_2)\text{-}0.05Li_3InO_3$	3.25E-4	0.35					278
$0.9(0.6Li_2S\text{-}0.4SiS_2)\text{-}0.1Li_3InO_3$	6.84E-5	0.40					278
$0.95(0.6Li_2S\text{-}0.4SiS_2)\text{-}0.05Li_4SiO_4$	1.54E-3	0.38					279

$0.9(0.6Li_2S\text{-}0.4SiS_2)\text{-}0.1Li_4SiO_4$	4.39E-4	0.40					279
$0.95(0.6Li_2S\text{-}0.4SiS_2)\text{-}0.05Li_2SO_4$	4.53E-4	0.41					279
$0.9(0.6Li_2S\text{-}0.4SiS_2)\text{-}0.1Li_2SO_4$	4.70E-5	0.45					279
$0.5Li_2O\text{-}0.1TiO_2\text{-}0.4P_2O_5$	5.67E-8	0.56					280
$0.5025Li_2O\text{-}0.0025Al_2O_3\text{-}0.095TiO_2\text{-}0.4P_2O_5$	1.56E-8	0.55					280
$0.505Li_2O\text{-}0.005Al_2O_3\text{-}0.09TiO_2\text{-}0.4P_2O_5$	1.78E-7	0.50					280
$0.5075Li_2O\text{-}0.0075Al_2O_3\text{-}0.085TiO_2\text{-}0.4P_2O_5$	2.51E-7	0.57					280
$0.51Li_2O\text{-}0.01Al_2O_3\text{-}0.08TiO_2\text{-}0.4P_2O_5$	1.58E-7	0.55					280
$0.515Li_2O\text{-}0.015Al_2O_3\text{-}0.07TiO_2\text{-}0.4P_2O_5$	1.25E-7	0.56					280
$0.525Li_2O\text{-}0.025Al_2O_3\text{-}0.05TiO_2\text{-}0.4P_2O_5$	2.17E-7	0.56					280
$0.53Li_2O\text{-}0.03Al_2O_3\text{-}0.04TiO_2\text{-}0.4P_2O_5$	2.72E-7	0.54					280
$0.54Li_2O\text{-}0.04Al_2O_3\text{-}0.02TiO_2\text{-}0.4P_2O_5$	1.97E-7	0.55					280
$0.545Li_2O\text{-}0.045Al_2O_3\text{-}0.01TiO_2\text{-}0.4P_2O_5$	7.14E-8	0.56					280
$0.95(0.6Li_2S\text{-}0.4SiS_2)\text{-}0.05Li_4SiO_4$	1.51E-3	0.34					281
$0.90(0.6Li_2S\text{-}0.4SiS_2)\text{-}0.1Li_4SiO_4$	4.34E-4	0.37					281
$0.8(0.6Li_2S\text{-}0.4SiS_2)\text{-}0.2Li_4SiO_4$	1.63E-4	0.43					281

$0.95(0.6Li_2S\text{-}0.4SiS_2)\text{-}0.05Li_3PO_4$	9.32E-4	0.35					281
$0.9(0.6Li_2S\text{-}0.4SiS_2)\text{-}0.1Li_3PO_4$	4.55E-4	0.37					281
$0.7(0.6Li_2S\text{-}0.4SiS_2)\text{-}0.3Li_3PO_4$	2.08E-5	0.46					281
$0.6(0.6Li_2S\text{-}0.4SiS_2)\text{-}0.4Li_3PO_4$	5.33E-6	0.51					281
$0.95(0.6Li_2S\text{-}0.4SiS_2)\text{-}0.05Li_4GeO_4$	1.21E-3	0.28					281
$0.9(0.6Li_2S\text{-}0.4SiS_2)\text{-}0.1Li_4GeO_4$	3.18E-4	0.34					281
$0.85(0.6Li_2S\text{-}0.4SiS_2)\text{-}0.15Li_4GeO_4$	1.14E-4	0.41					281
Li_7PS_6	8.0E-5						282
$0.7Li_2S\text{-}0.3P_2S_5$	3.2E-3	0.12					283
$0.95(0.6Li_2S\text{-}0.4SiS_2)\text{-}0.05Li_3BO_3$	1.40E-3						284
$0.93(0.6Li_2S\text{-}0.4SiS_2)\text{-}0.07Li_3BO_3$	3.71E-4						284
$0.85(0.6Li_2S\text{-}0.4SiS_2)\text{-}0.15Li_3BO_3$	3.39E-4						284
$0.75(0.6Li_2S\text{-}0.4SiS_2)\text{-}0.25Li_3BO_3$	7.15E-5						284
$0.95(0.6Li_2S\text{-}0.4SiS_2)\text{-}0.05Li_3AlO_3$	1.22E-3						284
$0.94(0.6Li_2S\text{-}0.4SiS_2)\text{-}0.06Li_3AlO_3$	6.67E-4						284
$0.92(0.6Li_2S\text{-}0.4SiS_2)\text{-}0.08Li_3AlO_3$	3.94E-4						284
$0.825(0.6Li_2S\text{-}0.4SiS_2)\text{-}0.175Li_3AlO_3$	1.25E-4						284

$0.975(0.6Li_2S\text{-}0.4SiS_2)\text{-}0.025Li_3GaO_3$	7.05E-4						284
$0.95(0.6Li_2S\text{-}0.4SiS_2)\text{-}0.05Li_3GaO_3$	3.36E-4						284
$0.92(0.6Li_2S\text{-}0.4SiS_2)\text{-}0.08Li_3GaO_3$	3.06E-4						284
$0.89(0.6Li_2S\text{-}0.4SiS_2)\text{-}0.11Li_3GaO_3$	1.20E-4						284
$0.97(0.6Li_2S\text{-}0.4SiS_2)\text{-}0.03Li_3InO_3$	3.11E-4						284
$0.95(0.6Li_2S\text{-}0.4SiS_2)\text{-}0.05Li_3InO_3$	2.99E-4						284
$0.90(0.6Li_2S\text{-}0.4SiS_2)\text{-}0.10Li_3InO_3$	6.81E-5						284
$(0.67Li_2S\text{-}0.33SiS_2)\text{-}(0.75Li_2S\text{-}0.25P_2S_5)$	1.2E-3	0.28					285
$0.2Li_3N\text{-}0.8SiS_2$	1.46E-6	0.45					286
$0.3Li_3N\text{-}0.7SiS_2$	2.97E-5	0.36					286
$0.4Li_3N\text{-}0.6SiS_2$	2.74E-4	0.30					286
$0.5Li_3N\text{-}0.5SiS_2$	4.47E-5	0.34					286
$0.6Li_3N\text{-}0.4SiS_2$	2.25E-8	0.63					286
$0.6Li_2S\text{-}0.4P_2S_3$	5.70E-6						287
$0.63Li_2S\text{-}0.37P_2S_3$	2.55E-5						287
$0.667Li_2S\text{-}0.333P_2S_3$	1.1E-4	0.40					287
$0.7Li_2S\text{-}0.3P_2S_3$	7.90E-5						287
$0.75Li_2S\text{-}0.25P_2S_3$	5.08E-5						287
$0.6Li_2S\text{-}0.4SiS_2$	5.1E-4	0.33					288
$0.555Li_2S\text{-}0.4SiS_2\text{-}0.045Li_3N$	1.5E-3	0.28					288

$0.525Li_2S$-$0.4SiS_2$-$0.075Li_3N$	9.6E-4	0.29					288
$0.1Li_2O$-$0.1LiCl$-$0.65B_2O_3$-$0.1SiO_2$-$0.05Al_2O_3$	1.9E-4	0.427					289
$0.75Li_2O$-0.25P2S5	1.80E-5	0.48					290
$0.75(0.7Li_2O$-$0.3Li_2S)$-0.25P2S5	2.42E-5	0.48					290
$0.75(0.5Li_2O$-$0.5Li_2S)$-0.25P2S5	2.83E-5	0.46					290
$0.75(0.4Li_2O$-$0.6Li_2S)$-0.25P2S5	4.99E-5	0.44					290
$0.75(0.3Li_2O$-$0.7Li_2S)$-0.25P2S5	8.89E-5	0.40					290
$0.75(0.2Li_2O$-$0.8Li_2S)$-0.25P2S5	1.63E-4	0.38					290
$0.75(0.1Li_2O$-$0.9Li_2S)$-0.25P2S5	2.27E-4	0.36					290
$0.75Li_2S$-0.25P2S5	1.80E-4	0.41					290
$0.45Li_2$-$0.55SiS_2$	1.08E-4	0.40					291
$0.5Li_2$-$0.5SiS_2$	3.36E-4	0.32					291
$0.55Li_2$-$0.45SiS_2$	6.53E-4	0.30					291
$0.60Li_2$-$0.4SiS_2$	1.19E-3	0.29					291
$0.63Li_2$-$0.37SiS_2$	1.05E-3	0.30					291
$0.65Li_2$-$0.35SiS_2$	7.41E-4	0.33					291
$0.95(0.5Li_2$-$0.5SiS_2)$-$0.05(0.5Li_2O$-$0.5P_2O_5)$	4.27E-4	0.38					291
$0.95(0.53Li_2$-$0.47SiS_2)$-$0.05(0.53Li_2O$-$0.47P_2O_5)$	5.91E-4	0.33					291

$0.95(0.55Li_2S\text{-}0.45SiS_2)\text{-}0.05(0.55Li_2O\text{-}0.45P_2O_5)$	1.01E-3	0.34					291
$0.95(0.58Li_2S\text{-}0.42SiS_2)\text{-}0.05(0.58Li_2O\text{-}0.42P_2O_5)$	1.06E-3	0.34					291
$0.95(0.6Li_2S\text{-}0.4SiS_2)\text{-}0.05(0.6Li_2O\text{-}0.4P_2O_5)$	1.01E-3	0.27					291
$0.95(0.63Li_2S\text{-}0.37SiS_2)\text{-}0.05(0.63Li_2O\text{-}0.37P_2O_5)$	8.71E-4	0.33					291
$0.95(0.65Li_2S\text{-}0.35SiS_2)\text{-}0.05(0.65Li_2O\text{-}0.35P_2O_5)$	5.34E-4	0.32					291
$0.95(0.67Li_2S\text{-}0.33SiS_2)\text{-}0.05(0.67Li_2O\text{-}0.33P_2O_5)$	1.99E-4	0.37					291
$0.8(0.55Li_2S\text{-}0.45SiS_2)\text{-}0.2(0.55Li_2O\text{-}0.45P_2O_5)$	7.88E-5	0.41					291
$0.8(0.6Li_2S\text{-}0.4SiS_2)\text{-}0.2(0.6Li_2O\text{-}0.4P_2O_5)$	7.69E-5	0.41					291
$0.8(0.65Li_2S\text{-}0.35SiS_2)\text{-}0.2(0.65Li_2O\text{-}0.35P_2O_5)$	5.21E-5	0.42					291
$0.65Li_2S\text{-}0.35P_2S_5$	4.14E-5						292
$0.675Li_2S\text{-}0.325P_2S_5$	7.84E-5						292
$0.7Li_2S\text{-}0.3P_2S_5$	1.58E-3	0.39					292
$0.725Li_2S\text{-}0.275P_2S_5$	4.51E-4						292
$0.75Li_2S\text{-}0.25P_2S_5$	3.67E-4						292
$0.6Li_2S\text{-}0.4SiS_2$	1.69E-4						293
$0.1LiI\text{-}0.9(0.6Li_2S\text{-}0.4SiS_2)$	2.35E-4						293
$0.2LiI\text{-}0.8(0.6Li_2S\text{-}0.4SiS_2)$	3.52E-4						293

0.3LiI-0.7(0.6Li_2S-0.4SiS_2)	7.42E-4						293
0.5Li_2S-0.5SiS_2	1.58E-6						293
0.1LiI-0.9(0.5Li_2S-0.5SiS_2)	3.99E-5						293
0.2LiI-0.8(0.6Li_2S-0.4SiS_2)	1.23E-4						293
0.3LiI-0.7(0.6Li_2S-0.4SiS_2)	3.62E-4						293
$Li_6Si_2S_7$	4.11E-4	0.37					294
0.95$Li_6Si_2S_7$-0.05$Li_6B_4O_9$	4.11E-4	0.35					294
0.9$Li_6Si_2S_7$-0.1$Li_6B_4O_9$	3.76E-4	0.39					294
0.875$Li_6Si_2S_7$-0.125$Li_6B_4O_9$	2.77E-4	0.39					294
0.75$Li_6Si_2S_7$-0.25$Li_6B_4O_9$	1.42E-4	0.40					294
0.95$Li_6Si_2S_7$-0.05$Li_6B_4S_9$	4.90E-4	0.37					294
0.925$Li_6Si_2S_7$-0.075$Li_6B_4S_9$	3.65E-4	0.38					294
0.9$Li_6Si_2S_7$-0.1$Li_6B_4S_9$	4.73E-4	0.38					294
0.875$Li_6Si_2S_7$-0.125$Li_6B_4S_9$	4.40E-4	0.37					294
0.75$Li_6Si_2S_7$-0.25$Li_6B_4S_9$	5.02E-4	0.36					294
0.63$Li_6Si_2S_7$-0.37$Li_6B_4S_9$	4.39E-4	0.39					294
$(Li_2S)_{60}(SiS_2)_{28}(P_2S_5)_{12}$	1.23E-3	0.34					295
$Li_7La_3Zr_2O_{12}$–5 wt% $LiPO_3$	2.5E-6	0.51					120

$Li_7La_3Zr_2O_{12}$–3 wt% $65Li_2O{\cdot}27B_2O_3{\cdot}8SiO_2$	1.5E-5	0.44					120
$Li_7La_3Zr_2O_{12}$–5 wt% $40.2Li_2O{\cdot}5.7Y_2O_3{\cdot}54.1SiO_2$	2.5E-5	0.39					120
$0.6Li_2S$-$0.4P_2S_5$	3.32E-6	0.52					296
$0.667Li_2S$-$0.333P_2S_5$	3.836E-5	0.44					296
$0.7Li_2S$-$0.3P_2S_5$	3.77E-5	0.45					296
$0.75Li_2S$-$0.25P_2S_5$	2.79E-4	0.40					296
$0.8Li_2S$-$0.2P_2S_5$	1.32E-4	0.44					296
($0.75Li_2S$-$0.25P_2S_5$)	2.68E-4	0.26					297
$0.95(0.75Li_2S$-$0.25P_2S_5)$-$0.05LiBH_4$	3.98E-4	0.25					297
$0.89(0.75Li_2S$-$0.25P_2S_5)$-$0.11LiBH_4$	6.18E-4	0.26					297
$0.67(0.75Li_2S$-$0.25P_2S_5)$-$0.33LiBH_4$	1.13E-3	0.21					297
$Li_7P_{2.9}S_{10.85}Mo_{0.01}$	4.8E-3	0.24					298
$Li_7P_3S_{11}$	2.6E-3	0.29					298
$Li_7P_{2.9}Mn_{0.1}S_{10.7}I_{0.3}$	5.6E-3	0.22					299
$Li_{11}AlP_2S_{12}$	8.02E-4	0.26					300
Li_3PS_4	1.78E-4	0.33					301
Li_3PS_4 – 2 wt% Al_2O_3	2.27E-4	0.35					301
Li_3PS_4 – 5 wt% Al_2O_3	1.96E-4	0.35					301
Li_3PS_4 – 8 wt% Al_2O_3	1.60E-4	0.36					301
Li_3PS_4 – 10 wt% Al_2O_3	1.50E-4	0.36					301
Li_3PS_4 – 30 wt% Al_2O_3	9.96E-5	0.36					301
Li_3PS_4 – 50 wt% Al_2O_3	9.38E-7	0.44					301

Li_3PS_4 – 70 wt% Al_2O_3	3.92E-8	0.60					301
Li_3PS_4 – 90 wt% Al_2O_3	1.54E-9	0.79					301
Li_3PS_4 – 2 wt% SiO_2	2.28E-4	0.32					301
Li_3PS_4 – 5 wt% SiO_2	1.96E-4	0.33					301
Li_3PS_4 – 8 wt% SiO_2	1.60E-4	0.33					301
Li_3PS_4 – 10 wt% SiO_2	1.50E-4	0.33					301
Li_3PS_4 – 30 wt% SiO_2	1.00E-4	0.35					301
Li_3PS_4 – 50 wt% SiO_2	3.80E-5	0.36					301
Li_3PS_4 – 70 wt% SiO_2	5.92E-6	0.38					301
Li_3PS_4 – 90 wt% SiO_2	8.53E-9	0.41					301
Li_3PS_4 – 5 wt% $Li_6ZnNb_4O_{14}$	2.28E-4	0.29					301
Li_3PS_4 – 10 wt% $Li_6ZnNb_4O_{14}$	2.43E-4	0.31					301
Li_3PS_4 – 15 wt% $Li_6ZnNb_4O_{14}$	2.41E-4	0.32					301
Li_3PS_4 – 20 wt% $Li_6ZnNb_4O_{14}$	2.22E-4	0.33					301
Li_3PS_4 – 30 wt% $Li_6ZnNb_4O_{14}$	1.87E-4	0.34					301
Li_3PS_4 – 50 wt% $Li_6ZnNb_4O_{14}$	1.42E-4	0.36					301
Li_3PS_4 – 70 wt% $Li_6ZnNb_4O_{14}$	7.23E-5	0.38					301
Li_3PS_4 – 90 wt% $Li_6ZnNb_4O_{14}$	2.99E-7	0.40					301
Li_3PS_4	1.46E-4	0.38					302
Li_3PS_4 – 10 wt% $Li_7La_3Zr_2O_{12}$	2.96E-4	0.36					302

Li_3PS_4 – 20 wt% $Li_7La_3Zr_2O_{12}$	3.70E-4	0.35					302
Li_3PS_4 – 25 wt% $Li_7La_3Zr_2O_{12}$	4.10E-4	0.35					302
Li_3PS_4 – 30 wt% $Li_7La_3Zr_2O_{12}$	5.38E-4	0.36					302
Li_3PS_4 – 35 wt% $Li_7La_3Zr_2O_{12}$	4.00E-4	0.36					302
Li_3PS_4 – 40 wt% $Li_7La_3Zr_2O_{12}$	3.33E-4	0.36					302
Li_3PS_4 – 60 wt% $Li_7La_3Zr_2O_{12}$	2.19E-4	0.40					302
Li_3PS_4 – 70 wt% $Li_7La_3Zr_2O_{12}$	1.26E-5	0.43					302
Li_3PS_4 – 90 wt% $Li_7La_3Zr_2O_{12}$	6.04E-6	0.44					302
$Li_7La_3Zr_2O_{12}$	5.20E-8	0.47					302
$Li_{3.45}Ge_{0.45}P_{0.55}S_{3.1}Se_{0.9}$	9.8E-4						303
$Li_{3.4}Ge_{0.4}P_{0.6}S_{3.2}Se_{0.8}$	1.17E-3						303
$Li_{3.35}Ge_{0.35}P_{0.65}S_{3.3}Se_{0.7}$	1.20E-3						303
$Li_{3.3}Ge_{0.3}P_{0.7}S_{3.4}Se_{0.6}$	1.33E-3						303
$Li_{3.25}Ge_{0.25}P_{0.75}S_{3.5}Se_{0.5}$	5.03E-4						303
$Li_{3.20}Ge_{0.20}P_{0.8}S_{3.6}Se_{0.4}$	1.08E-3						303
$Li_{3.15}Ge_{0.15}P_{0.85}S_{3.7}Se_{0.3}$	8.16E-4						303
$Li_{3.1}Ge_{0.1}P_{0.9}S_{3.8}Se_{0.2}$	1.13E-3						303
$Li_{3.05}Ge_{0.05}P_{0.95}S_{3.9}Se_{0.1}$	1.41E-3						303
Li_3PS_4	9.35E-4						303
$0.8Li_2O$-$0.2P_2S_5$	1.54E-5						304
$0.05Li_2S$-$0.75Li_2O$-$0.2P_2S_5$	1.39E-5						304

$0.1Li_2S$-$0.7Li_2O$-$0.2P_2S_5$	1.59E-5						304
$0.15Li_2S$-$0.65Li_2O$-$0.2P_2S_5$	2.32E-5						304
$0.2Li_2S$-$0.6Li_2O$-$0.2P_2S_5$	2.89E-5						304
$0.25Li_2S$-$0.55Li_2O$-$0.2P_2S_5$	3.80E-5						304
$0.3Li_2S$-$0.5Li_2O$-$0.2P_2S_5$	4.35E-5						304
$0.35Li_2S$-$0.45Li_2O$-$0.2P_2S_5$	5.26E-5						304
$0.4Li_2S$-$0.4Li_2O$-$0.2P_2S_5$	4.45E-5						304
$0.45Li_2S$-$0.35Li_2O$-$0.2P_2S_5$	6.35E-5						304
$0.5Li_2S$-$0.3Li_2O$-$0.2P_2S_5$	8.11E-5						304
$0.55Li_2S$-$0.25Li_2O$-$0.2P_2S_5$	1.12E-4						304
$0.6Li_2S$-$0.2Li_2O$-$0.2P_2S_5$	1.12E-4						304
$0.65Li_2S$-$0.15Li_2O$-$0.2P_2S_5$	1.13E-4						304
$0.7Li_2S$-$0.1Li_2O$-$0.2P_2S_5$	1.09E-4						304
$0.75Li_2S$-$0.05Li_2O$-$0.2P_2S_5$	1.43E-4						304
$0.8Li_2S$-$0.2P_2S_5$	2.99E-4						304
$0.75Li_2O$-$0.25P_2S_5$	1.55E-5						304
$0.05Li_2S$-$0.7Li_2O$-$0.25P_2S_5$	1.42E-5						304

$0.1Li_2S$-$0.65Li_2O$-$0.25P_2S_5$	2.52E-5						304
$0.15Li_2S$-$0.6Li_2O$-$0.25P_2S_5$	2.67E-5						304
$0.2Li_2S$-$0.55Li_2O$-$0.25P_2S_5$	2.74E-5						304
$0.25Li_2S$-$0.5Li_2O$-$0.25P_2S_5$	3.80E-5						304
$0.3Li_2S$-$0.45Li_2O$-$0.25P_2S_5$	5.88E-5						304
$0.35Li_2S$-$0.4Li_2O$-$0.25P_2S_5$	1.33E-5						304
$0.4Li_2S$-$0.35Li_2O$-$0.25P_2S_5$	2.44E-5						304
$0.45Li_2S$-$0.3Li_2O$-$0.25P_2S_5$	2.30E-5						304
$0.5Li_2S$-$0.25Li_2O$-$0.25P_2S_5$	9.56E-6						304
$0.55Li_2S$-$0.2Li_2O$-$0.25P_2S_5$	7.06E-5						304
$0.6Li_2S$-$0.15Li_2O$-$0.25P_2S_5$	9.27E-5						304
$0.65Li_2S$-$0.1Li_2O$-$0.25P_2S_5$	1.15E-4						304
$0.7Li_2S$-$0.05Li_2O$-$0.25P_2S_5$	9.76E-5						304
$0.75Li_2S$-$0.25P_2S_5$	1.60E-4						304
$0.7Li_2O$-$0.3P_2S_5$	5.78E-11						304
$0.05Li_2S$-$0.65Li_2O$-$0.3P_2S_5$	1.51E-8						304
$0.1Li_2S$-$0.6Li_2O$-$0.3P_2S_5$	7.78E-8						304

$0.15Li_2S$-$0.55Li_2O$-$0.3P_2S_5$	2.90E-7						304
$0.2Li_2S$-$0.5Li_2O$-$0.3P_2S_5$	1.67E-5						304
$0.25Li_2S$-$0.45Li_2O$-$0.3P_2S_5$	8.64E-7						304
$0.3Li_2S$-$0.4Li_2O$-$0.3P_2S_5$	1.62E-6						304
$0.35Li_2S$-$0.35Li_2O$-$0.3P_2S_5$	3.68E-6						304
$0.4Li_2S$-$0.3Li_2O$-$0.3P_2S_5$	5.86E-6						304
$0.45Li_2S$-$0.25Li_2O$-$0.3P_2S_5$	5.10E-6						304
$0.5Li_2S$-$0.2Li_2O$-$0.3P_2S_5$	8.33E-6						304
$0.55Li_2S$-$0.15Li_2O$-$0.3P_2S_5$	1.01E-5						304
$0.6Li_2S$-$0.1Li_2O$-$0.3P_2S_5$	2.29E-5						304
$0.65Li_2S$-$0.05Li_2O$-$0.3P_2S_5$	2.48E-5						304
$0.7Li_2S$- $0.3P_2S_5$	5.34E-5						304
$0.9Li_3PS_4 \cdot 10ZnO$	2.9E-4						305
$0.7Li_2S$-$0.3P_2S_5$	7.10E-4	0.23					306
$0.7Li_2S$-$0.29P_2S_5$-$0.01Li_3PO_4$	1.83E-3	0.19					306
$0.7Li_2S$-$0.28P_2S_5$-$0.02Li_3PO_4$	9.89E-4	0.21					306
$0.7Li_2S$-$0.27P_2S_5$-$0.03Li_3PO_4$	4.40E-4	0.25					306
$0.7Li_2S$-$0.25P_2S_5$-$0.05Li_3PO_4$	2.67E-4	0.29					306

$0.7Li_2S$-$0.3P_2S_5$	1.67E-3	0.23					307
$0.99(0.7Li_2S$-$0.3P_2S_5)$-$0.01Li_2ZrO_3$	2.86E-3	0.18					307
$0.98(0.7Li_2S$-$0.3P_2S_5)$-$0.02Li_2ZrO_3$	1.22E-3	0.25					307
$0.95(0.7Li_2S$-$0.3P_2S_5)$-$0.05Li_2ZrO_3$	7.42E-4	0.29					307
$Li_{2.7}PO_{3.9}$	7E-8	0.68					308
$Li_{3.6}(Si_{0.19}P_{0.82})O_{4.2}$	2.0E-7	0.57					308
$Li_{3.1}PO_{3.8}N_{0.16}$	2.00E-6	0.57					308
$Li_{3.3}PO_{3.8}N_{0.22}$	2.40E-6	0.56					308
$Li_{2.9}PO_{3.3}N_{0.46}$	3.30E-6	0.54					308
$Li_{4.4}PO_{4.3}$	9.39E-7	0.64					309
$Li_{4.0}PO_{3.9}N_{0.4}$	1.70E-6	0.62					309
$Li_{3.7}PO_{3.4}N_{0.7}$	2.36E-6	0.60					309
$Li_{3.5}PO_{3.2}N_{0.8}$	2.59E-6	0.59					309
$Li_{3.4}PO_{3.1}N_{0.9}$	2.81E-6	0.58					309
$Li_{3.2}PO_{3.0}N$	2.99E-6	0.57					309
$Li_{2.9}PO_{2.6}N_{0.91}$	2.1E-6	0.52					310
$Li_{1.8}PO_{1.2}N_{1.5}$	1.7E-6	0.49					310
$Li_{3.3}PO_{2.9}N_{0.83}$	3.1E-6	0.47					310
$0.45B_2S_3$-$0.55Li_2S$	8.19E-5	0.23					311
$0.815(0.45B_2S_3$-$0.55Li_2S)$-$0.185LiI$	3.08E-4	0.20					311
$0.69(0.45B_2S_3$-$0.55Li_2S)$-$0.31LiI$	7.58E-4	0.23					311
$0.33B_2S_3$-$0.67Li_2S$	2.26E-4	0.31					311

$0.95(0.33B_2S_3$-$0.67Li_2S)$-$0.05LiI$	4.37E-4	0.29					311
$0.9(0.33B_2S_3$-$0.67Li_2S)$-$0.1LiI$	4.81E-4	0.28					311
$0.85(0.33B_2S_3$-$0.67Li_2S)$-$0.15LiI$	4.92E-4	0.28					311
$0.75(0.33B_2S_3$-$0.67Li_2S)$-$0.25LiI$	6.10E-4	0.27					311
$0.66(0.33B_2S_3$-$0.67Li_2S)$-$0.34LiI$	5.22E-4	0.32					311
$0.6(0.33B_2S_3$-$0.67Li_2S)$-$0.4LiI$	4.89E-4	0.35					311
$0.29B_2S_3$-$0.71Li_2S$	2.71E-4	0.32					311
$0.95(0.29B_2S_3$-$0.71Li_2S)$-$0.05LiI$	3.72E-4	0.31					311
$0.875(0.29B_2S_3$-$0.71Li_2S)$-$0.125LiI$	6.27E-4	0.29					311
$0.78(0.29B_2S_3$-$0.71Li_2S)$-$0.22LiI$	6.56E-4	0.29					311
$0.64(0.29B_2S_3$-$0.71Li_2S)$-$0.36LiI$	8.10E-4	0.36					311
$0.25B_2S_3$-$0.75Li_2S$	3.03E-4	0.36					311
$0.92(0.25B_2S_3$-$0.75Li_2S)$-$0.08LiI$	3.83E-4	0.30					311
$0.89(0.25B_2S_3$-$0.75Li_2S)$-$0.11LiI$	3.48E-4	0.33					311
$0.5Li_2S$-$0.5SiS_2$	4.80E-5						312
$0.985(0.5Li_2S$-$0.5SiS_2)$-$0.015Li_3PO_4$	6.28E-5						312
$0.975(0.5Li_2S$-$0.5SiS_2)$-$0.025Li_3PO_4$	8.76E-5						312
$0.95(0.5Li_2S$-$0.5SiS_2)$-$0.05Li_3PO_4$	8.68E-5						312

$0.9(0.5Li_2S\text{-}0.5SiS_2)\text{-}0.1Li_3PO_4$	6.76E-5						312
$0.6Li_2S\text{-}0.4SiS_2$	1.85E-4						312
$0.99(0.6Li_2S\text{-}0.4SiS_2)\text{-}0.01Li_3PO_4$	2.53E-4						312
$0.97(0.6Li_2S\text{-}0.4SiS_2)\text{-}0.03Li_3PO_4$	3.97E-4						312
$0.95(0.6Li_2S\text{-}0.4SiS_2)\text{-}0.05Li_3PO_4$	2.03E-4						312
$0.9(0.6Li_2S\text{-}0.4SiS_2)\text{-}0.1Li_3PO_4$	5.20E-5						312
$0.61Li_2S\text{-}0.39SiS_2$	5.24E-4						312
$0.99(0.61Li_2S\text{-}0.39SiS_2)\text{-}0.01Li_3PO_4$	5.05E-4						312
$0.985(0.61Li_2S\text{-}0.39SiS_2)\text{-}0.015Li_3PO_4$	5.96E-4						312
$0.98(0.61Li_2S\text{-}0.39SiS_2)\text{-}0.02Li_3PO_4$	7.69E-4						312
$0.975(0.61Li_2S\text{-}0.39SiS_2)\text{-}0.025Li_3PO_4$	6.36E-4						312
$0.97(0.61Li_2S\text{-}0.39SiS_2)\text{-}0.03Li_3PO_4$	5.83E-4						312
$0.95(0.61Li_2S\text{-}0.39SiS_2)\text{-}0.05Li_3PO_4$	4.68E-4						312
$0.9(0.61Li_2S\text{-}0.39SiS_2)\text{-}0.1Li_3PO_4$	1.28E-4						312
$0.99(0.65Li_2S\text{-}0.35SiS_2)\text{-}0.01Li_3PO_4$	3.60E-4						312
$0.97(0.65Li_2S\text{-}0.35SiS_2)\text{-}0.03Li_3PO_4$	2.62E-4						312
$0.95(0.65Li_2S\text{-}0.35SiS_2)\text{-}0.05Li_3PO_4$	1.81E-4						312

$0.9(0.65Li_2S\text{-}0.35SiS_2)\text{-}0.1Li_3PO_4$	7.13E-5						312
$0.7Li_2S\text{-}0.3P_2S_5$	5.2E-3						313
LiI	3.07E-7						314
$0.998LiI\text{-}0.002CaI_2$	9.80E-7						314
$0.99LiI\text{-}0.01CaI_2$	5.54E-6	0.43					314
LiI	2.74E-8	0.43					315
$0.8LiI\text{-}0.2Al_2O_3$	6.84E-6	0.35					315
$0.7LiI\text{-}0.3Al_2O_3$	2.07E-5	0.33					315
$0.6LiI\text{-}0.4Al_2O_3$	3.94E-5	0.33					315
$0.5LiI\text{-}0.5Al_2O_3$	2.58E-5	0.33					315
$0.4LiI\text{-}0.6Al_2O_3$	6.76E-6	0.37					315
$Li_{3.5}P_{0.5}Si_{0.5}O_4$	4.27E-7	0.57					19
$Li_{3.5}P_{0.5}Ge_{0.5}O_4$	7.89E-6	0.56					19
$Li_{3.5}As_{0.5}Si_{0.5}O_4$	4.05E-6	0.55					19
$Li_{3.5}V_{0.5}Si_{0.5}O_4$	1.20E-5	0.53					19
$Li_{3.5}As_{0.5}Ge_{0.5}O_4$	2.83E-5	0.51					19
$Li_{3.5}V_{0.5}Ge_{0.5}O_4$	3.00E-5						19
$Li_{3.5}As_{0.5}Ti_{0.5}O_4$	3.22E-5	0.52					19
$Li_{3.5}As_{0.5}V_{0.5}O_4$	4.01E-5	0.49					19
$LiHf_2(PO_4)_3\text{-}0.1Li_2O$	1.12E-4						19
$LiHf_2(PO_4)_3\text{-}0.2Li_2O$	2.78E-5						19
$LiHf_2(PO_4)_3\text{-}0.3Li_2O$	2.58E-5						19
$LiHf_2(PO_4)_3\text{-}0.4Li_2O$	3.40E-5						19
$LiTi_2(PO_4)_3$	1.69E-6	0.30					316

$0.95LiTi_2(PO_4)_3$-$0.05Li_3PO_4$	5.52E-5	0.29					316
$0.9LiTi_2(PO_4)_3$-$0.1Li_3PO_4$	1.38E-4	0.28					316
$0.8LiTi_2(PO_4)_3$-$0.2Li_3PO_4$	1.93E-4	0.31					316
$0.7LiTi_2(PO_4)_3$-$0.3Li_3PO_4$	2.45E-4	0.30					316
$0.95LiTi_2(PO_4)_3$-$0.05Li_3BO_3$	3.59E-5	0.30					316
$0.9LiTi_2(PO_4)_3$-$0.1Li_3BO_3$	2.54E-4	0.30					316
$0.8LiTi_2(PO_4)_3$-$0.2Li_3BO_3$	2.97E-4	0.30					316
$0.7LiTi_2(PO_4)_3$-$0.3Li_3BO_3$	2.45E-4	0.29					316
$0.5LiTi_2(PO_4)_3$-$0.5Li_3BO_3$	2.73E-5	0.31					316
$LiTi_2(PO_4)_3$	1.00E-4						317
$LiTi_2(PO_4)_3$-$0.15LiPO_4$	6.00E-4						317
$LiTi_2(PO_4)_3$-$0.3LiPO_4$	9.92E-4						317
$LiTi_2(PO_4)_3$-$0.6LiPO_4$	1.23E-3						317
$LiTi_2(PO_4)_3$-$0.9LiPO_4$	1.10E-3						317
$LiTi_2(PO_4)_3$-$0.15LiBO_3$	4.80E-4						317
$LiTi_2(PO_4)_3$-$0.3LiBO_3$	1.66E-3						317
$LiTi_2(PO_4)_3$-$0.6LiBO_3$	1.12E-3						317
$LiTi_2(PO_4)_3$-$0.9LiBO_3$	8.91E-4						317
$LiTi_2(PO_4)_3$-$1.5LiBO_3$	6.48E-4						317
$LiTi_2(PO_4)_3$-$0.2Li_2SO_4$	8.35E-4						317
$LiTi_2(PO_4)_3$-$0.4Li_2SO_4$	1.66E-3						317

$LiTi_2(PO_4)_3$-0.6Li_2SO_4	5.67E-4						317
$LiTi_2(PO_4)_3$-0.4LiCl	6.45E-4						317
$LiTi_2(PO_4)_3$-0.8LiCl	1.28E-3						317
$LiTi_2(PO_4)_3$-1.2LiCl	1.02E-3						317
$LiTi_2(PO_4)_3$-0.4$LiNO_3$	1.18E-3						317
$LiTi_2(PO_4)_3$-0.8$LiNO_3$	1.49E-3						317
$LiTi_2(PO_4)_3$-1.2$LiNO_3$	9.95E-4						317
$Li_{0.39}La_{0.54}TiO_3$	1.08E-3	0.316					318
$(Li_{0.39}La_{0.54})_{1.006}Al_{0.006}Ti_{0.994}O_3$	1.13E-3	0.308					318
$(Li_{0.39}La_{0.54})_{1.01}Al_{0.02}Ti_{0.98}O_3$	1.58E-3	0.278					318
$(Li_{0.39}La_{0.54})_{1.03}Al_{0.06}Ti_{0.94}O_3$	1.39E-3	0.290					318
$(Li_{0.39}La_{0.54})_{1.005}Cr_{0.01}Ti_{0.99}O_3$	9.52E-4	0.300					318
$(Li_{0.39}La_{0.54})_{1.01}Cr_{0.02}Ti_{0.98}O_3$	1.01E-3	0.315					318
$(Li_{0.39}La_{0.54})_{1.025}Cr_{0.05}Ti_{0.95}O_3$	1.04E-3	0.298					318
$La_{0.51}Li_{0.34}TiO_{2.94}$	1E-3	0.38					319
$La_{0.57}Li_{0.26}TiO_{2.99}$	1E-3	0.34					319
$La_{0.6}Li_{0.16}TiO_{3.01}$	6.3E-4	0.33					319
$La_{0.64}Li_{0.067}TiO_3$	7.9E-5	0.36					319
$(La_{0.5}Li_{0.5})_{0.95}Sr_{0.05}TiO_3$	1.49E-3						319
$(La_{0.5}Li_{0.5})_{0.9}Sr_{0.1}TiO_3$	1.30E-3						319
$(La_{0.5}Li_{0.5})_{0.75}Sr_{0.25}TiO_3$	8.99E-5						319
$(La_{0.5}Li_{0.5})_{0.95}Ba_{0.05}TiO_3$	7.61E-4						319

$La_{0.63}Li_{0.1}Mg_{0.5}W_{0.5}O_3$	1.69E-6	0.39					319
$Li_{0.5}La_{0.5}TiO_3$	8.67E-4	0.28					320
$Li_{0.5}La_{0.5}Ti_{0.98}Sn_{0.02}O_3$	4.86E-4						320
$Li_{0.5}La_{0.5}Ti_{0.96}Sn_{0.04}O_3$	3.89E-4						320
$Li_{0.5}La_{0.5}Ti_{0.94}Sn_{0.06}O_3$	3.52E-4	0.294					320
$Li_{0.5}La_{0.5}Ti_{0.9}Sn_{0.1}O_3$	2.60E-4						320
$Li_{0.5}La_{0.5}Ti_{0.98}Zr_{0.02}O_3$	4.16E-4						320
$Li_{0.5}La_{0.5}Ti_{0.96}Zr_{0.04}O_3$	2.86E-4						320
$Li_{0.5}La_{0.5}Ti_{0.94}Zr_{0.06}O_3$	2.23E-4						320
$Li_{0.5}La_{0.5}Ti_{0.9}Zr_{0.1}O_3$	7.05E-5						320
$Li_{0.5}La_{0.5}Ti_{0.998}Mn_{0.002}O_3$	9.12E-4						320
$Li_{0.5}La_{0.5}Ti_{0.996}Mn_{0.004}O_3$	9.64E-4						320
$Li_{0.5}La_{0.5}Ti_{0.994}Mn_{0.006}O_3$	1.08E-3						320
$Li_{0.5}La_{0.5}Ti_{0.992}Mn_{0.008}O_3$	1.13E-3						320
$Li_{0.5}La_{0.5}Ti_{0.99}Mn_{0.01}O_3$	1.13E-3						320
$Li_{0.5}La_{0.5}Ti_{0.998}Ge_{0.002}O_3$	9.12E-4						320
$Li_{0.5}La_{0.5}Ti_{0.996}Ge_{0.004}O_3$	9.64E-4						320
$Li_{0.5}La_{0.5}Ti_{0.994}Ge_{0.006}O_3$	1.08E-3						320
$Li_{0.5}La_{0.5}Ti_{0.992}Ge_{0.008}O_3$	1.13E-3	0.265					320
$Li_{0.5}La_{0.5}Ti_{0.99}Ge_{0.01}O_3$	1.13E-3						320
$La_{0.58}Li_{0.36}Ti_{0.95}Mg_{0.05}O_3$	2.1E-4	0.29					321
$La_{0.56}Li_{0.36}Ti_{0.95}Al_{0.05}O_3$	6.4E-4	0.26					321
$La_{0.55}Li_{0.36}Ti_{0.95}Mn_{0.05}O_3$	1.9E-4	0.29					321
$La_{0.55}Li_{0.36}Ti_{0.95}Ge_{0.05}O_3$	3.6E-4	0.29					321
$La_{0.55}Li_{0.36}Ti_{0.95}Ru_{0.05}O_3$	5.2E-5	0.28					321

$La_{0.51}Li_{0.36}Ti_{0.95}W_{0.05}O_3$	7.3E-4	0.27					321
$La_{0.55}Li_{0.36}Ti_{0.9}W_{0.1}O_3$	4.4E-4	0.27					321
$La_{0.55}Li_{0.36}Ti_{0.995}Al_{0.005}O_3$	1.1E-3	0.28					321
$La_{0.55}Li_{0.36}Ti_{0.992}Al_{0.008}O_3$	6.5E-4	0.29					321
$La_{0.54}Li_{0.36}Ti_{0.995}W_{0.005}O_3$	2.6E-4	0.30					321
$La_{0.54}Li_{0.36}TiO_3$	8.9E-4	0.29					321
$La_{0.606}Li_{0.06}Ti_{0.94}Al_{0.06}O_3$	1.68E-6	0.36					322
$La_{0.566}Li_{0.1}Ti_{0.9}Al_{0.1}O_3$	7.34E-6	0.35					322
$La_{0.516}Li_{0.15}Ti_{0.85}Al_{0.15}O_3$	9.66E-6	0.36					322
$La_{0.466}Li_{0.2}Ti_{0.8}Al_{0.2}O_3$	4.28E-5	0.33					322
$La_{0.416}Li_{0.25}Ti_{0.75}Al_{0.25}O_3$	7.66E-5	0.35					322
$La_{0.366}Li_{0.3}Ti_{0.7}Al_{0.3}O_3$	1.72E-5	0.33					322
$Li_{0.12}La_{o.63}TiO_3$	2.00E-4						323
$Li_{0.18}La_{o.61}TiO_3$	4.43E-4						323
$Li_{0.24}La_{o.59}TiO_3$	9.93E-4						323
$Li_{0.3}La_{o.57}TiO_3$	1.10E-3						323
$Li_{0.39}La_{o.54}TiO_3$	1.02E-3						323
$Li_{0.45}La_{o.52}TiO_3$	9.05E-4						323
$LiZr_2(PO_4)_3$	4.77E-7						324
$Li_{1.05}Al_{0.05}Zr_{1.9}(PO_4)_3$	5.79E-7						324
$Li_{1.1}Al_{0.1}Zr_{1.8}(PO_4)_3$	6.35E-7						324
$Li_{1.2}Al_{0.2}Zr_{1.6}(PO_4)_3$	1.90E-6	0.48					324
$Li_{1.225}Al_{0.225}Zr_{1.55}(PO_4)_3$	2.13E-6	0.48					324
$Li_{1.25}Al_{0.25}Zr_{1.5}(PO_4)_3$	2.06E-6	0.48					324
$Li_{1.275}Al_{0.275}Zr_{1.45}(PO_4)_3$	3.05E-6	0.48					324

$Li_{1.3}Al_{0.3}Zr_{1.4}(PO_4)_3$	1.91E-6	0.48					324
$LiHf_2(P0_4)_3$	3.42E-6						325
$LiHfTi(P0_4)_3$	5.63E-7						325
$Li_{0.1}Zr_{1.1}Nb_{0.9}P_3O_{12}$	6E-6						325
$LiTi_2(PO_4)_3$	1.04E-7						326
$Li_{1.1}Sc_{0.1}Ti_{1.9}(PO_4)_3$	1.75E-5						326
$Li_{1.2}Sc_{0.2}Ti_{1.8}(PO_4)_3$	4.11E-5	0.34					326
$Li_{1.3}Sc_{0.3}Ti_{1.7}(PO_4)_3$	4.06E-5						326
$Li_{1.4}Sc_{0.4}Ti_{1.6}(PO_4)_3$	9.43E-6						326
$Li_{1.5}Sc_{0.5}Ti_{1.5}(PO_4)_3$	5.42E-7						326
$Li_{1.1}Y_{0.1}Ti_{1.9}(PO_4)_3$	2.94E-7						326
$Li_{1.2}Y_{0.2}Ti_{1.8}(PO_4)_3$	7.95E-7						326
$Li_{1.3}Y_{0.3}Ti_{1.7}(PO_4)_3$	1.01E-6	0.40					326
$Li_{1.4}Y_{0.4}Ti_{1.6}(PO_4)_3$	2.97E-7						326
$LiTi_2(PO_4)_3$-0.5LiF	2.318E-4	0.28					327
$LiTi_2(PO_4)_3$	7.181E-6	0.48					327
$14Li_2O$-$9Al_2O_3$-$38TiO_2$-$39P_2O_5$	1.3E-3	0.33					328
$Li_{6.6}La_3Zr_{1.6}Ta_{0.4}O_{12}$	3.13E-4	0.38					329
$Li_{6.6}La_{2.875}Y_{0.125}Zr_{1.6}Ta_{0.4}O_{12}$	3.17E-4	0.35					329
$Li_{6.6}La_{2.75}Y_{0.25}Zr_{1.6}Ta_{0.4}O_{12}$	4.36E-4	0.34					329
$Li_{6.6}La_{2.5}Y_{0.5}Zr_{1.6}Ta_{0.4}O_{12}$	2.26E-4	0.39					329
Li_2ZrS_3	7.3E-6						330
$Li_{2.2}Zn_{0.1}Zr_{0.9}S_3$	1.2E-4						330

$0.7Li_2S$-$0.3P_2S_5$	8.1E-5	0.425					[12]
Li_7PS_6	1.61E-6	0.16					[176]

II. Labels for comparing all descriptors-simplification combinations

A subset of the digitized labels was used for comparing between the different semi-supervised learning models. In total, the label subset is comprised of 155 structures. The subset is required because not all structures are compatible with all the descriptor transformations. Some descriptor-structure combinations produce coding errors, imaginary values, or infinite values. To directly compare all the descriptors, its necessary to have a common set of labels. The 155 labels that worked for all descriptors is listed in the subsequent table:

Compound	$\sigma_{25°C}$ (S cm^{-1})	E_a (eV)	Space Group	Space Group #	Other names	ICSD	Citation
$Li_4P_2O_7$	<1E-10	1.617	$P\bar{1}$	2		248414	[8]
$Li_7P_3S_{11}$	3.2E-3	0.124	$P\bar{1}$	2		157654	[5]
Li_7BiO_6	8.80E-07	0.58	$P\bar{1}$	2		155950	[3]
Li_7SbO_6	6.70E-08	0.7	$P\bar{1}$	2		413370	[3]
$Li_6CuB_4O_{10}$	1.00E-13	0.92	$P\bar{1}$	2	β-$Li_6CuB_4O_{10}$	4819	[10]
$LiAlSi_3O_8$	1.30E-10		$C\bar{1}$	2		81980	[1]
$Li_3BP_2O_8$	9.60E-12	0.62	$P\bar{1}$	2		248343	[7]
$LiSn_2(PO_4)_3$	2.04E-9		$P\bar{1}$	2		83832	[2]
$LiV(PO_4)F$	8.1E-7	0.23	$P\bar{1}$	2		183876	[6]
$Li_2NaBP_2O_8$	4.40E-18	1.21	$P\bar{1}$	2		291512	[7]
$LiMgSO_4F$	5.40E-08	0.54	$P\bar{1}$	2		281119	[9]
Li_2ZnGeO_4	1.00E-07	0.4	Pc	7		34362	[13]
Li_4SiO_4	5.00E-10	0.55	$P2_1/m$	11		238603	[17]
$Li_{3.7}P_{0.3}Si_{0.7}O_4$	3.84E-7		$P2_1/m$	11		35168	[19]
$Li_{7.22}Si_{1.5}P_{0.5}O_8$	1.64E-7	0.48	$P2_1/m$	11		238602	[16]
Li_3InCl_6	2.04E-3	0.35	C2/m	12		89617	[20]
$Li_2P_2S_6$	7.80E-11	0.48	C2/m	12		253894	[21]
$LiPO_3$	1.00E-09		P2/c	13		51630	[28]

$LiAlSi_4O_{10}$	1.01E-10		P2/c	13		194284	[1]
$LaLiO_2$	<1E-10	0.92	$P2_1/c$	14		239278	[36]
$LiBO_2$	1.00E-08	0.71	$P2_1/c$	14		200891	[34]
$LiSbO_2$	<1E-10	0.88	$P2_1/c$	14		262075	[39]
$LiYO_2$	1.80E-08	0.72	$P2_1/c$	14		45511	[33]
$LiAlCl_4$	1.00E-06	0.47	$P2_1/c$	14		35275	[32]
Li_3BO_3	7.40E-11	0.63	$P2_1/c$	14		9105	[30]
Li_2SO_4	1.40E-14	1.1	$P2_1/c$	14		2512	[29]
$Li_6Ge_2O_7$	8.50E-07	0.43	$P2_1/c$	14		31050	[31]
LiGaBr4	7.00E-6	0.54	$P2_1/c$	14		61337	[25]
$Li_4Zn(PO_4)_2$	<1E-10	1.3	$P2_1/c$	14	α-$Li_4Zn(PO_4)_2$	255464	[38]
$La(Li_{0.76}Mg_{0.08})O_2$	7.27E-10	0.66	$P2_1/c$	14		239280	[36]
$(La_{0.9}Sr_{0.1})LiO_2$	6.29E-10	0.62	$P2_1/c$	14		239279	[36]
$Li_2Sr_2Al(PO_4)_3$	<1E-10	1.02	$P2_1/c$	14		431319	[40]
$Li_{2.5}V_2(PO_4)_3$	1.9E-7		$P2_1/c$	14		240269	[37]
Li_2SnS_3	1.50E-05	0.59	C2/c	15		251656	[43]
LiVO3	2.048E-9		C2/c	15		51443	[48]
$Li_6Zr_2O_7$	5.20E-10	0.68	C2/c	15		73835	[41]
Li_3AlF_6	5.00E-07	0.54	C2/c	15		85171	[42]
$LiTa_2PO_8$	1.6E-3	0.32	C2/c	15		267438	[44]
$LiBaP_2O_7$	1.00E-10		C2/c	15		280927	[45]
$Li_3Na_5(TiS_4)_2$	8.80E-06	0.4	C2/c	15		391258	[46]
$LiGd(PO_3)_4$	<1E-10	1.7	C2/c	15		416442	[47]
$Li_{3.7}Zn_{0.7}Ga_{0.3}(PO_4)_2$	<1E-10	0.91	$P2_12_12_1$	19	β'-$Li_{3.7}Zn_{0.7}$	255466	[38]

					$Ga_{0.3}(PO_4)_2$		
Li_3SbS_4	1.5E-6	0.518	$Pmn2_1$	31		8407	[51]
Li_3PS_4	2.60E-07	0.49	$Pmn2_1$	31	γ-Li_3PS_4	180318	[52]
Li_3SbS_3	1.00E-07	0.4	$Pna2_1$	33		424834	[55]
$LiGaO_2$	2.40E-14	0.86	$Pna2_1$	33		18152	[53]
LiB_6O_9F	5.40E-24	1.38	$Pna2_1$	33		420286	[54]
$LiSi_2N_3$	6.17E-08	0.64	$Cmc2_1$	36		34118	[56]
$Li_2(PO_2N)$	<1E-10	0.57	$Cmc2_1$	36		188493	[57]
$LiGa_2GeS_6$	3.80E-08	0.47	Fdd2	43		254406	[58]
Li_5AlO_4	5.00E-10	0.99	Pmmn	59		16229	[64]
$Li_{14}Nd_5(Si_{11}N_{19}O_5)O_2F_2$	1.7E-10	0.69	Pmmn	59		262923	[65]
Li_2SiN_2	1.60E-07		Pbca	61		420126	[66]
Li_5GaO_4	5.00E-09	0.71	Pbca	61	α-Li_5GaO_4	9082	[64]
Li_3PS_4	1.60E-04	0.36	Pnma	62	β-Li_3PS_4	180319	[52]
Li_3PO_4	4.2E-18	1.24	Pnma	62	γ-Li_3PO_4	79427	[70]
Li_3PO_4	<1E-10	1.14	Pnma	62	γ-Li_3PO_4	20208	[68]
Li_4SnS_4	7.0E-5	0.29	Pnma	62		290832	[80]
Li_4SnSe_4	2E-5	0.45	Pnma	62		193768	[76]
Li_4GeS_4	2.00E-07	0.53	Pnma	62		290831	[79]
Li_4GeS_4	2E-7	0.53	Pnma	62		92200	[71]
Li_2ZnI_4	4.00E-08	0.58	Pnma	62		402062	[81]
$Li_{3.5}Ge_{0.5}V_{0.5}O_4$	1.77E-5		Pnma	62		66576	[84]
$Li_{6.6}SiPO_8$	1.48E-7	0.49	Pnma	62		238601	[16]
$Li_{3.75}Ge_{0.75}V_{0.25}O_4$	5.66E-6		Pnma	62		150918	[73]

$Li_4Zn(PO_4)_2$	<1E-10	1.1	Pnma	62	β-$Li_4Zn(PO_4)_2$	255465	[38]
$Li_{2.88}PO_{3.73}N_{0.14}$	1.4E-13	0.97	Pnma	62		79426	[70]
$Li_2Mg_2(MoO_4)_3$	<1E-10	0.71	Pnma	62		170956	[75]
$Li_{3.70}Ge_{0.85}W_{0.15}O_4$	3.80E-5		Pnma	62		150920	[73]
$Li_{14}Zn(GeO_4)_4$	1.00E-06	0.24	Pnma	62		100169	[72]
$Nd_{0.54}Li_{0.36}TiO_3$	3.42E-8	0.50	Pnma	62		81047	[86]
$Li_{6.5}O_8P_{1.5}Si_{0.5}$	4.49E-07	0.44	Pnma	62		238600	[16]
$Pr_{0.51}Li_{0.39}TiO_{2.96}$	5.34E-7	0.44	Pnma	62		81048	[86]
$LiZnSO_4F$	2.80E-05	0.2455	Pnma	62		261343	[78]
$Li_{3.5}Zn_{0.5}Ga_{0.5}(PO_4)_2$	<1E-10	1.02	Pnma	62	β-$Li_{3.5}Zn_{0.5}Ga_{0.5}(PO_4)_2$	255468	[38]
$Li_4H_8Cl_4O_4$	1E-8	0.777	Cmcm	63	$LiCl*H_2O$	281198	[88]
Li_2MgBr_4	7.80E-10	0.77	Cmmm	65		73276	[89]
$Li_{0.18}La_{0.61}TiO_3$	2.0E-4	0.432	Cmmm	65		99398	[90]
$LiBiO_2$	3.80E-08	0.1	Ibam	72		46022	[30]
$LiZnPS_4$	5.4E-8		$I\bar{4}$	82		95785	[69]
$(Li_{1.19}Zn_{0.9})PS_4$	0.65E-5	0.25	$I\bar{4}$	82		264463	[69]
$(Li_{1.69}Zn_{0.66})PS_4$	1.30E-4	0.181	$I\bar{4}$	82		264462	[69]
$(Li_{0.5}Ce_{0.5})(MoO_4)$	1.3E-8	0.4	$I4_1/a$	88		186450	[91]
$(Li_{0.5}Ce_{0.25}Sm_{0.25})(MoO_4)$	1.8E-10	0.5	$I4_1/a$	88		186452	[91]
$(Li_{0.5}Ce_{0.25}Pr_{0.25})(MoO_4)$	1E-9	0.5	$I4_1/a$	88		186451	[91]
Li_2TeO_4	<1E-10	1.129	$P4_122$	91		1485	[92]
Li_3BN_2	1.60E-10	0.67	$P4_22_12$	94	α-Li_3BN_2	655673	[93]

$Li_2B_4O_7$	1.00E-10		$I4_1cd$	110		65930	[94]
$La_{0.52}Li_{0.45}TiO_3$	5.01E-4		P4/mmm	123		50434	[97]
$Li(NdTiO_4)$	<1E-10	0.87	P4/nmmZ	129		91844	[99]
Li_4PS_4I	1.2E-4	0.37	P4/nmmZ	129		432169	[101]
$Li(LaTiO_4)$	<1E-10	0.83	P4/nmmZ	129		91843	[99]
$La_{0.62}$ $Li_{0.14}(Mg_{0.5}W_{0.5})O_3$	1.2E-5	0.37	P4/nmm	129		151902	[100]
Li_6ZnO_4	9.40E-09	0.61	$P4_2/nmc$	137		62137	[64]
$Li_{10}SnP_2S_{12}$	7E-3	0.27	$P4_2/nmc$ C	137		193755	[107]
$Li_{10}SnP_2S_{12}$	3.98E-3	0.305	$P4_2/nmc$	137		255750	[108]
$Li_{10}GePS_{12}$	1.21E-2		$P4_2/nmc$	137		188887	[104]
$Li_{10}GeP_2S_{12}$	2.46E-2	0.274	$P4_2/nmc$	137		241439	[108]
$Li_{10}GeP_2S_{12}$	1.20E-02	0.25	$P4_2/nmc$	137		255749	[110]
$Li_{10.35}Ge_{1.35}P_{1.65}S_{12}$	1.44E-2	0.269	$P4_2/nmc$ S	137		193947	[104]
$Li_{10.35}Si_{1.35}P_{1.65}S_{12}$	6.5E-3		$P4_2/nmcS$	137		252037	[109]
$Li_{9.81}Sn_{0.81}P_{2.19}S_{12}$	5.5E-3		$P4_2/nmc$	137		252040	[109]
$Li_{10.2}(Sn_{0.2}Si_{0.8})1.2P_{1.8}S_{12}$	7.82E-3		$P4_2/nmcS$	137		5667	[111]
$Li_{10.2}(Sn_{0.2}Si_{0.8})_{1.2}P_{1.8}S_{12}$	2.69E-3		$P4_2/nmcS$	137		257948	[111]
$Li_{10.5}(Sn_{0.2}Si_{0.8})_{1.5}P_{1.5}S_{12}$	8.79E-3		$P4_2/nmcS$	137		5668	[111]
$Li_{10}(Ge_{0.776}Sn_{0.224})P_2S_{12}$	1.41E-2	0.276	$P4_2/nmc$	137		255748	[108]
$LiLaNb_2O_7$	<1E-8		I4/mmm	139		72566	[114]
$Li_4Sr_3Nb_6O_{20}$	<1E-10		I4/mmm	139		87824	[115]
$Li_4Sr_{3.056}Nb_6O_{20}$	<1E-10	0.74	I4/mmm	139		109168	[115]
$Li_4Sr_3Nb_{5.77}Fe_{0.23}O_{19.77}$	<1E-10		I4/mmm	139		87823	[115]
Li_4SrN_2	2.30E-13	0.9	$I4_1/amd$	141		87413	[116]

$LiAlO_2$	1.10E-12	0.97	$I4_1/amd$	141	r-$LiAlO_2$	99517	[33]
$LiScO_2$	<1E-10	1.047	$I4_1/amd$	141		257819	[117]
$LiScO_2$	1.00E-12	0.87	$I4_1/amd$	141		36124	[33]
$Li_{0.9}Sc_{0.9}Zr_{0.1}O_2$	<1E-10	0.912	$I4_1/amd$	141		257820	[117]
$Li_7La_3Zr_2O_{12}$	1.63E-6	0.54	$I4_1/acdZ$	142	“tetragonol-LLZO”	183684	[119]
$LiAlGeO_4$	<1E-10	0.97	R3H	146		257741	[123]
$LiGaSiO_4$	3.00E-16	0.9	R3H	146		65125	[122]
$LiGa_{0.5}Al_{0.5}GeO_4$	<1E-10	1.06	R3H	146		257740	[123]
$LiNaSO_4$	8.80E-10		P31c	159		14364	[125]
Li_5NCl_2	1.20E-06	0.5	$R\bar{3}m$	166		84763	[131]
$LiGe_2(PO_4)_3$	4.83E-9	0.654	$R\bar{3}cH$	167		69763	[133]
$LiZr_2(PO_4)_3$	2.96E-10		$R\bar{3}cH$	167		201935	[2]
$LiTi_2(PO_4)_3$	7.61E-6	0.38	$R\bar{3}cH$	167		95979	[132]
$LiGe_2(PO_4)_3$	3.33E-7		$R\bar{3}cH$	167		263767	[2]
$Li_{1.3}(Al_{0.23}Y_{0.07}Ti_{1.7})(PO_4)_3$	3.84E-8		$R\bar{3}cH$	167		253243	[138]
$Li_9Mg_3(PO_4)_4F_3$	<1E-10	0.835	$P6_3$	173		426103	[148]
$LiLa_9Si_6O_{26}$	<1E-10		$P6_3/m$	176		291218	[150]
$Li_{0.284}Sm_{4.512}Si_3O_{12.91}$	<1E-10		$P6_3/m$	176		83279	[150]
$Pb_{6.12}Ca_{1.9}Li_{1.96}(PO_4)_6$	<1E-10	1.05	$P6_3/m$	176		59615	[149]
$Li_5La_3Nb_2O_{12}$	8E-6	0.43	$I2_13$	199		54865	[159]
$(K_{0.1}Li_{0.9})(SbO_3)$	1.36E-8		$Pn\bar{3}Z$	201		200984	[160]
$Li_2CoTi_3O_8$	<1E-10	1.33	$P4_332$	212		86166	[163]
$Li_2ZnGe_3O_8$	<1E-10	2.14	$P4_332$	212		86169	[163]
$Li_2MgTi_3O_8$	<1E-10	0.71	$P4_332$	212		86165	[163]

$(Li_{0.55}Mg_{0.45})(Li_{0.445}Mg_{0.055})Ti_{1.5}O_4$	1.53E-11	0.786	$P4_332$	212		168145	[164]
$(Li_{0.61}Mg_{0.39})(Li_{0.46}Mg_{0.005}Ti_{0.035})Ti_{1.5}O_4$	6.56E-10	0.685	$P4_332$	212		168144	[164]
Li_2VCl_4	6.95E-6		$F\bar{4}3m$	216		74959	[166]
Li_5NI_2	4.00E-6		$F\bar{4}3m$	216		16800	[165]
Li_6PO_5Cl	5.54E-10	0.66	$F\bar{4}3m$	216		421479	[173]
Li_7PN_4	1.60E-07	0.4	$P\bar{4}3n$	218		69017	[95]
Li_9NS_3	8.30E-07	0.52	$Pm\bar{3}m$	221		240749	[185]
Li_3OBr	1.10E-06	0.74	$Pm\bar{3}m$	221		67265	[194,195]
$Li_2(OH)Br$	1.20E-6	0.75	$Pm\bar{3}m$	221		200874	[184]
LiI	1E-7		$Fm\bar{3}m$	225		414244	[197]
$Li_{7.2}N_{1.6}Cl_{2.4}$	8.4E-7	0.49	$Fm\bar{3}m$	225		49646	[131]
$Li_{0.19}La_{0.67}(Ti_{0.9}Co_{0.1})O_3$	1.08E-4		$Fm\bar{3}m$	225		151535	[182]
$LiCdCl_4$	5.80E-07	0.44	$Fd\bar{3}m$	227		74958	[199]
Li_2MnCl_4	4.79E-6		$Fd\bar{3}m$	227		69678	[166]
Li_2MgCl_4	6.24E-7		$Fd\bar{3}m$	227		74957	[166]
$LiSrTa_2O_6F$	<1E-10	0.604	$Fd\bar{3}m$	227		236010	[200]
$Li_{1.9}Mn_{0.9}Ga_{0.1}Cl_4$	2.37E-7		$Fd\bar{3}m$	227		50305	[198]
$Li(Li_{0.34}Ti_{1.66})O_4$	6.03E-8	0.506	$Fd\bar{3}m$	227		168137	[164]
$(Li_{0.74}Mg_{0.26})(Li_{0.40}Mg_{0.04}Ti_{1.56})O_4$	1.51E-9	0.639	$Fd\bar{3}m$	227		168142	[164]
$(Li_{0.826}Mg_{0.174})(Li_{0.374}Mg_{0.026}Ti_{1.60})O_4$	4.24E-9	0.615	$Fd\bar{3}m$	227		168141	[164]

III. Labels used for the final SOAP model

Once the best-performing descriptor-simplification is identified, an expanded set of labels can be employed. The mathematical transformation for the SOAP descriptor is compatible with most of the ~26,000 structures. In addition to the 155 labels used for descriptor comparisons, 64 labels were added. The full list of labels is included in the table below:

Compound	$\sigma_{25°C}$ (S cm^{-1})	E_a (eV)	Space Group	Space Group #	Other names	ICSD	Citation
$Li_4P_2O_7$	<1E-10	1.617	$P\bar{1}$	2		248414	[8]
$Li_7P_3S_{11}$	3.2E-3	0.124	$P\bar{1}$	2		157654	[5]
Li_7BiO_6	8.80E-07	0.58	$P\bar{1}$	2		155950	[3]
Li_7SbO_6	6.70E-08	0.7	$P\bar{1}$	2		413370	[3]
$Li_6CuB_4O_{10}$	1.00E-13	0.92	$P\bar{1}$	2	β-$Li_6CuB_4O_{10}$	4819	[10]
$LiAlSi_3O_8$	1.30E-10		$C\bar{1}$	2		81980	[1]
$Li_3BP_2O_8$	9.60E-12	0.62	$P\bar{1}$	2		248343	[7]
$LiSn_2(PO_4)_3$	2.04E-9		$P\bar{1}$	2		83832	[2]
$LiV(PO_4)F$	8.1E-7	0.23	$P\bar{1}$	2		183876	[6]
$LiMgSO_4F$	5.40E-08	0.54	$P\bar{1}$	2		281119	[9]
$Li_2NaBP_2O_8$	4.40E-18	1.21	$P\bar{1}$	2		291512	[7]
Li_2ZnGeO_4	1.00E-07	0.4	Pc	7		34362	[13]
Li_4SiO_4	5.00E-10	0.55	$P2_1/m$	11		238603	[17]
Li_4SiS_4	5.00E-08	0.56	$P2_1/m$	11		59708	[15]
$Li_{3.7}P_{0.3}Si_{0.7}O_4$	3.84E-7		$P2_1/m$	11		35168	[19]
$Li_{7.22}Si_{1.5}P_{0.5}O_8$	1.64E-7	0.48	$P2_1/m$	11		238602	[16]
$Li_2P_2S_6$	7.80E-11	0.48	C2/m	12		253894	[21]
Li_3InCl_6	2.04E-3	0.35	C2/m	12		89617	[20]
$Li_{17}Sb_{13}S_{28}$	1.05E-9	0.4	C2/m	12		429902	[24]

$LiPO_3$	1.00E-09		P2/c	13		51630	[28]
$LiAlSi_4O_{10}$	1.01E-10		P2/c	13		194284	[1]
$LaLiO_2$	<1E-10	0.92	$P2_1/c$	14		239278	[36]
$LiBO_2$	1.00E-08	0.71	$P2_1/c$	14		200891	[34]
$LiSbO_2$	<1E-10	0.88	$P2_1/c$	14		262075	[39]
$LiYO_2$	1.80E-08	0.72	$P2_1/c$	14		45511	[33]
Li_3BO_3	7.40E-11	0.63	$P2_1/c$	14		9105	[30]
Li_2SO_4	1.40E-14	1.1	$P2_1/c$	14		2512	[29]
LiGaBr4	7.00E-6	0.54	$P2_1/c$	14		61337	[25]
$LiAlCl_4$	1.00E-06	0.47	$P2_1/c$	14		35275	[32]
$Li_6Ge_2O_7$	8.50E-07	0.43	$P2_1/c$	14		31050	[31]
$Li_4Zn(PO_4)_2$	<1E-10	1.3	$P2_1/c$	14	α-$Li_4Zn(PO_4)_2$	255464	[38]
$Li_{2.5}V_2(PO_4)_3$	1.9E-7		$P2_1/c$	14		240269	[37]
$La(Li_{0.76}Mg_{0.08})O_2$	7.27E-10	0.66	$P2_1/c$	14		239280	[36]
$(La_{0.9}Sr_{0.1})LiO_2$	6.29E-10	0.62	$P2_1/c$	14		239279	[36]
$Li_2Sr_2Al(PO_4)_3$	<1E-10	1.02	$P2_1/c$	14		431319	[40]
$LiClC_3H_7NO$	1.6E-4	0.881	$P2_1/c$	14		238683	[35]
Li_2CrCl_4	<1E-10	1.22	C2/c	15		202627	[49]
Li_2ZrO_3	6.10E-10	0.78	C2/c	15		94894	[33]
$Li_6Zr_2O_7$	5.20E-10	0.68	C2/c	15		73835	[41]
Li_3AlF_6	5.00E-07	0.54	C2/c	15		85171	[42]
Li_2SnS_3	1.50E-05	0.59	C2/c	15		251656	[43]
LiVO3	2.048E-9		C2/c	15		51443	[48]
$LiTa_2PO_8$	1.6E-3	0.32	C2/c	15		267438	[44]

$LiBaP_2O_7$	1.00E-10		C2/c	15		280927	[45]
$LiGd(PO_3)_4$	<1E-10	1.7	C2/c	15		416442	[47]
$Li_3Na_5(TiS_4)_2$	8.80E-06	0.4	C2/c	15		391258	[46]
$Li_{3.7}Zn_{0.7}Ga_{0.3}(PO_4)_2$	<1E-10	0.91	$P2_12_12_1$	19	β'-$Li_{3.7}Zn_{0.7}Ga_{0.3}(PO_4)_2$	255466	[38]
Li_3SbS_4	1.5E-6	0.518	$Pmn2_1$	31		8407	[51]
Li_3PS_4	2.60E-07	0.49	$Pmn2_1$	31	γ-Li_3PS_4	180318	[52]
Li_3SbS_3	1.00E-07	0.4	$Pna2_1$	33		424834	[55]
$LiGaO_2$	2.40E-14	0.86	$Pna2_1$	33		18152	[53]
LiB_6O_9F	5.40E-24	1.38	$Pna2_1$	33		420286	[54]
$LiSi_2N_3$	6.17E-08	0.64	$Cmc2_1$	36		34118	[56]
$Li_2(PO_2N)$	<1E-10	0.57	$Cmc2_1$	36		188493	[57]
$LiGa_2GeS_6$	3.80E-08	0.47	Fdd2	43		254406	[58]
$La_{0.595}Li_{0.215}TiO_3$	8.53E-4		Pmmm	47		92234	[59]
$La_{0.62}Li_{0.14}TiO_3$	4.42E-4		Pmmm	47		92231	[59]
$La_{0.64}Li_{0.08}TiO_3$	3.35E-4		Pmmm	47		92228	[59]
$Li_{0.02}Na_{0.48}La_{0.5}Nb_2O_6$	3.99E-6		Pmmm	47		180635	[60]
$Li_{0.04}Na_{0.46}La_{0.5}Nb_2O_6$	5.91E-6		Pmmm	47		180634	[60]
$Li_{0.07}Na_{0.43}La_{0.5}Nb_2O_6$	1.23E-5		Pmmm	47		180633	[60]
$Li_{0.1}Na_{0.4}La_{0.5}Nb_2O_6$	1.21E-5		Pmmm	47		180632	[60]
$Li_{0.2}Na_{0.3}La_{0.5}Nb_2O_6$	1.18E-5		Pmmm	47		180631	[60]
$Li_{0.3}Na_{0.2}La_{0.5}Nb_2O_6$	1.11E-5		Pmmm	47		180630	[60]
$Li_{0.4}Na_{0.1}La_{0.5}Nb_2O_6$	9.92E-6		Pmmm	47		180629	[60]
Li_5AlO_4	5.00E-10	0.99	Pmmn	59		16229	[64]
$Li_{14}Nd_5(Si_{11}N_{19}O_5)O_2F_2$	1.7E-10	0.69	Pmmn	59		262923	[65]

Li_2SiN_2	1.60E-07		Pbca	61		420126	[66]
Li_5GaO_4	5.00E-09	0.71	Pbca	61	α-Li_5GaO_4	9082	[64]
Li_3PO_4	4.2E-18	1.24	Pnma	62	γ-Li_3PO_4	79427	[70]
Li_3PO_4	<1E-10	1.14	Pnma	62	γ-Li_3PO_4	20208	[68]
Li_3PS_4	1.60E-04	0.36	Pnma	62	β-Li_3PS_4	180319	[52]
Li_4SnS_4	7.0E-5	0.29	Pnma	62		290832	[80]
Li_4SnSe_4	2E-5	0.45	Pnma	62		193768	[76]
Li_4GeS_4	2.00E-07	0.53	Pnma	62		290831	[79]
Li_4GeS_4	2E-7	0.53	Pnma	62		92200	[71]
$Li(BH_4)$	1E-8		Pnma	62		239763	[77]
Li_2ZnI_4	4.00E-08	0.58	Pnma	62		402062	[81]
$Li_4Zn(PO_4)_2$	<1E-10	1.1	Pnma	62	β-$Li_4Zn(PO_4)_2$	255465	[38]
$Li_2Mg_2(MoO_4)_3$	<1E-10	0.71	Pnma	62		170956	[75]
$Li_{0.2}Ca_{0.4}TaO_3$	3.53E-9	0.54	Pnma	62		151936	[74]
$Li_{3.5}Ge_{0.5}V_{0.5}O_4$	1.77E-5		Pnma	62		66576	[84]
$Li_{3.75}Ge_{0.75}V_{0.25}O_4$	5.66E-6		Pnma	62		150918	[73]
$Li_{14}Zn(GeO_4)_4$	1.00E-06	0.24	Pnma	62		100169	[72]
$Li_{3.70}Ge_{0.85}W_{0.15}O_4$	3.80E-5		Pnma	62		150920	[73]
$Li_{6.6}SiPO_8$	1.48E-7	0.49	Pnma	62		238601	[16]
$Li_{2.88}PO_{3.73}N_{0.14}$	1.4E-13	0.97	Pnma	62		79426	[70]
$Li_{6.5}O_8P_{1.5}Si_{0.5}$	4.49E-07	0.44	Pnma	62		238600	[16]
$Nd_{0.54}Li_{0.36}TiO_3$	3.42E-8	0.50	Pnma	62		81047	[86]
$Pr_{0.51}Li_{0.39}TiO_{2.96}$	5.34E-7	0.44	Pnma	62		81048	[86]

$LiZnSO_4F$	2.80E-05	0.2455	Pnma	62		261343	[78]
$Li_{3.5}Zn_{0.5}Ga_{0.5}(PO_4)_2$	<1E-10	1.02	Pnma	62	β-$Li_{3.5}Zn_{0.5}Ga_{0.5}(PO_4)_2$	255468	[38]
$Li_{0.2}(Ca_{0.36}Sr_{0.04})TaO_3$	9.2E-9		Pnma	62		151937	[74]
Li_4GeO_4	2.80E-10	0.73	Cmcm	63		18096	[87]
$Li_4H_8Cl_4O_4$	1E-8	0.777	Cmcm	63	$LiCl*H_2O$	281198	[88]
Li_2MgBr_4	7.80E-10	0.77	Cmmm	65		73276	[89]
$Li_{0.18}La_{0.61}TiO_3$	2.0E-4	0.432	Cmmm	65		99398	[90]
$LiBiO_2$	3.80E-08	0.1	Ibam	72		46022	[30]
$LiZnPS_4$	5.4E-8		$I\bar{4}$	82		95785	[69]
$(Li_{1.19}Zn_{0.9})PS_4$	0.65E-5	0.25	$I\bar{4}$	82		264463	[69]
$(Li_{1.69}Zn_{0.66})PS_4$	1.30E-4	0.181	$I\bar{4}$	82		264462	[69]
$(Li_{0.5}Ce_{0.5})(MoO_4)$	1.3E-8	0.4	$I4_1/a$	88		186450	[91]
$(Li_{0.5}Ce_{0.25}Sm_{0.25})(MoO_4)$	1.8E-10	0.5	$I4_1/a$	88		186452	[91]
$(Li_{0.5}Ce_{0.25}Pr_{0.25})(MoO_4)$	1E-9	0.5	$I4_1/a$	88		186451	[91]
Li_2TeO_4	<1E-10	1.129	$P4_122$	91		1485	[92]
Li_3BN_2	1.60E-10	0.67	$P4_22_12$	94	α-Li_3BN_2	655673	[93]
$Li_2B_4O_7$	1.00E-10		$I4_1cd$	110		65930	[94]
$LiY(BH_4)_4$	1.26E-6		$P\bar{4}2c$	112		239762	[77]
$LiPN_2$	1.6E-7	0.40	$I\bar{4}2d$	122		66007	[95]
$Li_{0.33}La_{0.5}TiO_3$	1E-3	0.15	P4/mmm	123		82671	[96]
$La_{0.5}Li_{0.5}TiO_3$	9.25E-4	0.39	P4/mmm	123		92236	[59]
$La_{0.52}Li_{0.45}TiO_3$	5.01E-4		P4/mmm	123		50434	[97]
$La_{0.565}Li_{0.305}TiO_3$	9.57E-4		P4/mmm	123		92235	[59]

$La_{0.58}Li_{0.27}TiO3$	5.99E-4		P4/mmm	123		82672	[97]
Li_4PS_4I	1.2E-4	0.37	P4/nmmZ	129		432169	[101]
$Li(LaTiO_4)$	<1E-10	0.83	P4/nmmZ	129		91843	[99]
$Li(NdTiO_4)$	<1E-10	0.87	P4/nmmZ	129		91844	[99]
$La_{0.62}$ $Li_{0.14}(Mg_{0.5}W_{0.5})O_3$	1.2E-5	0.37	P4/nmm	129		151902	[100]
$La_{0.63}Li_{0.11}(Mg_{0.5}W_{0.5})O_3$	6.8E-6	0.38	P4/nmm	129		151901	[100]
$La_{0.65}Li_{0.05}(Mg_{0.5}W_{0.5})O_3$	1.8E-7	0.46	P4/nmm	129		151900	[100]
Li_6ZnO_4	9.40E-09	0.61	$P4_2/nmc$	137		62137	[64]
$Li_{10}SnP_2S_{12}$	3.98E-3	0.305	$P4_2/nmc$	137		255750	[108]
$Li_{10}SnP_2S_{12}$	7E-3	0.27	$P4_2/nmc$ C	137		193755	[107]
$Li_{10}GePS_{12}$	1.21E-2		$P4_2/nmc$	137		188887	[104]
$Li_{10}GeP_2S_{12}$	1.20E-02	0.25	$P4_2/nmc$	137		255749	[110]
$Li_{10}GeP_2S_{12}$	2.46E-2	0.274	$P4_2/nmc$	137		241439	[108]
$Li_{10.35}Ge_{1.35}P_{1.65}S_{12}$	1.44E-2	0.269	$P4_2/nmc$ S	137		193947	[104]
$Li_{10.35}Si_{1.35}P_{1.65}S_{12}$	6.5E-3		$P4_2/nmcS$	137		252037	[109]
$Li_{9.81}Sn_{0.81}P_{2.19}S_{12}$	5.5E-3		$P4_2/nmc$	137		252040	[109]
$Li_{10}(Ge_{0.776}Sn_{0.224})P_2S_{12}$	1.41E-2	0.276	$P4_2/nmc$	137		255748	[108]
$Li_{10.2}(Sn_{0.2}Si_{0.8})1.2P_{1.8}S_{12}$	7.82E-3		$P4_2/nmcS$	137		5667	[111]
$Li_{10.2}(Sn_{0.2}Si_{0.8})_{1.2}P_{1.8}S_{12}$	2.69E-3		$P4_2/nmcS$	137		257948	[111]
$Li_{10.5}(Sn_{0.2}Si_{0.8})_{1.5}P_{1.5}S_{12}$	8.79E-3		$P4_2/nmcS$	137		5668	[111]
$LiLaNb_2O_7$	<1E-8		I4/mmm	139		72566	[114]
$Li_4Sr_3Nb_6O_{20}$	<1E-10		I4/mmm	139		87824	[115]
$Li_4Sr_{3.056}Nb_6O_{20}$	<1E-10	0.74	I4/mmm	139		109168	[115]
$Li_4Sr_3Nb_{5.77}Fe_{0.23}O_{19.77}$	<1E-10		I4/mmm	139		87823	[115]

Li_3BN_2	8.70E-08	0.55	$I4_1/amd$	141	β-Li_3BN_2	155126	[93]
$LiScO_2$	<1E-10	1.047	$I4_1/amd$	141		257819	[117]
$LiScO_2$	1.00E-12	0.87	$I4_1/amd$	141		36124	[33]
Li_4SrN_2	2.30E-13	0.9	$I4_1/amd$	141		87413	[116]
$LiAlO_2$	1.10E-12	0.97	$I4_1/amd$	141	r-$LiAlO_2$	99517	[33]
$Li_{0.9}Sc_{0.9}Zr_{0.1}O_2$	<1E-10	0.912	$I4_1/amd$	141		257820	[117]
$Li_7La_3Zr_2O_{12}$	1.63E-6	0.54	$I4_1/acdZ$	142	“tetragonol-LLZO”	183684	[119]
$Li_7La_3Zr_2O_{12}$	9.9E-6	0.43	$I4_1/acdZ$	142		238687	[121]
$Li_7La_3HfO_{12}$	9.85E-7	0.53	$I4_1/acdZ$	142	“tetragonal-LLHO”	174202	[118]
$LiAlGeO_4$	<1E-10	0.97	R3H	146		257741	[123]
$LiGaSiO_4$	3.00E-16	0.9	R3H	146		65125	[122]
$LiGa_{0.5}Al_{0.5}GeO_4$	<1E-10	1.06	R3H	146		257740	[123]
$LiGaGeO_4$	<1E-10	1.12	$R\bar{3}$	148		257739	[123]
$LiNaSO_4$	8.80E-10		P31c	159		14364	[125]
$Li_4P_2S_6$	2.38E-07	0.29	$P\bar{3}1m$	162		242170	[127]
$Li_{2.667}Mg_{0.667}P_2S_6$	4.00E-06	0.46	$P\bar{3}1m$	162		95607	[126]
$Li_{3.333}Mg_{0.333}P_2S_6$	8.20E-8	0.517	$P\bar{3}1m$	162		95606	[126]
Li_3ErCl_6	3.3E-4	0.41	$P\bar{3}m1$	164		50151	[129]
Li_5NCl_2	1.20E-06	0.5	$R\bar{3}m$	166		84763	[131]
$LiGe_2(PO_4)_3$	3.33E-7		$R\bar{3}cH$	167		263767	[2]
$LiGe_2(PO_4)_3$	4.83E-9	0.654	$R\bar{3}cH$	167		69763	[133]
$LiZr_2(PO_4)_3$	2.96E-10		$R\bar{3}cH$	167		201935	[2]
$LiTi_2(PO_4)_3$	7.61E-6	0.38	$R\bar{3}cH$	167		95979	[132]

$Li(Ti_{0.4}Sn_{1.6})(PO_4)_3$	3.15E-6		$R\bar{3}cH$	167		183677	[135]
$Li(Ti_{0.6}Sn_{1.4})(PO_4)_3$	9.42E-6		$R\bar{3}cH$	167		183676	[135]
$Li(Ti_{1.4}Sn_{0.6})(PO_4)_3$	2.28E-5	0.32	$R\bar{3}cH$	167		183672	[135]
$Li_{1.3}Al_{0.3}Ti_{1.7}(PO_4)_3$	7E-4		$R\bar{3}cH$	167		257190	[139]
$Li_{1.3}(Al_{0.3}Ti_{1.7})(PO_4)_3$	8.02E-7		$R\bar{3}cH$	167		253240	[138]
$Li_{1.2}Al_{0.2}Ge_{1.8}(PO_4)_3$	4.83E-5	0.387	$R\bar{3}cH$	167		263760	[133]
$Li_{1.3}(Al_{0.23}Y_{0.07}Ti_{1.7})(PO_4)_3$	3.84E-8		$R\bar{3}cH$	167		253243	[138]
$Li_{1.3}(Al_{0.23}Sc_{0.07}Ti_{1.7})(PO_4)_3$	1.94E-7		$R\bar{3}cH$	167		253242	[138]
$Li_{1.3}(Al_{0.23}Ga_{0.07}Ti_{1.7})(PO_4)_3$	4.46E-6		$R\bar{3}cH$	167		253241	[138]
$LiIO_3$	1.90E-07		$P6_3$	173		35473	[147]
$Li_9Mg_3(PO_4)_4F_3$	<1E-10	0.835	$P6_3$	173		426103	[148]
$LiEu_9Si_6O_{26}$	<1E-10		$P6_3/m$	176		291220	[150]
$LiLa_9Si_6O_{26}$	<1E-10		$P6_3/m$	176		291218	[150]
$Li_{0.284}Sm_{4.512}Si_3O_{12.91}$	<1E-10		$P6_3/m$	176		83279	[150]
$Pb_{6.12}Ca_{1.9}Li_{1.96}(PO_4)_6$	<1E-10	1.05	$P6_3/m$	176		59615	[149]
$Li_3(NH_2)_2I$	1E-5	0.58	$P6_3mc$	186		167528	[152]
$Ba_3LiTa_5ZrSi_4O_{26}$	<1E-10	0.79	$P\bar{6}2m$	189		239277	[153]
Li_3N	1.2E-3	0.25	P6/mmm	191		26540	[154]
Li_3N	3.00E-04	0.26	P6/mmm	191		156894	[155]
$Fe_2Na_2K(Li_3Si_{12}O_{30})$	<1E-10	1.22	P6/mcc	192		235750	[156]
Li_3P	7.03E-4	0.18	$P6_3/mmc$	194		642223	[157]
$Li_5La_3Nb_2O_{12}$	8E-6	0.43	$I2_13$	199		54865	[159]
$(K_{0.1}Li_{0.9})(SbO_3)$	1.36E-8		$Pn\bar{3}Z$	201		200984	[160]
Li_8SiP_4	4.5E-5	0.404	$Pa\bar{3}$	205		235186	[161]

Li_8GeP_4	1.8E-5	0.435	$Pa\bar{3}$	205	α-Li_8GeP_4	235184	[161]
Li_3AlN_2	5.00E-08	0.45	$Ia\bar{3}$	206		257464	[162]
$Li_2ZnGe_3O_8$	<1E-10	2.14	$P4_332$	212		86169	[163]
$Li_2MgTi_3O_8$	<1E-10	0.71	$P4_332$	212		86165	[163]
$Li_2CoTi_3O_8$	<1E-10	1.33	$P4_332$	212		86166	[163]
$(Li_{0.55}Mg_{0.45})(Li_{0.445}Mg_{0.055})Ti_{1.5}O_4$	1.53E-11	0.786	$P4_332$	212		168145	[164]
$(Li_{0.61}Mg_{0.39})(Li_{0.46}Mg_{0.005}Ti_{0.035})Ti_{1.5}O_4$	6.56E-10	0.685	$P4_332$	212		168144	[164]
Li_2VCl_4	6.95E-6		$F\bar{4}3m$	216		74959	[166]
Li_5NI_2	4.00E-6		$F\bar{4}3m$	216		16800	[165]
Li_6PO_5Cl	5.54E-10	0.66	$F\bar{4}3m$	216		421479	[173]
$LiCe(BH_4)_3Cl$	1.03E-4		$I\bar{4}3m$	217		185218	[178]
Li_7PN_4	1.60E-07	0.4	$P\bar{4}3n$	218		69017	[95]
$Li_4B_7O_{12}Cl$	2.4E-5		$F\bar{4}3c$	219		1125	[179]
Li_9NS_3	8.30E-07	0.52	$Pm\bar{3}m$	221		240749	[185]
Li_3OBr	1.10E-06	0.74	$Pm\bar{3}m$	221		67265	[194,195]
$Li_2(OH)Br$	1.20E-6	0.75	$Pm\bar{3}m$	221		200874	[184]
$(La_{0.55}Li_{0.45})(Ti_{0.9}Al_{0.1})O_3$	1.51E-3		$Pm\bar{3}m$	221		254045	[186]
$(La_{0.6}Li_{0.4})(Ti_{0.8}Al_{0.2})O_3$	5.68E-4		$Pm\bar{3}m$	221		254046	[186]
$(La_{0.65}Li_{0.35})(Ti_{0.7}Al_{0.3})O_3$	1.61E-4		$Pm\bar{3}m$	221		254047	[186]
$(La_{0.402}Li_{0.368}Sr_{0.230})(TiO_3)$	2.87E-5	0.36	$Pm\bar{3}m$	221		190827	[183]
$(La_{0.46}Li_{0.429}Sr_{0.111})(TiO_3)$	1.97E-4	0.33	$Pm\bar{3}m$	221		190826	[183]
$(La_{0.49}Li_{0.461}Sr_{0.049})(TiO_3)$	7.09E-4	0.33	$Pm\bar{3}m$	221		190825	[183]

$(Li_{0.16}Sr_{0.69})(Ga_{0.25}Ta_{0.75})O_3$	3.69E-6	0.359	$Pm\bar{3}m$	221		291520	[187]
$Li_{0.31}La_{0.63}((Ti_{0.9}Co_{0.1})O_3$	2.60E-4		$Pm\bar{3}m$	221		151533	[182]
LiI	1E-7		$Fm\bar{3}m$	225		414244	[197]
$Li_{7.2}N_{1.6}Cl_{2.4}$	8.4E-7	0.49	$Fm\bar{3}m$	225		49646	[131]
$Li_{0.19}La_{0.67}(Ti_{0.9}Co_{0.1})O_3$	1.08E-4		$Fm\bar{3}m$	225		151535	[182]
$LiCdCl_4$	5.80E-07	0.44	$Fd\bar{3}m$	227		74958	[199]
Li_2MgCl_4	6.24E-7		$Fd\bar{3}m$	227		74957	[166]
Li_2MnCl_4	4.79E-6		$Fd\bar{3}m$	227		69678	[166]
$Li(Li_{0.34}Ti_{1.66})O_4$	6.03E-8	0.506	$Fd\bar{3}m$	227		168137	[164]
$Li_{1.9}Mn_{0.9}Ga_{0.1}Cl_4$	2.37E-7		$Fd\bar{3}m$	227		50305	[198]
$(Li_{0.74}Mg_{0.26})(Li_{0.40}Mg_{0.04}Ti_{1.56})O_4$	1.51E-9	0.639	$Fd\bar{3}m$	227		168142	[164]
$(Li_{0.826}Mg_{0.174})(Li_{0.374}Mg_{0.026}Ti_{1.60})O_4$	4.24E-9	0.615	$Fd\bar{3}m$	227		168141	[164]
$LiSrTa_2O_6F$	<1E-10	0.604	$Fd\bar{3}m$	227		236010	[200]

IV. W_σ optimization

Ward's minimum variance method applied to the conductivity labels (W_σ) is used to assess the utility of each descriptor-simplification combination. The W_σ is calculated after agglomerative clustering, for each clustering set:

$$W_\sigma = \sum_{k=1}^{n_C} \sum_{i \in C_k} \left[\log(\sigma_{RT})_i - \overline{\log(\sigma_{RT})_k}\right]^2$$

where n_C is the number of clusters in a set, C_k is cluster k, and where $\overline{\log(\sigma_{RT})_k}$ denotes the mean for all labels in cluster k. Lower W_σ values indicate that the descriptor-simplification combination results in clustering where structures with similar conductivity are grouped together. Whereas a large W_σ indicates that the clusters have little correlation to the conductivity labels.

A frozen-state strategy is employed to prevent any label from dropping out of the W_σ calculation. The frozen-state strategy operates by calculating the partial variance (PV) for each label at each clustering depth:

$$PV_{x,C_k} = \left[\log(\sigma_{RT})_x - \overline{\log(\sigma_{RT})_k}\right]^2$$

where PV_{x,C_k} is the partial variance for label x, when label x is assigned to cluster k. The PV for each label is saved before summing all the partial variances to yield the W_σ. At each subsequent clustering depth, all new clusters are checked to determine whether any cluster contains a single label. If a label is the only label in a cluster, then that label's partial variance is frozen: its PV_{x,C_k} becomes equal to the saved state from the previous cluster depth:

$$PV_{x,C_j} = PV_{x,C_k}$$

where C_j denotes the cluster with only one label and C_k denotes the cluster that label x previously resided in. Without the frozen state strategy, poor models will reach desirable W_σ values at sufficient depths of clustering. The artificial depression of the W_σ value occurs because clusters that contain a single label evaluate to 0 (the label mean and cluster mean are the same). Whereas the frozen state strategy effectively "remembers" how well (or poorly) the label was clustered before it drops out.

Hyperparameter tuning was employed for some of the descriptors. At least one W_σ representation exists for each unique combination of structure simplification and descriptor. However, some of the descriptors can be altered by tuning associated hyperparameters, resulting in more W_σ representations. The descriptors with hyperparameter tuning are the global instability index, radial distribution function, smooth overlap of atomic positions (SOAP), and mXRD. A grid search was done over the hyperparameters, for each descriptor, with parameters shown in table S1.

Descriptor	**Hyper-parameter**	**Description**	**Values attempted in grid search**
Global instability index	r_cut	The distance, in angstroms, to search for neighbors when calculating bond valences.	[1.0, 1.1, …, 5.9, 6.0]

Radial distribution function	cutoff	The distance, in angstroms, over which the radial distribution function should be calculated.	[1, 2, …, 29, 30]
	bin_size	The radial distance, in angstroms, for each bin.	[0.01, 0.02, …, 0.09, 0.1, 0.2, …, 0.9, 1.0]
Smooth overlap of atomic positions (SOAP)	rcut	The radial cutoff for the local region in angstroms.	[1, 2, …, 29, 30]
	nmax	The number of radial basis functions used.	[2, 3, …, 8, 9]
	lmax	The maximum degree of spherical harmonics used.	[1, 2, …, 8, 9]
	average	The averaging mode.	[‘outer’, ‘inner’]
mXRD	pattern_length	The number of 2θ values that will be calculated between 0° and 90°.	[101, 201, …, 901, 1001]

Ultimately, the SOAP-CAN descriptor-simplification outperforms all other descriptor-simplifications when the averaging hyperparameter is set to ‘outer’. Setting the ‘outer’ hyperparameter results in averaging over the power spectrum of different sites. Whereas the ‘inner’ setting averages over the sites first, before summing up the magnetic quantum numbers. The other three hyperparameters (rcut, nmax, and lmax) are less consequential, with most combinations tested outperforming all other non-SOAP descriptors. To illustrate the point, three different SOAP–CAN outcomes are depicted in Figure S1, plotted against the best-performing outcomes from density-CAN, mXRD-A40, orbital field matrix, and structure heterogeneity-A40. The three SOAP-CAN outcomes are those with the lowest W_σ mean for the depth of clustering ranges: 2-100, 101-200, and 201-300. The respective hyperparameters for the three SOAP-CAN descriptors are [rcut=2, nmax=4, lmax=2], [rcut=4, nmax=2, lmax=2], and [rcut=3, nmax=5, lmax=3].

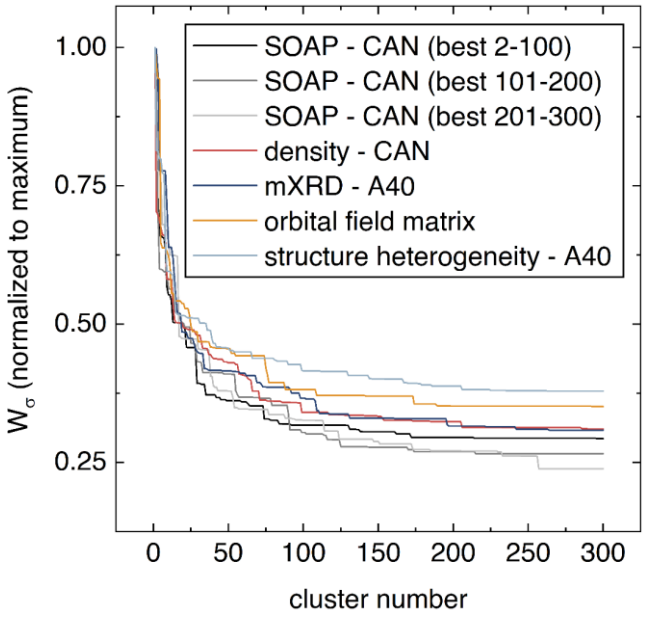

Figure S1. *W_σ* ***vs. cluster number for three different SOAP-CAN models compared with the best-performing models for density-CAN, mXRD-A40, orbital field matrix, and structure heterogeneity-A40.*** *The three SOAP-CAN models are those with the lowest W_σ mean for the clustering ranges: 2-100, 101-200, and 201-300. Almost all SOAP-CAN models outperformed the best non-SOAP models, irrespective of the specific combination of rcut, nmax, and lmax hyperparameters.*

V. W_{Ea} optimization

Each clustering outcome is also assessed by labeling with approximate activation energies for ion hopping. The activation energies are calculated using a bond valence site energy (BVSE) method developed by Adams and Rao[331,332]. The strategy approximates the E_a as the sum of an attractive Morse-type potential term and a repulsive Coulombic interaction term. The Morse-type potential term represents mobile ion interactions with lattice anions. While the Coulombic interaction term represents mobile ion interactions with lattice cations. Relative to DFT-based methods, the BVSE method is a computationally lean approach that can be used to readily assess thousands of structures. However, the BVSE method tends to overestimate activation energies because it (1) does not allow for structural relaxation as the mobile ion moves and (2) does not consider repulsive interactions between mobile ions[331,332]. The BVSE method has been implemented by He et al. and is available for use through their python API[333]. Using the BVSE method, we label 6845 structures with activation energies (6845 is the number of structures successfully solved given a computing time cutoff of 20-minutes for each structure). Ward's minimum variance method applied to the activation energy labels (W_{Ea}) is calculated in a similar manner to the W_σ:

$$W_{Ea} = \sum_{k=1}^{n_C} \sum_{i \in C_k} \left[\left(E_{a,BVSE}\right)_i - \left(\overline{E_{a,BVSE}}\right)_k \right]^2$$

where n_C is the number of clusters in a set, C_k is cluster k, and where $\left(\overline{E_{a,BVSE}}\right)_k$ denotes the mean for all labels in cluster k. Each descriptor's W_{Ea} results are shown in Figure S2 for the first 50 clustering sets. For simplicity, only the best-performing simplification-descriptor combination is shown for each descriptor.

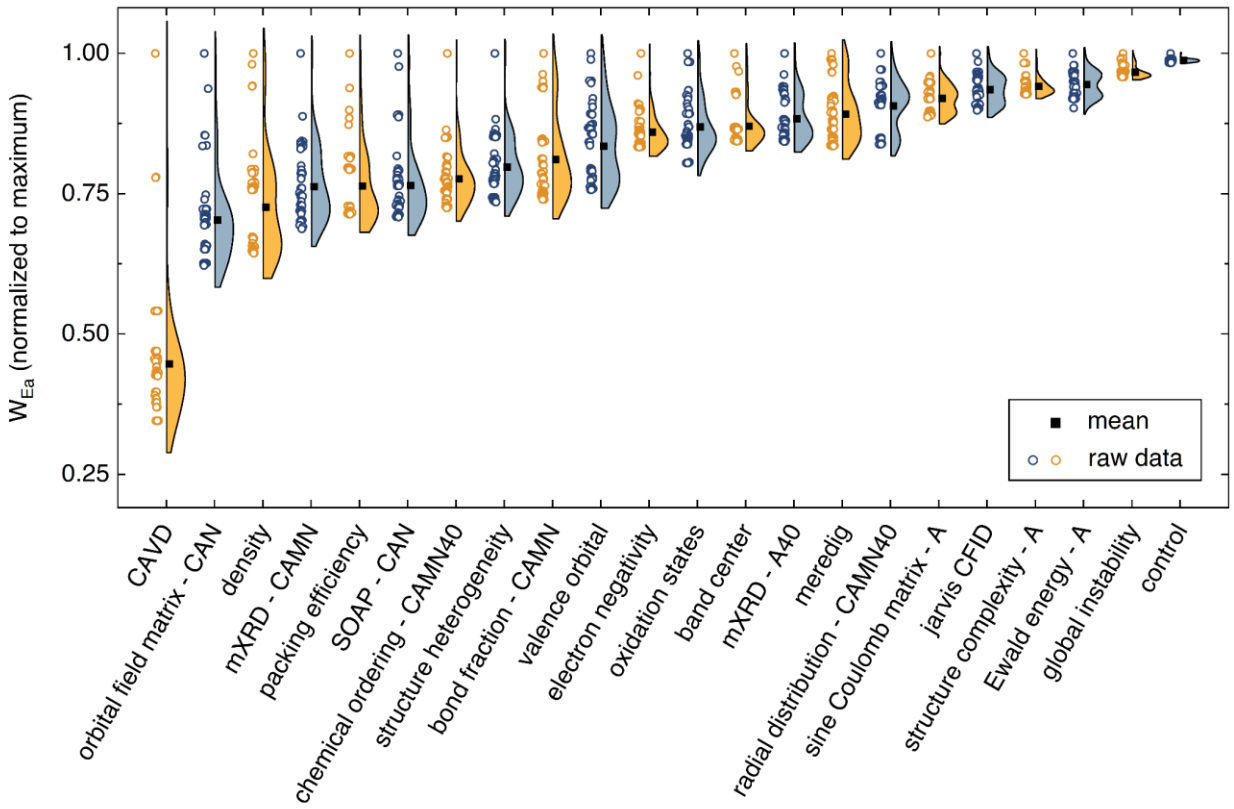

Figure S2. The W_{Ea} for the first 50 clusters generated using each descriptor. *Half-violin plots show the raw W_{Ea} score for each cluster as symbols next to the violin distribution. Simplification-descriptor combinations are sorted in order of ascending mean. The control is a random assignment of clusters, with W_{Ea} values averaged over 100 randomly assigned sets.*

For E_a labels, all descriptor-simplification pairings result in better semi-supervised ML performance than randomized clustering. The SOAP descriptor performs well relative to most, but five other descriptors outperform it: CAVD, orbital field matrix-CAN, density, mXRD-CAMN, and the packing efficiency descriptors. The favorable performance of CAVD is anticipated because the BVSE calculation directly uses the CAVD descriptor as a parameter. The favorable performance of the density and packing efficiency descriptors may be explained by their similarity to CAVD: the Voronoi decomposition to encode void space is dependent on the density and packing efficiency of the structure. Similarly, the orbital field matrix descriptor relies on calculation of Voronoi polyhedra to understand the coordination environment for each atom. A mXRD-CAMN descriptor-simplification performs well on the BVSE label set; however, the mXRD representation used by Toyota (mXRD – A40) drops from to 14th best on the E_a label set. The result may suggest that the mXRD – A40 pairing does not generalize well. When comparing the top 10 descriptors for each label set, 6 descriptors are common to both approaches: SOAP, density, mXRD, structure heterogeneity, orbital field matrix, and bond fraction.

VI. Second-order SOAP descriptor

Semi-supervised ML models may be further improved by merging descriptors and clustering on the union representation. Second order descriptor unions are examined by combining the best-performing descriptors with all other descriptors. The two input descriptor vectors (d_A and d_B) were combined with a mixing ratio (α) to yield the union representation (d_{AB}):

$$d_{AB} = d_A \cup \alpha d_B$$

The ideal mixing ratio is unknown for each union and we find that incremental changes to the mixing ratio do not result in continuous changes to the W_σ. Thus, outcomes are manually screened for mixing ratios from 10^{-6} to 10^{6} (see supplemental information – section VI). Most descriptor unions result in no improvement to the W_σ, across all mixing ratios. However, the W_σ for SOAP when mixing with the non-simplified sine Coulomb matrix descriptor (for $\alpha = 2\cdot10^{-6}$ - $4\cdot10^{-6}$) is lowered by 2-3%, with the exact percentage depending on the depth of clustering.

Almost no descriptor combinations are successful in reducing the W_σ. Excluding combinations that include the SOAP-CAN descriptor, no combinations outperform the 1st order SOAP-CAN representation. For combinations that include SOAP-CAN, some mixing ratios with the sine Coulomb matrix and the Ewald energy descriptors resulted in modest improvements in the W_σ. The best improvement is found when mixing SOAP-CAN with the sine Coulomb descriptor for $\alpha = 2\cdot10^{-6}$, $3\cdot10^{-6}$, and $4\cdot10^{-6}$. All three combinations result in the same improved curve, plotted below in Figure S3.

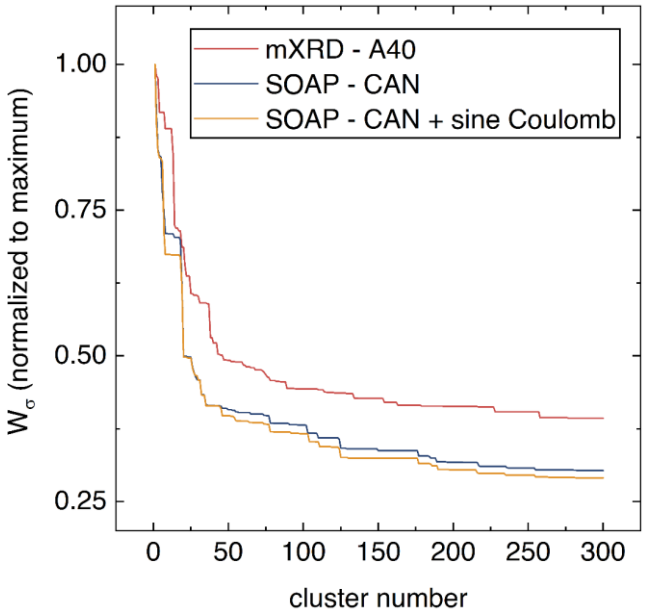

Figure S3. The best performing 2nd order descriptor: SOAP-CAN mixed with the sine Coulomb descriptor. *The clustering performance is shown for the full label set of 219. Since the mXRD – A40 representation is also compatible with the full label set, it is shown for reference. The 2nd order descriptor outperforms the 1st order SOAP-CAN descriptor at most depths of clustering.*

The agglomerative dendrogram in the main text shows that the 2nd-order SOAP-CAN descriptor facilitates aggregation of high-conductivity labels. In the simplified 9-cluster representation, most of the high-conductivity ($\sigma_{RT}>10^{-5}$ S cm^{-1}) labels are contained within the 2nd

"mega cluster". The 2nd mega cluster accounts for only 15% of the input structure. By clustering further, increasingly dense representations are found. For example, at the 241st clustering depth, the 21 high-conductivity labels have been sorted into five subclusters (Figure S4). Taken together, the five subclusters account for 52.5% of the high conductivity labels while containing only 2.2% of the input structures. We note that the control (random clustering) exhibits a Ward Variance 214% greater than the 2nd-order SOAP-CAN model at the 241st clustering depth. The difference in Ward Variance illustrates that the 2nd-order SOAP-CAN model is much better at identifying high-conductivity structures, relative to random selection.

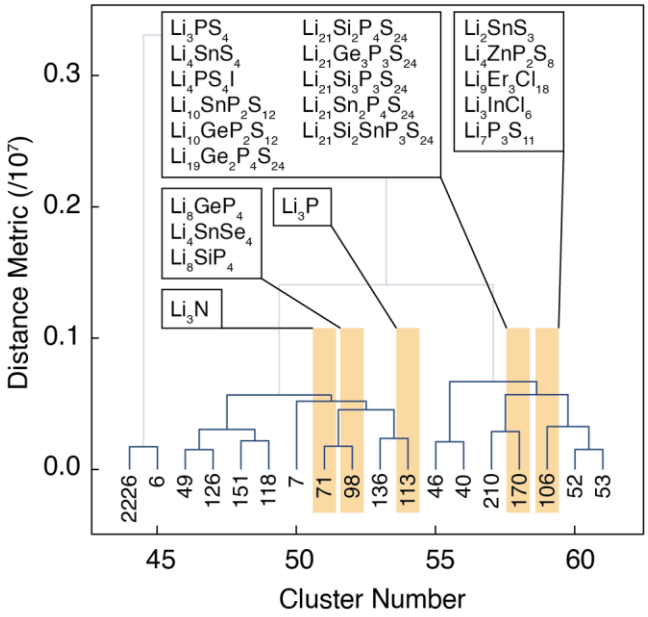

Figure S4. The partial agglomerative dendrogram generated for the 2nd-order SOAP-CAN descriptor-simplification. *The area shown is the 2nd mega cluster taken from Figure 3 of the main text. At a clustering depth of 241, the 21 high-conductivity labels are sorted into 5 clusters which account for 2.2% of the input structures.*

VII. Climbing Image – Nudged Elastic Band

Migration barriers for Li ion hopping are evaluated with the Climbing Image – Nudged Elastic Band (CI-NEB) method as implemented in the QuantumESPRESSO PWneb software package[334–337]. Density-functional theory (DFT) calculations are performed using the Perdew-Burke-Ernzerfof (PBE) generalized gradient approximation functional and projector-augmented wave (PAW) sets[338,339]. Convergence testing for the kinetic-energy cutoff of the plane-wave basis and the *k*-point sampling is performed for each structure to ensure an accuracy of 1 meV per atom. The lattice parameters and atomic positions of the as-retrieved structure are optimized. Supercells are created for each structure that are a minimum of 10 Å in each lattice direction to minimize interactions between periodic images of the mobile ion. To study the migration barrier in the dilute limit, a single Li vacancy is created in the boundary endpoint structures of each studied pathway. A uniform background charge is used to balance excess charge. Each boundary configuration is relaxed until the force on each atom is less than $3x10^{-4}$ eV/Å. Images are created by linearly interpolating framework atomic positions between the initial and final boundary configurations. The initial pathway for the mobile ion is generated from the BVSE output minimum energy pathway to promote faster convergence of the NEB calculation. An NEB force convergence threshold of 0.05 eV/ Å is used. The calculation is first converged using the default NEB algorithm and then restarted with the CI scheme to allow for the maximum energy of the pathway to be determined.

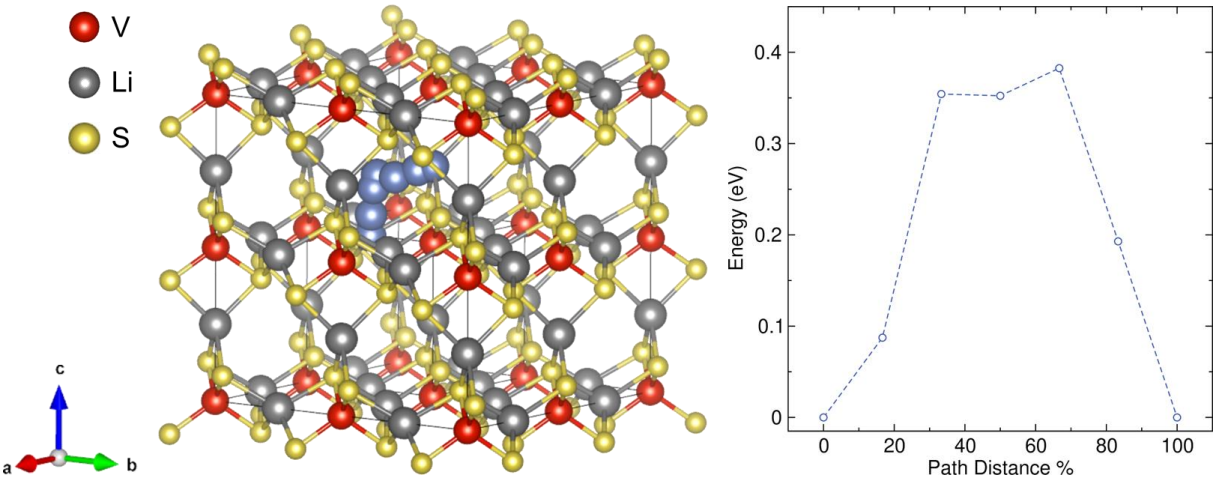

Figure S5. The 2x2x2 supercell of Li_3VS_4 used for the CI-NEB calculation of Li migration energy. *Blue atoms represent the Li position from the CI-NEB output images.*

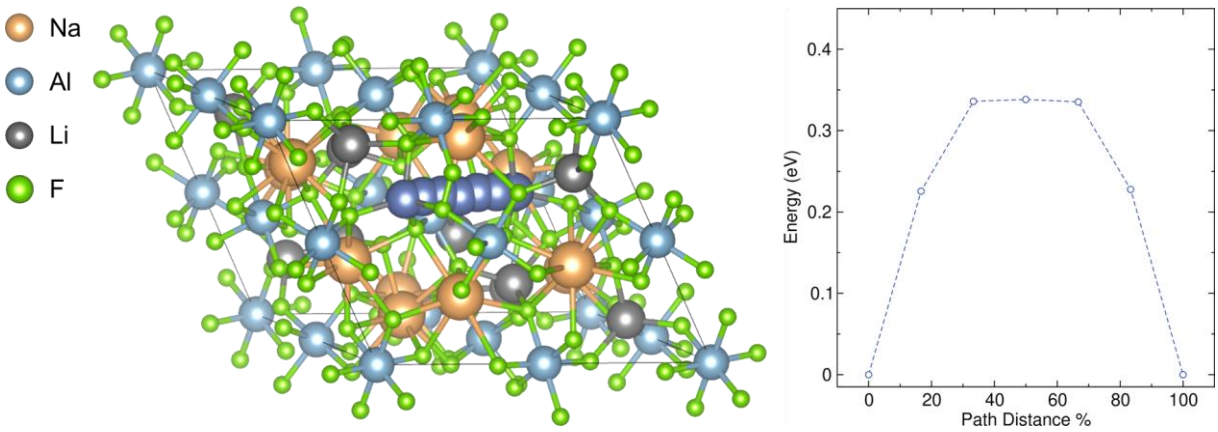

Figure S6. The primitive cell of $Na_3Li_3Al_2F_{12}$ used for the CI-NEB calculation of Li migration energy. *Blue atoms represent the Li position from the CI-NEB output images.*

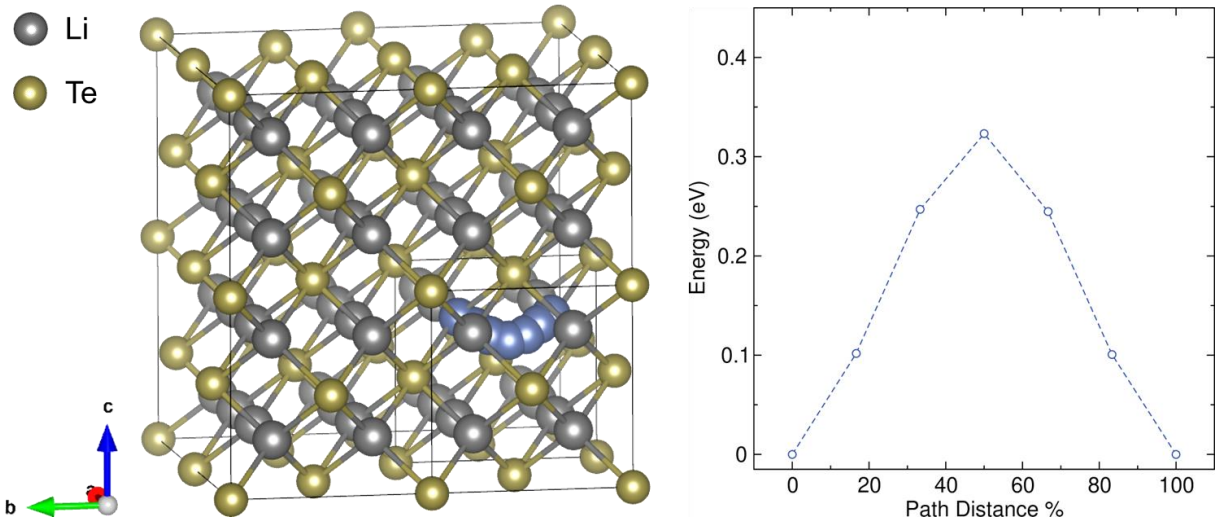

Figure S7. The 2x2x2 supercell of Li_2Te used for the CI-NEB calculation of Li migration energy. *Blue atoms represent the Li position from the CI-NEB output images.*

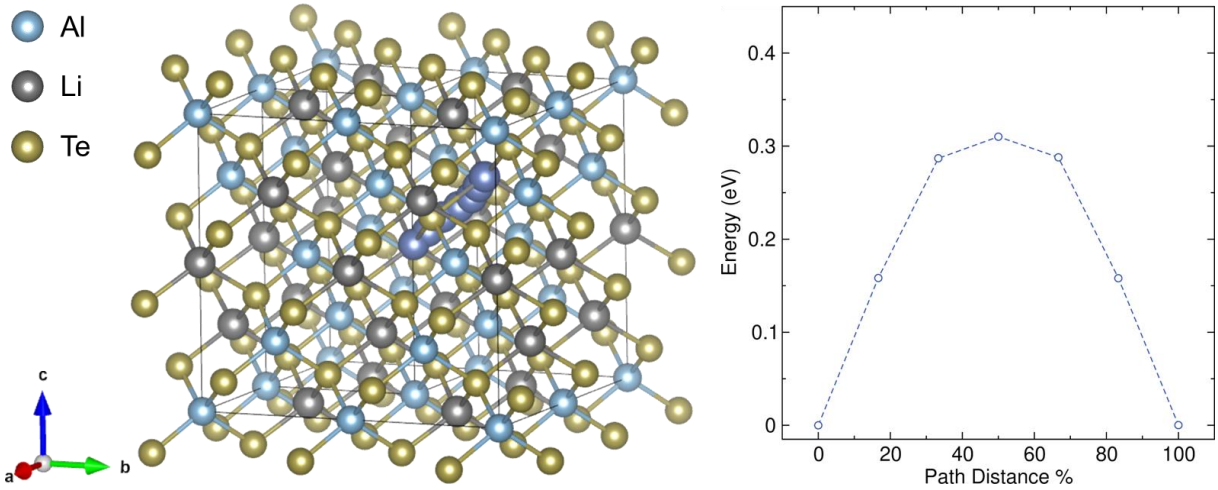

Figure S8. The 2x2x1 supercell of $LiAlTe_2$ used for the CI-NEB calculation of Li migration energy. *Blue atoms represent the Li position from the CI-NEB output images.*

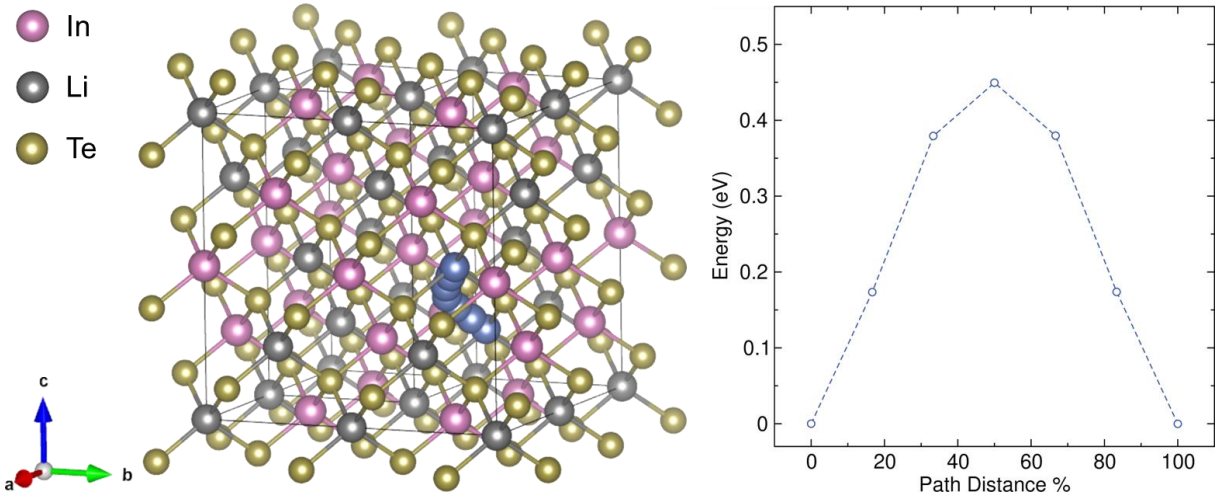

Figure S9. The 2x2x1 supercell of $LiInTe_2$ used for the CI-NEB calculation of Li migration energy. *Blue atoms represent the Li position from the CI-NEB output images.*

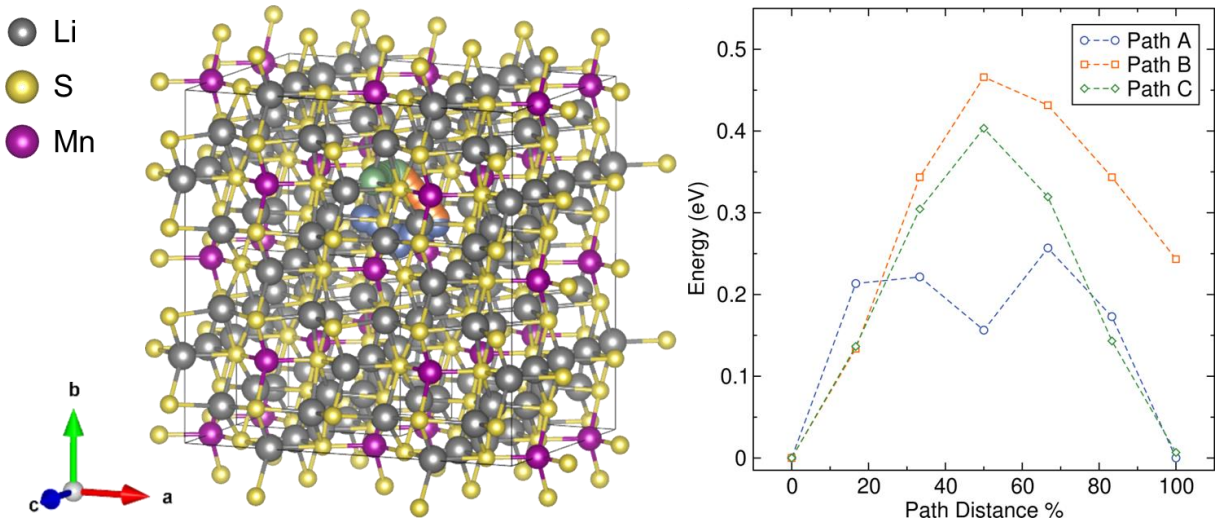

Figure S10. The 2x2x2 supercell of Li_6MnS_4 used for the CI-NEB calculation of Li migration energy. *Blue atoms represent the Li position from the CI-NEB output images.*

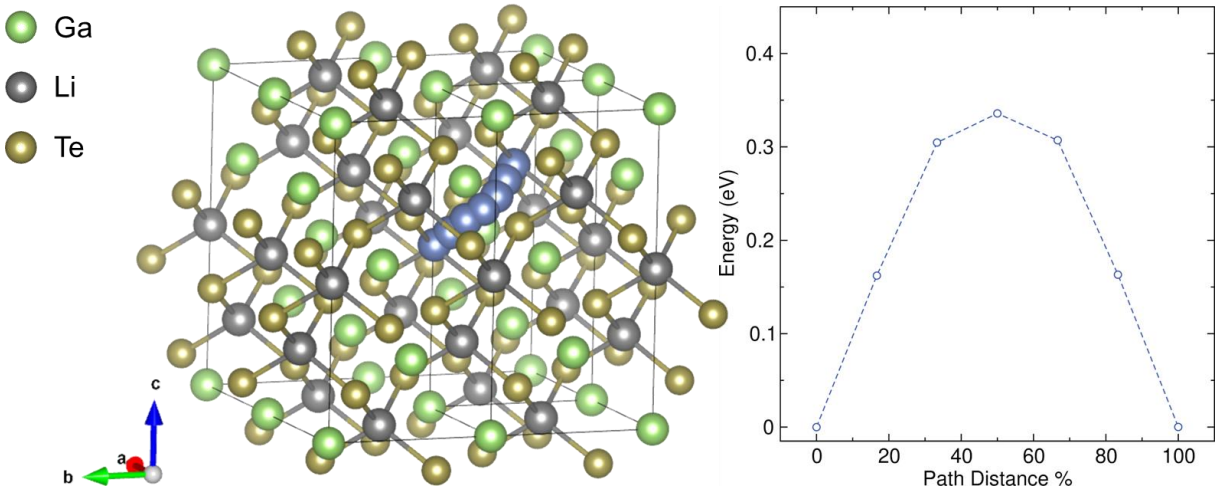

Figure S11. The 2x2x1 supercell of $LiGaTe_2$ used for the CI-NEB calculation of Li migration energy. *Blue atoms represent the Li position from the CI-NEB output images.*

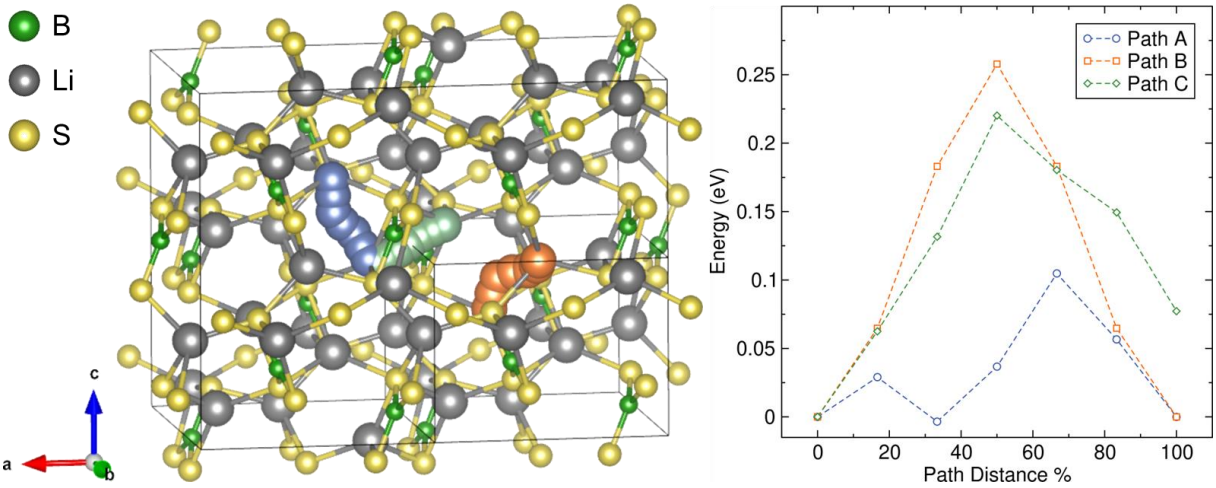

Figure S12. The 2x1x2 supercell of Li_3BS_3 used for the CI-NEB calculation of Li migration energy. *Blue, green, and orange atoms represent the Li position from the CI-NEB output images.*

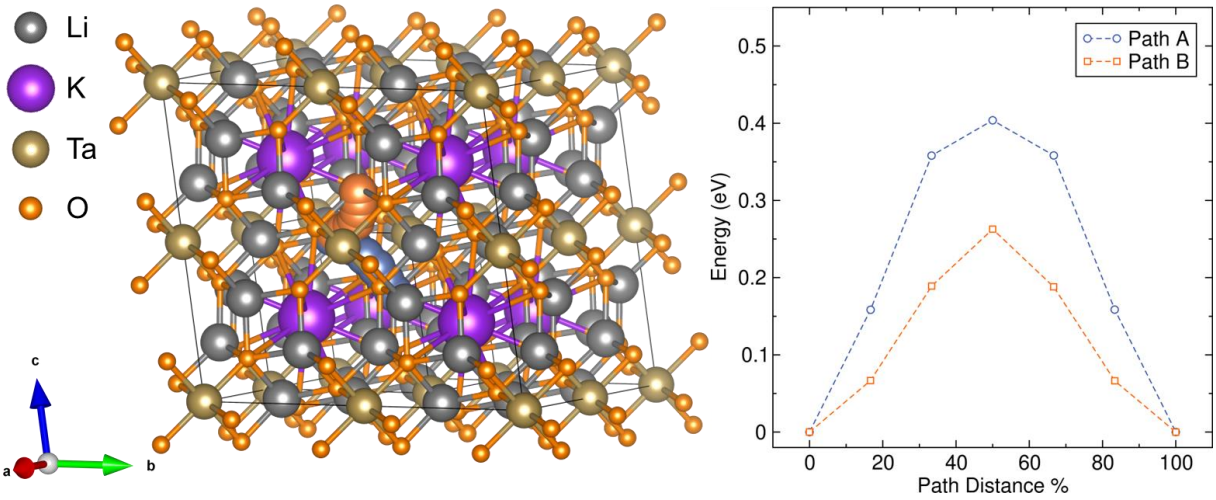

Figure S13. The 2x2x2 supercell of KLi_6TaO_6 used for the CI-NEB calculation of Li migration energy. *Blue and orange atoms represent the Li position from the CI-NEB output images.*

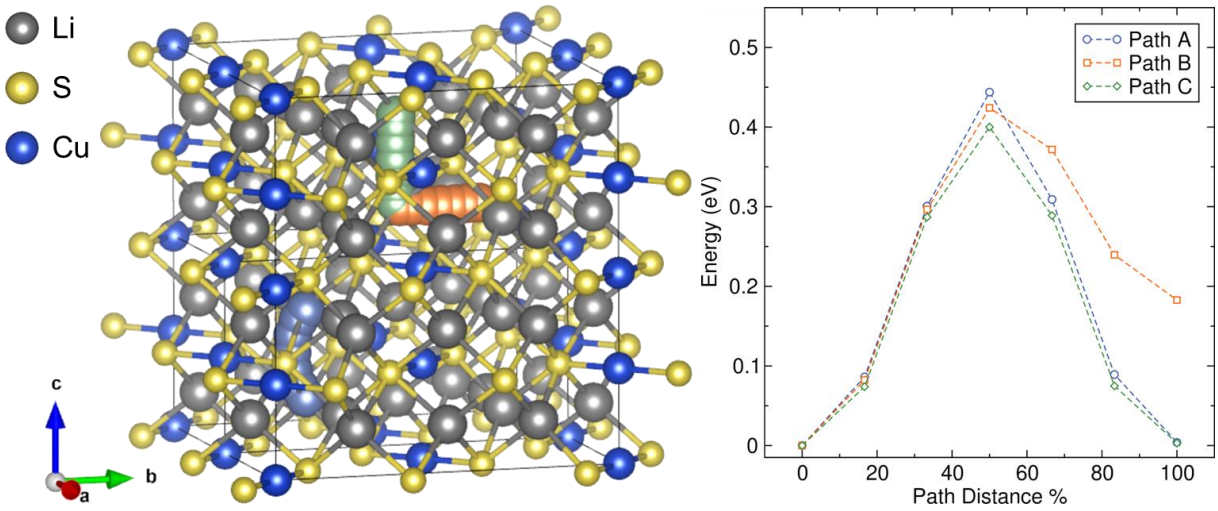

Figure S14. The 2x1x2 supercell of Li_3CuS_2 used for the CI-NEB calculation of Li migration energy. *Blue atoms represent the Li position from the CI-NEB output images.*

VIII. a-$Li_{2.95}B_{0.95}Si_{0.05}S_3$ impedance

Electrochemical impedance data for the amorphized Si-substituted Li_3BS_3 (a-$Li_{2.95}B_{0.95}Si_{0.05}S_3$) suggests the presence of two RC features. The VSP-300 potentiostat can supply a maximum sinusoidal frequency of 3 MHz, sufficient to resolve a partial semicircle in the Nyquist impedance plot (Figure S14). Attempted fits to the partial semicircle reveal that it would not intersect the origin at higher frequencies, suggesting the presence of an additional RC feature. It is plausible that two RC features exist, describing the bulk and grain-boundary transport of Li^+. A more conservative estimate of the conductivity (σ_{tot}) can be derived by extrapolating a linear of the Warburg tail to the x intercept. While the more conservative estimate is used in the main manuscript, we note here that the actual bulk conductivity is likely higher.

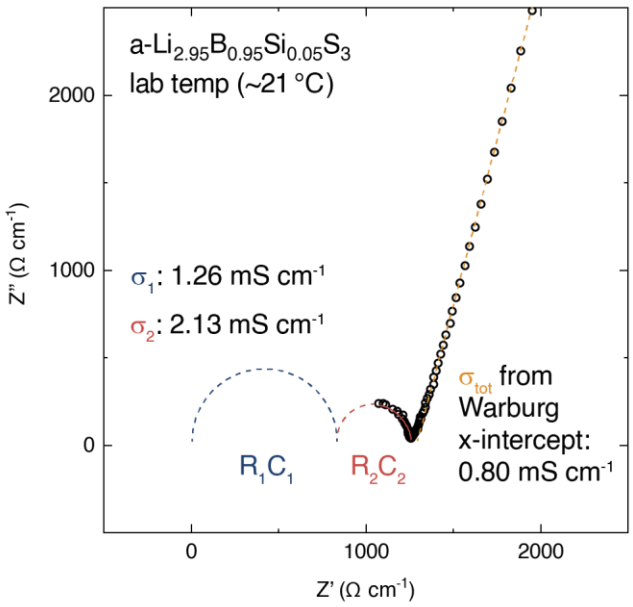

Figure S15. Nyquist data for a-$Li_{2.95}B_{0.95}Si_{0.05}S_3$ near room temperature. *The partially resolved semi-circular features suggests the presence of at least two RC circuit elements.*

IX. Full list of promising structures

Excluding the labeled dataset, there are 50 compounds that are predicted to be stable and to exhibit a Li-hopping activation energy below 600 meV. Ten of the predicted compounds have already been experimentally examined and are hereafter excluded: Li_2O, Li_2S, LiCl, LiI, LiBr, Li_6AsS_5I, $Li_4Ti_5O_{12}$, Li_2InCl_3, $LiInI_4$, Li_6NiCl_8. Another nine are excluded because they are used in cathodes, anodes, or glassy electrolyte formulations: $LiFeCl_4$, Li_2CO_3, Li_2PtO_3, $Li_2NiGe_3O_8$, Li_2CrO_4, Li_2SeO_4, LiAlS, $Li_2Mn_3NiO_8$, $LiInSe_2$. The remaining 31 promising structures are discussed below and plotted by ascending activation energy in Figure S15.

a. Stable compounds

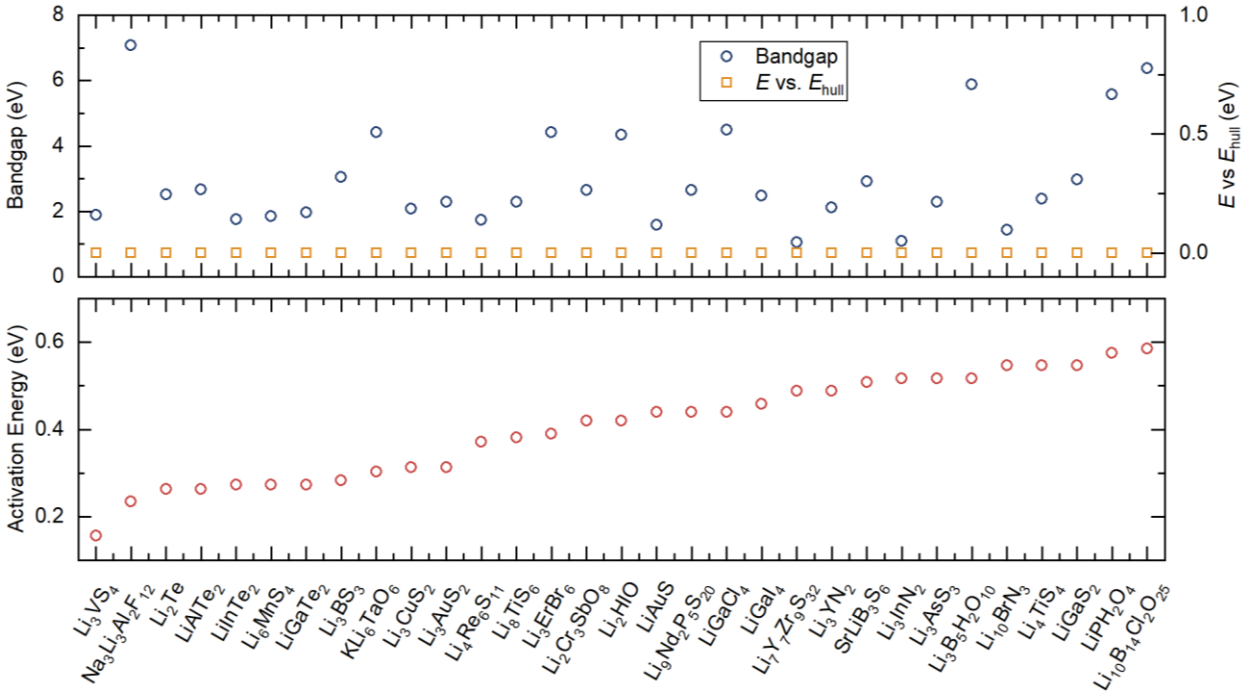

Figure S16. The 31 promising structures that are predicted to be stable and to exhibit Li-hopping activation energy below 600 meV.

Each structure is examined in order of ascending activation energy below.

Li_3VS_4

Material's Project ID	mp-760375
ICSD ID	None
Space Group	$P\bar{4}3m$ [215]
Calculated Band Gap	1.8951 eV
Calculated E above E_{hull}	0 eV
Predicted Activation Energy	156.25 meV

Notes: Explored for use as both an anode[340] and a cathode[341]. NEB has been employed to predict an activation energy of 95 meV.[342] All Li occupies tetrahedral sites that are edge sharing with adjacent V tetrahedra.

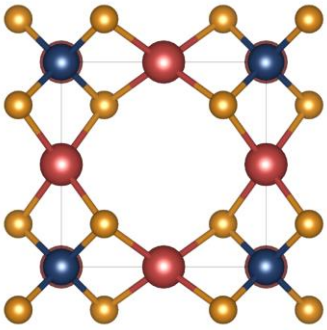

(a-axis view)

$Na_3Li_3Al_2F_{12}$

Material's Project ID	mp-6711
ICSD ID	9923
Space Group	$Ia\bar{3}d$ [230]
Calculated Band Gap	7.0872 eV
Calculated E above E_{hull}	0 eV
Predicted Activation Energy	234.38 meV

Notes: The structure appears to be unexplored. Discussion of structural motifs by Geller et al.[343] All Li atoms are in a tetrahedral bonding environment.

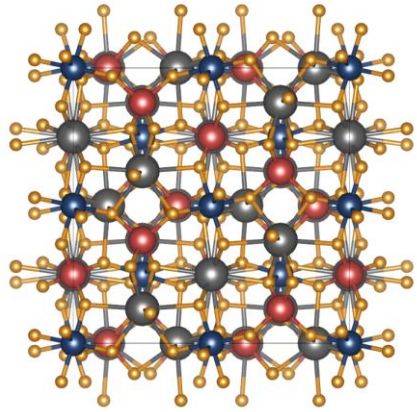

(a-axis view)

Li_2Te

Material's Project ID	mp-2530
ICSD ID	60434
Space Group	$Fm\bar{3}m$ [225]
Calculated Band Gap	2.5171 eV
Calculated E above E_{hull}	0 eV
Predicted Activation Energy	263.67 meV

Notes: A screening approach using bond valence site energy calculations identified the oxide as a promising structure: $Li_2Te_2O_5$.[344] All Li are in tetrahedral bonding environment.

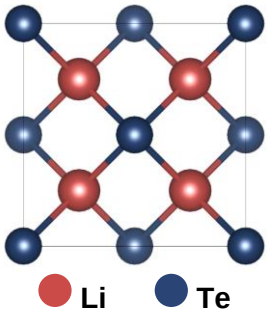

(a-axis view)

$LiAlTe_2$

Material's Project ID	mp-4586
ICSD ID	280226
Space Group	$I\bar{4}2d$ [122]
Calculated Band Gap	2.6599 eV
Calculated E above E_{hull}	0 eV
Predicted Activation Energy	263.67 meV

Notes: All Li are in a tetrahedral environment with corner sharing. The structure hasn't been examined as an ionic conductor – ongoing research is focused on optoelectronic properties.[345]

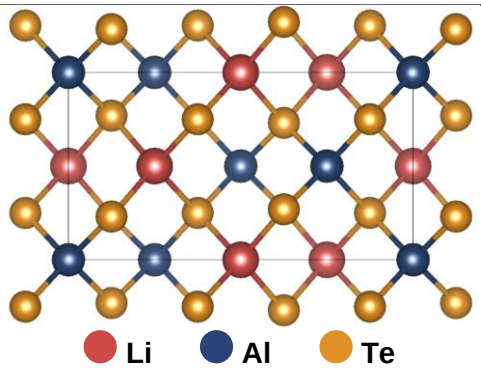

(b-axis view)

$LiInTe_2$

Material's Project ID	mp-20782
ICSD ID	658016
Space Group	$I\bar{4}2d$ [122]
Calculated Band Gap	1.7492 eV
Calculated E above E_{hull}	0 eV
Predicted Activation Energy	273.44 meV

Notes: All Li are in a tetrahedral environment with corner sharing. The structure hasn't been examined as an ionic conductor – ongoing research is focused on optoelectronic properties.[346]

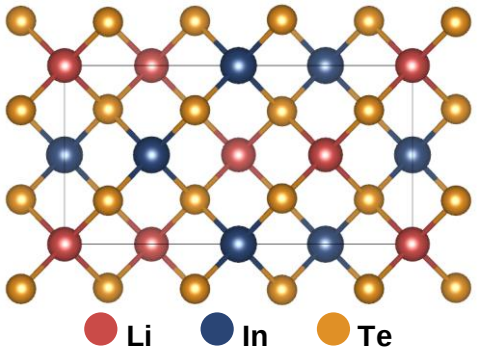

(b-axis view)

Li_6MnS_4

Material's Project ID	mp-756490
ICSD ID	NA
Space Group	$P4_2/nmc$ [137]
Calculated Band Gap	1.8508 eV
Calculated E above E_{hull}	0 eV
Predicted Activation Energy	273.44 meV

Notes: All Li are in an edge-sharing tetrahedral bonding environment. Augustine et al. posit that the structure could be a viable cathode material. They performed *ab-initio* calculations to measure the enthalpy of formation and have concluded that the structure should be stable.[347]

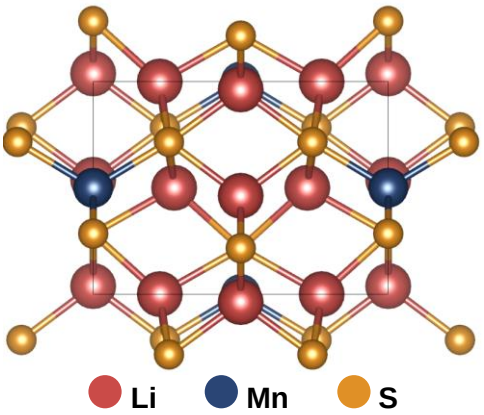

(a-axis view)

$LiGaTe_2$

Material's Project ID	mp-5048
ICSD ID	162555
Space Group	$I\bar{4}2d$ [122]
Calculated Band Gap	1.9666 eV
Calculated E above E_{hull}	0 eV
Predicted Activation Energy	273.44 meV

Notes: All Li are in a tetrahedral environment with corner sharing. The structure hasn't been examined as an ionic conductor – ongoing research is focused on optoelectronic properties.[348] Isaenko et al. report an experimental band gap of 2.41 eV.

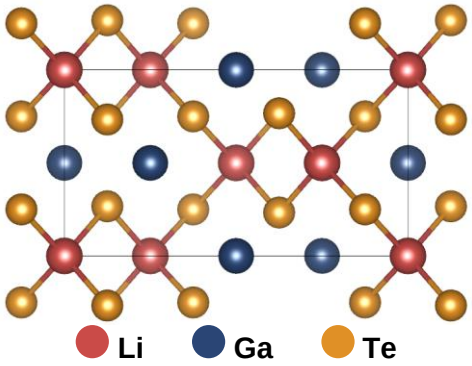

(b-axis view)

Li_3BS_3

Material's Project ID	mp-5614
ICSD ID	380104
Space Group	$Pnma$ [62]
Calculated Band Gap	3.0526 eV
Calculated E above E_{hull}	0 eV
Predicted Activation Energy	283.2 meV

Notes: All Li are in a tetrahedral bonding environment. Recent NEB work suggests an activation barrier of 250 meV.[349]

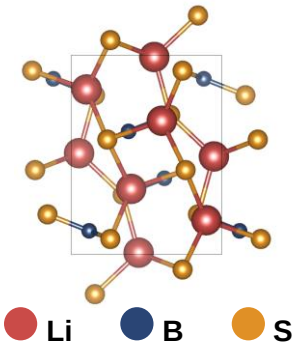

(b-axis view)

KLi_6TaO_6

Material's Project ID	mp-9059
ICSD ID	73159
Space Group	$R\bar{3}mH$ [166]
Calculated Band Gap	4.4134 eV
Calculated E above E_{hull}	0 eV
Predicted Activation Energy	302.73 meV

Notes: All Li are in a tetrahedral bonding environment with edge or corner sharing. Recent electrochemical characterization by Suzuki et al. found an ionic conductivity near 10^{-5} S cm^{-1} with aliovalent substitution of Sn.[350]

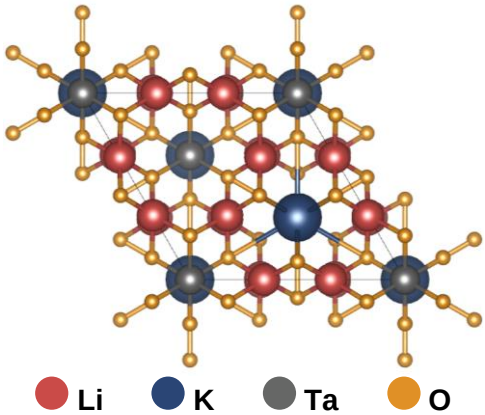

(c-axis view)

Li_3CuS_2

Material's Project ID	mp-1177695
ICSD ID	NA
Space Group	$Ibam$ [72]
Calculated Band Gap	2.0826 eV
Calculated E above E_{hull}	0 eV
Predicted Activation Energy	312.5 meV

Notes: All Li are in an edge-sharing tetrahedral bonding environment. Explored for use as a cathode by Kawasaki et al. in 2021.[351] They found an initial charge-discharge capacity of 380 mAh g^{-1} with average voltage of 2.1 V vs. Li/Li^+.

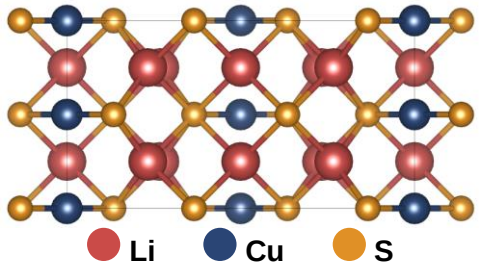

(a-axis view)

Li_3AuS_2

Material's Project ID	mp-15999
ICSD ID	280535
Space Group	$Ibam$ [72]
Calculated Band Gap	2.2827 eV
Calculated E above E_{hull}	0 eV
Predicted Activation Energy	312.5 meV

Notes: All Li are in an edge-sharing tetrahedral bonding environment. Never explored for battery purposes. Synthesis by Huang et al.[352]

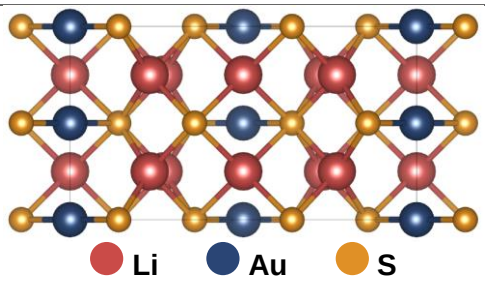

(a-axis view)

$Li_4Re_6S_{11}$

Material's Project ID	mp-1181012
ICSD ID	NA
Space Group	$Pccn$ [56]
Calculated Band Gap	1.7328 eV
Calculated E above E_{hull}	0 eV
Predicted Activation Energy	371.09 meV

Notes: All Li sits in four- and five-coordinate environments. Kahle et al. previously screened ~1400 Li-containing compounds and identified $Li_4Re_6S_{11}$ as a potentially promising SSE using molecular dynamics simulation.[353] Their simulations failed to resolve RT diffusion but found promising diffusivity at elevated temperatures.

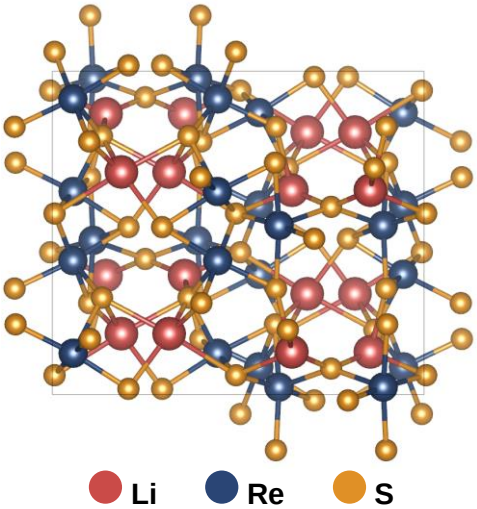

(a-axis view)

Li_8TiS_6

Material's Project ID	mp-753546
ICSD ID	NA
Space Group	$P6_3cm$ [185]
Calculated Band Gap	2.2925 eV
Calculated E above E_{hull}	0 eV
Predicted Activation Energy	380.86 meV

Notes: All Li are in a tetrahedral bonding environment.

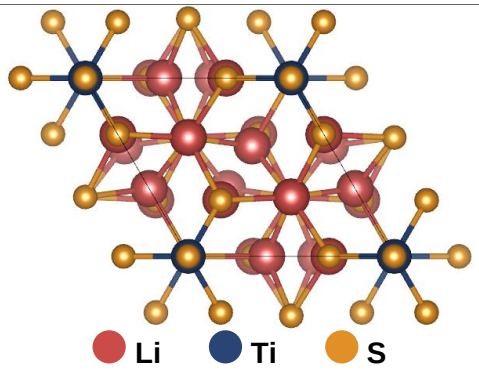

(c-axis view)

Li_3ErBr_6

Material's Project ID	mp-1222492
ICSD ID	NA
Space Group	$C2$ [5]
Calculated Band Gap	4.4222 eV
Calculated E above E_{hull}	0 eV
Predicted Activation Energy	390.63 meV

Notes: All Li are in an octahedral bonding environment. Muy et al. identify Li_3ErBr_6 as one of eighteen promising compounds using a phonon-band descriptor approach.[354] They synthesize the Cl analogue and report an experimental conductivity of 0.05-0.3 mS cm^{-1}. The material also mentioned briefly in perspective by Li et al.[355]

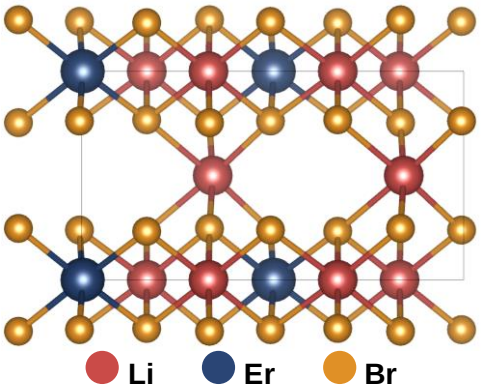

(a-axis view)

$Li_2Cr_3SbO_8$

Material's Project ID	mp-1178030
ICSD ID	NA
Space Group	$R\bar{3}m$ [166]
Calculated Band Gap	2.6513 eV
Calculated E above E_{hull}	0 eV
Predicted Activation Energy	419.92 meV

Notes: All Li are in a tetrahedral bonding environment.

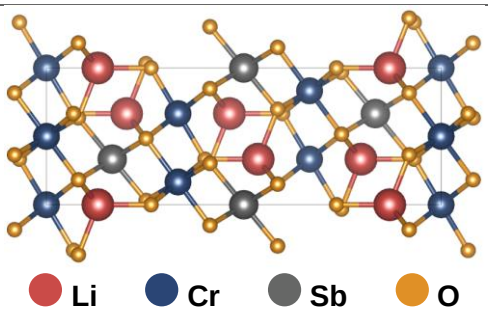

(b-axis view)

Li_2HIO

Material's Project ID	mp-643069
ICSD ID	NA
Space Group	$Pnma$ [62]
Calculated Band Gap	4.3363 eV
Calculated E above E_{hull}	0 eV
Predicted Activation Energy	419.92 meV

Notes: All Li are in a tetrahedral bonding environment. Sendek et al. identified Li_2HIO as promising using a combined ML and DFT approach.[356] They predicted a RT diffusion barrier of 350 meV.

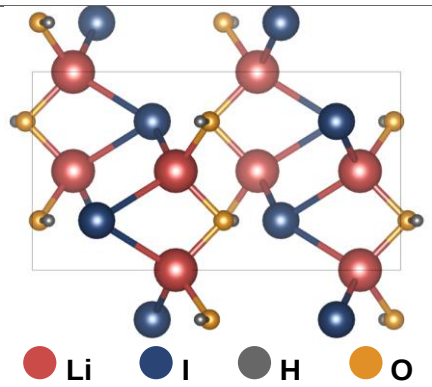

(c-axis view)

LiAuS

Material's Project ID	mp-29829
ICSD ID	165259
Space Group	$F22\bar{1}d$ [70]
Calculated Band Gap	1.587 eV
Calculated E above E_{hull}	0 eV
Predicted Activation Energy	439.45 meV

Notes: All Li are in an edge-sharing tetrahedral bonding environment. Synthesis via Huang et al.[352]

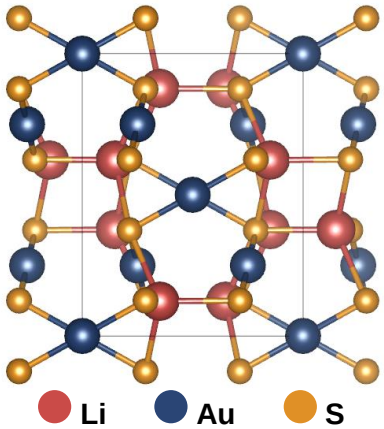

(c-axis view)

$Li_9Nd_2P_5S_{20}$

Material's Project ID	mp-1223032
ICSD ID	NA
Space Group	$C2/c$ [15]
Calculated Band Gap	2.6503 eV
Calculated E above E_{hull}	0 eV
Predicted Activation Energy	439.45 meV

Notes: Li ions are in a distorted octahedral and some 5-coordinate bonding environments.

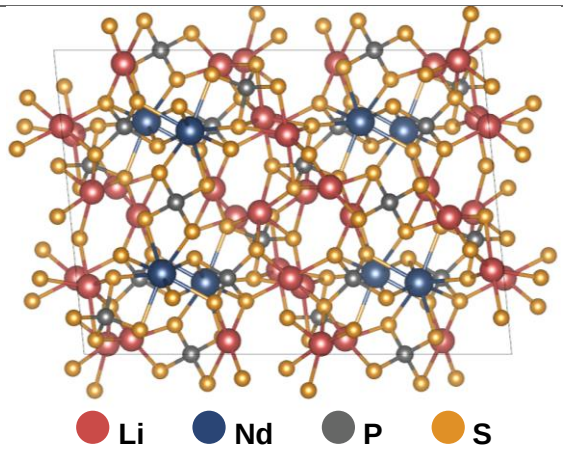

(b-axis view)

$LiGaCl_4$

Material's Project ID	mp-28341
ICSD ID	60849
Space Group	$P2_1/c$ [14]
Calculated Band Gap	4.4866 eV
Calculated E above E_{hull}	0 eV
Predicted Activation Energy	439.45 meV

Notes: All Li are in an octahedral bonding environment. Mentioned briefly in perspective by Li et al.[355]

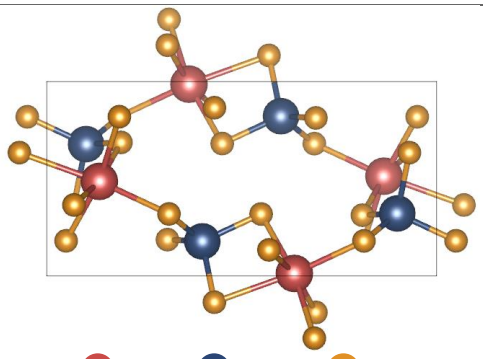

(c-axis view)

$LiGaI_4$

Material's Project ID	mp-567967
ICSD ID	60850
Space Group	$P2_1/c$ [14]
Calculated Band Gap	2.4872 eV
Calculated E above E_{hull}	0 eV
Predicted Activation Energy	458.98 meV

Notes: All Li are in an octahedral bonding environment. Discussed briefly in perspective by Li et al.[355] Predicted by Kahle et al. to be a fast ionic conductor using molecular dynamics simulations.[353] They predict an activation energy of 350 meV.

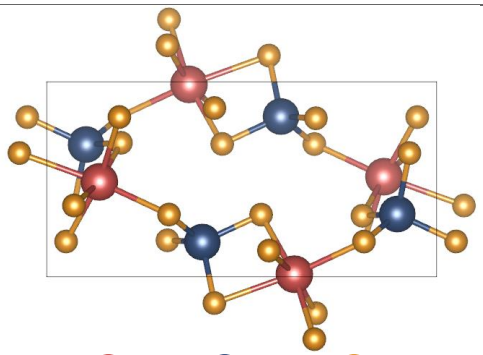

(c-axis view)

$Li_7Y_7Zr_9S_{32}$

Material's Project ID	mp-767467
ICSD ID	NA
Space Group	$P1$ [1]
Calculated Band Gap	1.0523 eV
Calculated E above E_{hull}	0 eV
Predicted Activation Energy	488.28 meV

Notes: All Li are in a tetrahedral bonding environments.

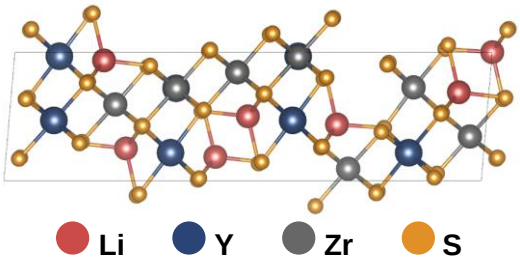

(b-axis view)

Li_3YN_2

Material's Project ID	mp-1029592
ICSD ID	NA
Space Group	$Ia\bar{3}$ [206]
Calculated Band Gap	2.119 eV
Calculated E above E_{hull}	0 eV
Predicted Activation Energy	488.28 meV

Notes: All Li are in a three coordinate bonding environment.

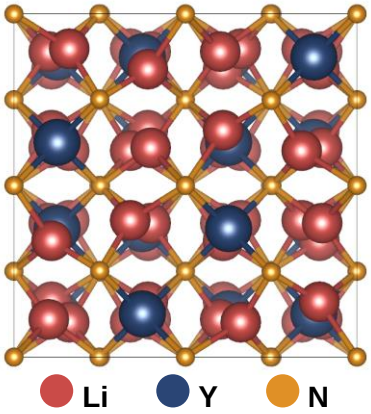

$SrLiB_3S_6$

Material's Project ID	mp-558219
ICSD ID	79616
Space Group	Cc [9]
Calculated Band Gap	2.918 eV
Calculated E above E_{hull}	0 eV
Predicted Activation Energy	507.81 meV

Notes: All Li are in a tetrahedral bonding environment. Optical properties and air-stability have been briefly discussed by Kim et al.[357]

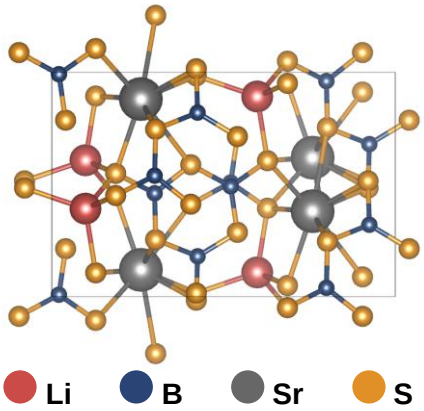

(c-axis view)

Li_3InN_2

Material's Project ID	mp-1029562
ICSD ID	NA
Space Group	$Ia\bar{3}$ [206]
Calculated Band Gap	1.0921 eV
Calculated E above E_{hull}	0 eV
Predicted Activation Energy	517.58 meV

Notes: All Li are in an edge-sharing tetrahedral bonding environment. Synthetic accounts appear to exist in some books.

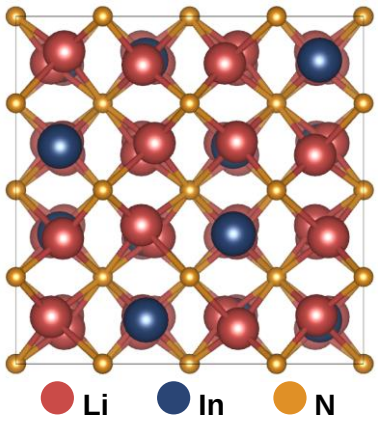

Li_3AsS_3

Material's Project ID	mp-28471
ICSD ID	424835
Space Group	$Pna2_1$ [33]
Calculated Band Gap	2.291 eV
Calculated E above E_{hull}	0 eV
Predicted Activation Energy	517.58 meV

Notes: Li are all in an edge-sharing tetrahedral bonding environment. Wang et al. predicted that this might be a high-conductivity structure by using a "structure matching" algorithm.[358]

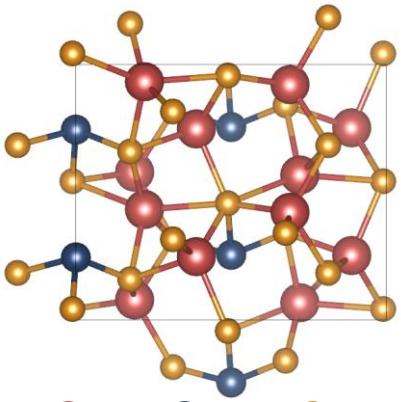

(b-axis view)

$Li_3B_5H_2O_8$

Material's Project ID	mp-1199091
ICSD ID	418166
Space Group	$P4_32_12$ [96]
Calculated Band Gap	5.8839 eV
Calculated E above E_{hull}	0 eV
Predicted Activation Energy	517.58 meV

Notes: All Li are in a 5-coordinate bonding environment. A hydrothermal synthetic method has been described by Li et al.[359]

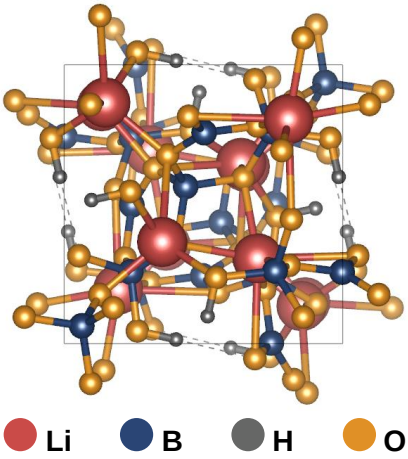

(c-axis view)

$Li_{10}BrN_3$

Material's Project ID	mp-28989
ICSD ID	78819
Space Group	$P\bar{6}m2$ [62]
Calculated Band Gap	1.4357 eV
Calculated E above E_{hull}	0 eV
Predicted Activation Energy	546.88 meV

Notes: All Li are in 3-coordinate or 2-coordinate bonding environments. Identified by Snydacker et al. as a suitable coating for Li anode passivation via convex hull calculations.[360]

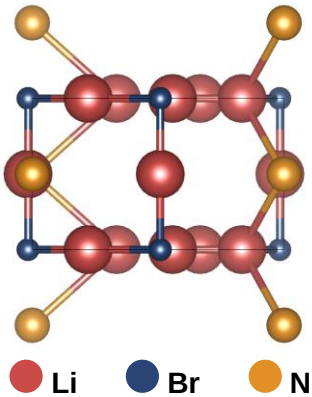

(a-axis view)

Li_4TiS_4

Material's Project ID	mp-766540
ICSD ID	NA
Space Group	$Pnma$ [62]
Calculated Band Gap	2.3811 eV
Calculated E above E_{hull}	0 eV
Predicted Activation Energy	546.88 meV

Notes: All Li are in octahedral or tetrahedral bonding environments. The tetrahedra sit between the octahedral layers. Amorphous Li_4TiS_4 is thought to form upon discharge of TiS_4-based cathodes.[361]

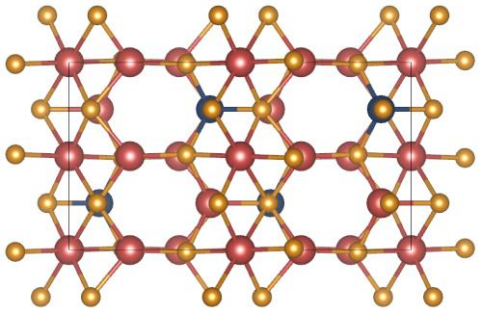

(c-axis view)

$LiGaS_2$

Material's Project ID	mp-3647
ICSD ID	68465
Space Group	$Pna2_1$ [33]
Calculated Band Gap	2.9659 eV
Calculated E above E_{hull}	0 eV
Predicted Activation Energy	546.88 meV

Notes: All Li are in a tetrahedral bonding environment. Wang et al. predicted that $LiGaS_2$ might be a high-conductivity structure by using a "structure matching" algorithm.[358] Separately, He et al. used ab initio calculation to predict the same.[362]

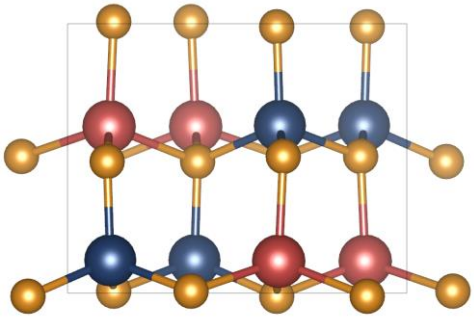

(a-axis view)

$LiPH_2O_4$

Material's Project ID	mp-24610
ICSD ID	182308
Space Group	$Pna2_1$ [33]
Calculated Band Gap	5.5778 eV
Calculated E above E_{hull}	0 eV
Predicted Activation Energy	576.17 meV

Notes: All Li are in a corner-sharing tetrahedral bonding environments.

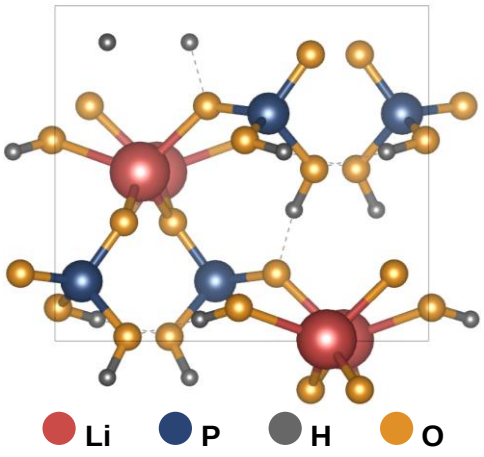

(a-axis view)

$Li_{10}B_{14}Cl_2O_{25}$

Material's Project ID	mp-23122
ICSD ID	200981
Space Group	$F23$ [196]
Calculated Band Gap	6.3849 eV
Calculated E above E_{hull}	0 eV
Predicted Activation Energy	585.94 meV

Notes: Li are mostly in tetrahedral bonding environments, although some 5-coordinate environments exist. Kahle et al. identified $Li_{10}B_{14}Cl_2O_{25}$ as a potentially promising SSE material using a "pinball" model.[353]

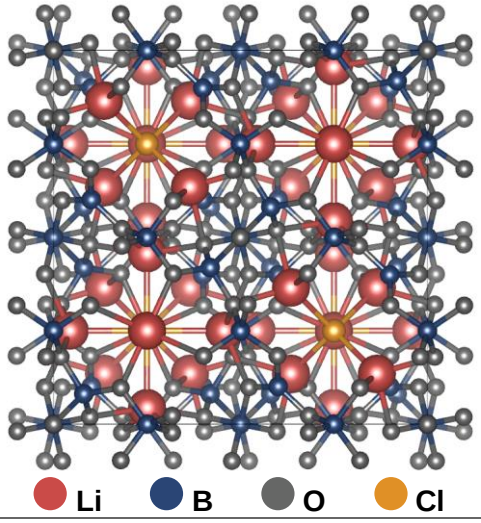

b. Quasi-stable compounds (E_{hull} below 15 meV)

Excluding the labeled dataset, there are 34 compounds that are predicted to be within 15 meV of the convex hull (E_{hull}) and to exhibit a Li-hopping activation energy below 600 meV. Ten of the predicted compounds have already been experimentally examined and are hereafter excluded: Li_3SbS_4, Li_6AsS_5I, Li_6PS_5I, Li_3ScCl_6, Li_2MnBr_4, Li_3N, $LiTi_2P_3O_{12}$, $Li_{10}SiP_2S_{12}$, Li_2ZnCl_4, Li_3InO_3. Another three are currently being excluded because they are used in cathodes: Li_3NbS_4, Li_3CuS_2, Li_6VCl_8. The remaining 21 promising structures are discussed below and plotted by ascending activation energy in Figure S16.

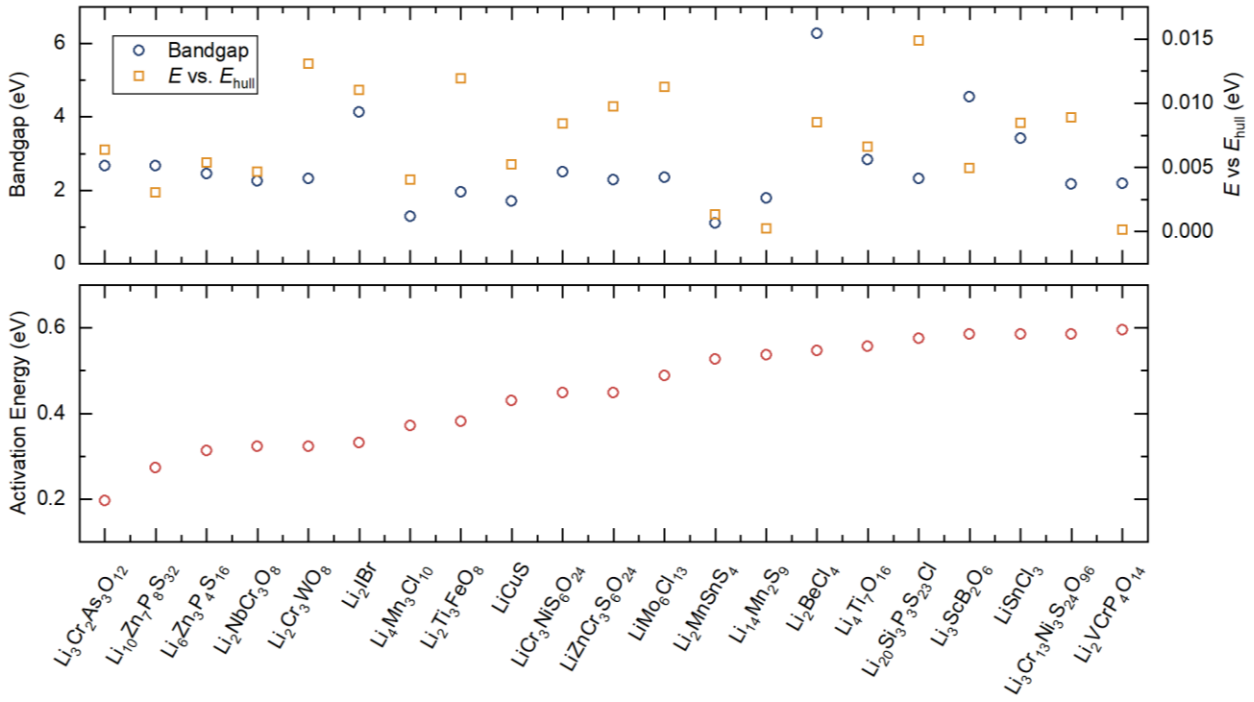

Figure S17. The 21 promising structures that are predicted to be within 15 meV of E_{hull} and to exhibit Li-hopping activation energy below 600 meV.

$Li_3Cr_2As_3O_{12}$

Material's Project ID	mp-779404
ICSD ID	NA
Space Group	$Ia\bar{3}d$ [230]
Calculated Band Gap	2.6702 eV
Calculated E above E_{hull}	6.37 meV
Predicted Activation Energy	165.31 meV

Notes: Li are in 8-coordinate sites surrounded by oxygens.

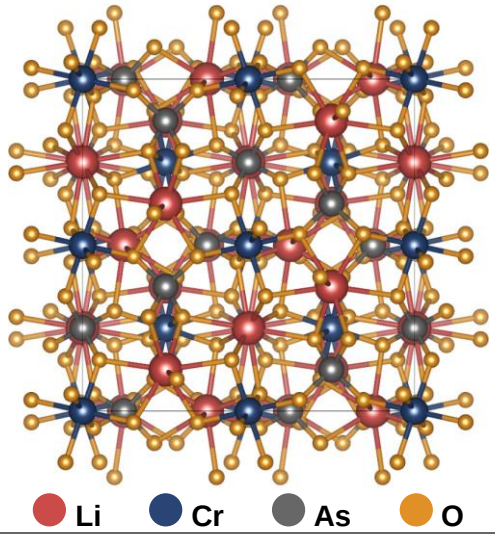

$Li_{10}Zn_7P_8S_{32}$

Material's Project ID	mp-1147627
ICSD ID	NA
Space Group	$P1$ [1]
Calculated Band Gap	2.6635 eV
Calculated E above E_{hull}	3.04 meV
Predicted Activation Energy	273.44 meV

Notes: All Li are in tetrahedral bonding environments – corner sharing with Zn and P tetrahedra. Richard's et al. used NEB to predict that $Li_{10}Zn_7P_8S_{32}$ has a 252 meV activation energy for Li diffusion.[363] They also predict a RT conductivity of 3.44 mS cm^{-1}.

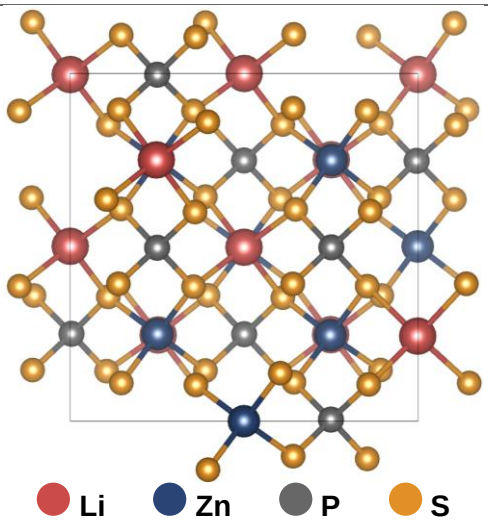

(a-axis view)

$Li_6Zn_3P_4S_{16}$

Material's Project ID	mp-1147596
ICSD ID	NA
Space Group	$P1$ [1]
Calculated Band Gap	2.4515 eV
Calculated E above E_{hull}	5.35 meV
Predicted Activation Energy	312.5 meV

Notes: All Li are in tetrahedral bonding environments – corner sharing with Zn and P tetrahedra. Richard's et al. used NEB to predict that $Li_6Zn_3P_4S_{16}$ has a 181 meV activation energy for Li diffusion.[363] They also predict a RT conductivity of 27.7 mS cm^{-1}.

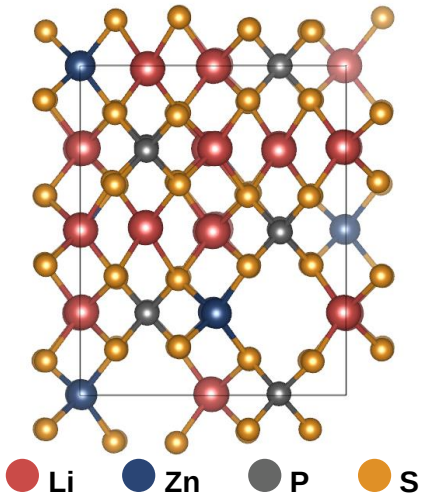

(c-axis view)

$Li_2NbCr_3O_8$

Material's Project ID	mp-775164
ICSD ID	NA
Space Group	$P4_332$ [212]
Calculated Band Gap	2.2504 eV
Calculated E above E_{hull}	4.65 meV
Predicted Activation Energy	322.27 meV

Notes: All Li are in tetrahedral bonding environments.

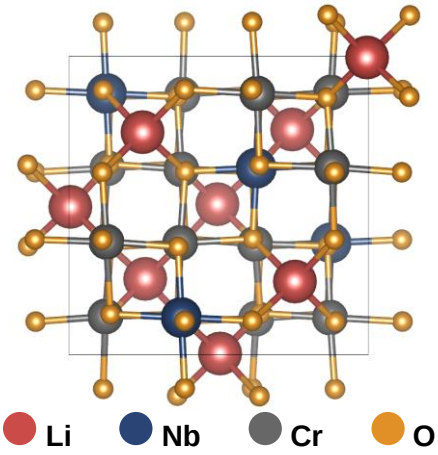

(a-axis view)

$Li_2Cr_3WO_8$

Material's Project ID	mp-758116
ICSD ID	NA
Space Group	$P4_332$ [212]
Calculated Band Gap	2.318 eV
Calculated E above E_{hull}	13.05 meV
Predicted Activation Energy	322.27 meV

Notes: All Li are in tetrahedral bonding environments.

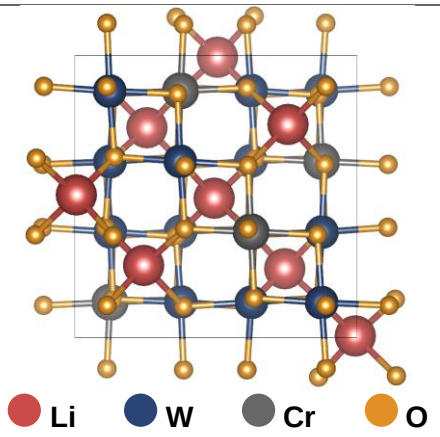

(a-axis view)

Li_2IBr

Material's Project ID	mp-1222669
ICSD ID	NA
Space Group	$P3m1$ [156]
Calculated Band Gap	4.1375 eV
Calculated E above E_{hull}	11.02 meV
Predicted Activation Energy	332.03 meV

Notes: All Li are in tetrahedral bonding environment.

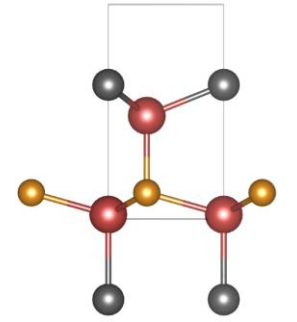

(a-axis view)

$Li_4Mn_3Cl_{10}$

Material's Project ID	mp-531376
ICSD ID	NA
Space Group	Cm [8]
Calculated Band Gap	1.2928 eV
Calculated E above E_{hull}	4.04 meV
Predicted Activation Energy	371.09 meV

Notes: Octahedral Li layers with Li tetrahedra interspersed between.

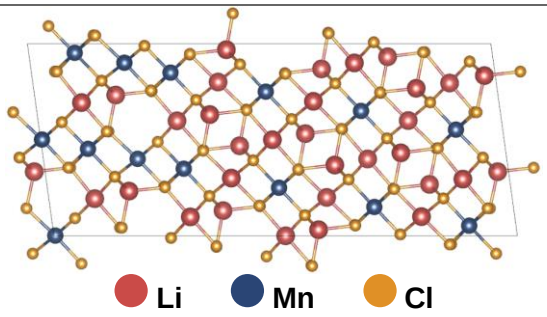

(b-axis view)

$Li_2Ti_3FeO_8$

Material's Project ID	mp-775306
ICSD ID	NA
Space Group	$R32$ [155]
Calculated Band Gap	1.9461 eV
Calculated E above E_{hull}	11.9 meV
Predicted Activation Energy	380.86 meV

Notes: All Li are in tetrahedral bonding environments.

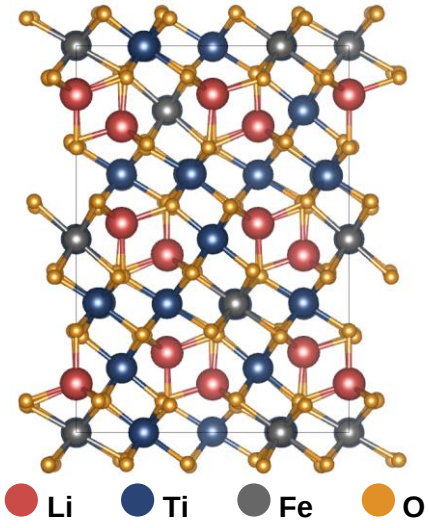

(a-axis view)

LiCuS

Material's Project ID	mp-774736
ICSD ID	NA
Space Group	Cc [9]
Calculated Band Gap	1.6984 eV
Calculated E above E_{hull}	5.2 meV
Predicted Activation Energy	429.69 meV

Notes: All Li are in edge-sharing tetrahedral bonding environments. Previously examined as a cathode material by Chen et al.[364]

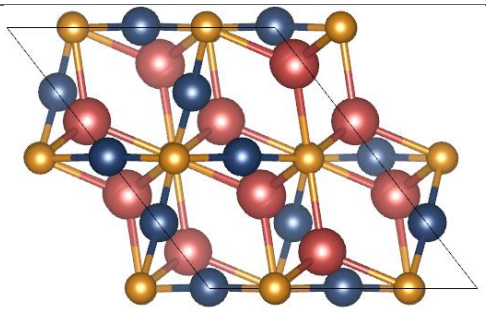

(b-axis view)

$LiCr_3NiS_6O_{24}$

Material's Project ID	mp-766088
ICSD ID	NA
Space Group	$P1$ [1]
Calculated Band Gap	2.5049 eV
Calculated E above E_{hull}	8.41 meV
Predicted Activation Energy	449.22 meV

Notes: All Li are in tetrahedral bonding environments.

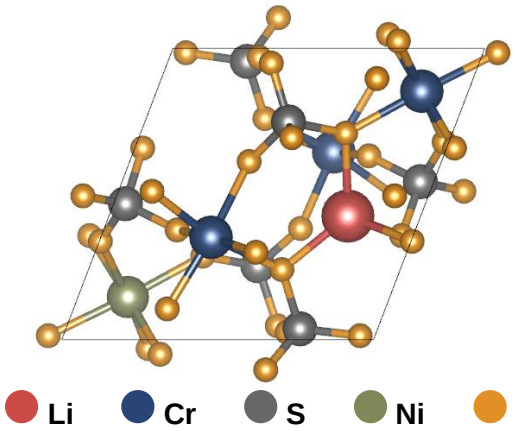

(c-axis view)

$LiZnCr_3S_6O_{24}$

Material's Project ID	mp-769549
ICSD ID	NA
Space Group	$P1$ [1]
Calculated Band Gap	2.2921 eV
Calculated E above E_{hull}	9.72 meV
Predicted Activation Energy	449.22 meV

Notes: All Li are in tetrahedral bonding environments.

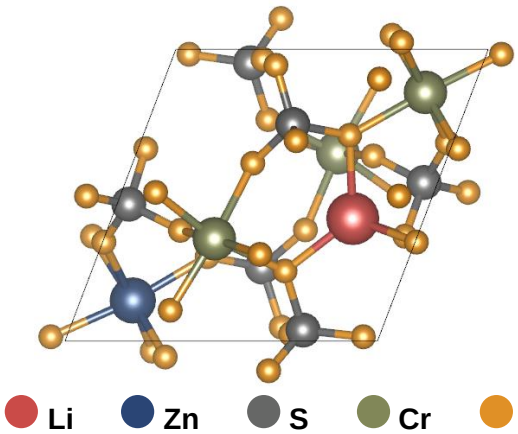

(c-axis view)

$LiMo_6Cl_{13}$

Material's Project ID	mp-680167
ICSD ID	410368
Space Group	$P\bar{1}$ [2]
Calculated Band Gap	2.3547 eV
Calculated E above E_{hull}	11.28 meV
Predicted Activation Energy	488.28 meV

Notes: All Li are in tetrahedral bonding environments.

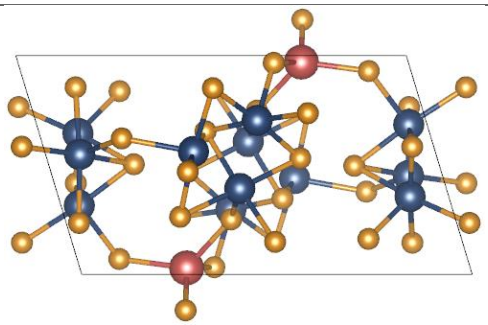

(b-axis view)

Li_2MnSnS_4

Material's Project ID	mp-1195603
ICSD ID	429817
Space Group	$Pna2_1$ [33]
Calculated Band Gap	1.1045 eV
Calculated E above E_{hull}	1.34 meV
Predicted Activation Energy	527.34 meV

Notes: All Li are in tetrahedral bonding environments. Devlin et al. have previously published a synthetic method for Li_2MnSnS_4.[365]

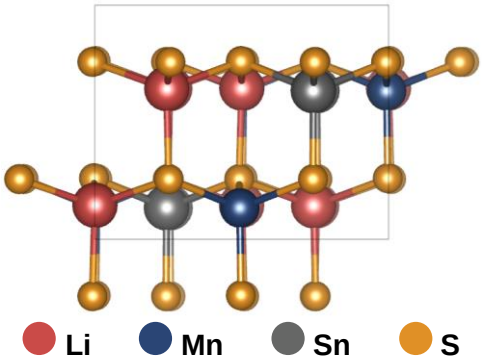

(a-axis view)

$Li_{14}Mn_2S_9$

Material's Project ID	mp-756198
ICSD ID	NA
Space Group	$P\bar{3}$ [147]
Calculated Band Gap	1.7888 eV
Calculated E above E_{hull}	0.25 meV
Predicted Activation Energy	537.11 meV

Notes: All Li are in edge-sharing tetrahedral bonding environments.

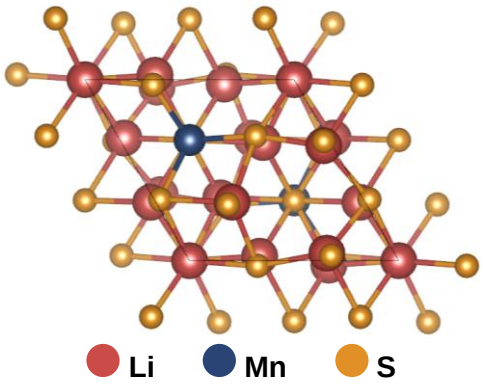

(a-axis view)

Li_2BeCl_4

Material's Project ID	mp-1210835
ICSD ID	NA
Space Group	$Pnma$ [62]
Calculated Band Gap	6.2881 eV
Calculated E above E_{hull}	8.52 meV
Predicted Activation Energy	546.88 meV

Notes: All Li are in edge-sharing octahedral bonding environments. A synthetic method has been published by Steiner et al.[366]

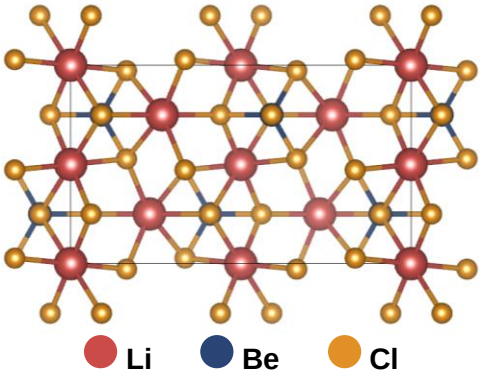

(c-axis view)

$Li_4Ti_7O_{16}$

Material's Project ID	mp-531820
ICSD ID	NA
Space Group	$Pnnm$ [58]
Calculated Band Gap	2.8323 eV
Calculated E above E_{hull}	6.62 meV
Predicted Activation Energy	556.64 meV

Notes: All Li are in tetrahedral bonding environments.

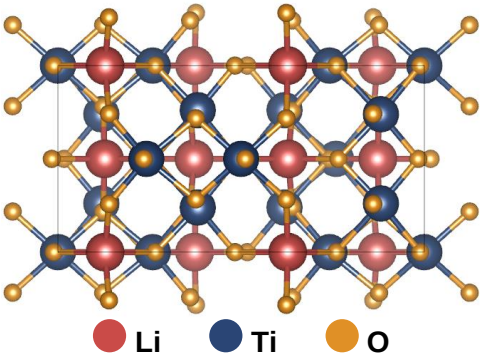

(a-axis view)

$Li_{20}Si_3P_3S_{23}Cl$

Material's Project ID	mp-1097035
ICSD ID	NA
Space Group	Pm [6]
Calculated Band Gap	2.3126 eV
Calculated E above E_{hull}	14.89 meV
Predicted Activation Energy	576.17 meV

Notes: All Li are in corner-sharing tetrahedral bonding environments. $Li_{10}Si_3P_3S_{23}Cl$ was theoretically studied by Rao et al.[367] They used it is a model system for a neural-network molecular dynamics pipeline.

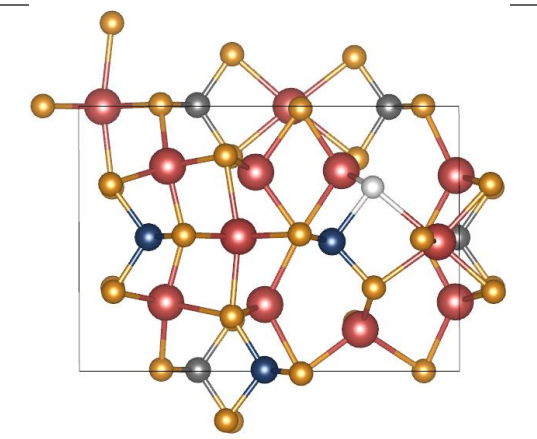

(b-axis view)

$Li_3ScB_2O_6$

Material's Project ID	mp-557012
ICSD ID	241234
Space Group	$P2_1/c$ [14]
Calculated Band Gap	4.5457 eV
Calculated E above E_{hull}	4.93 meV
Predicted Activation Energy	585.94 meV

Notes: All Li are in tetrahedral or octahedral bonding environments.

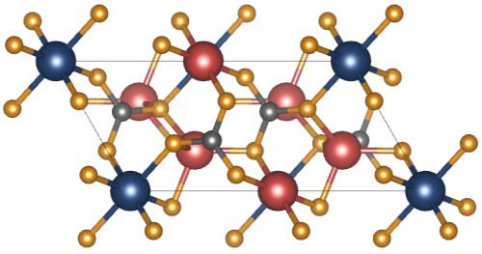

(b-axis view)

$LiSnCl_3$

Material's Project ID	mp-998591
ICSD ID	NA
Space Group	$R3c$ [161]
Calculated Band Gap	3.4153 eV
Calculated E above E_{hull}	8.45 meV
Predicted Activation Energy	585.94 meV

Notes: All Li are in octahedral bonding environments. Muy et al. examined $LiSnCl_3$ using a phonon-band descriptor approach.[354] Despite a promising band-center value, they suggest it has a low stability window. Körbel et al. identify it as a promising piezoelectric material.[368]

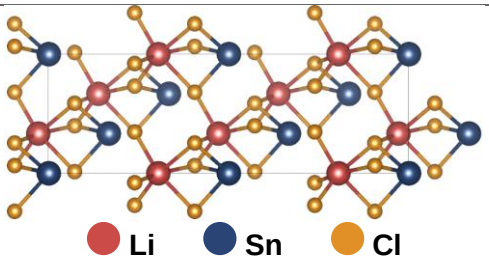

(b-axis view)

$Li_3Cr_{13}Ni_3S_{24}O_{96}$

Material's Project ID	mp-695469
ICSD ID	NA
Space Group	$P1$ [1]
Calculated Band Gap	2.1679 eV
Calculated E above E_{hull}	8.9 meV
Predicted Activation Energy	585.94 meV

Notes: All Li are in tetrahedral bonding environments.

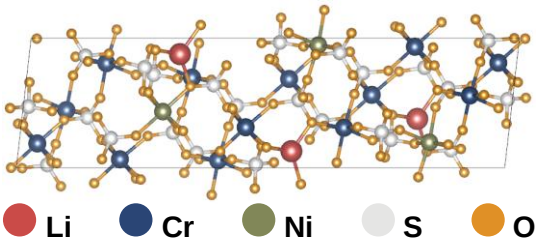

(b-axis view)

$Li_2VCrP_4O_{14}$

Material's Project ID	mp-759753
ICSD ID	NA
Space Group	$P1$ [1]
Calculated Band Gap	2.1798 eV
Calculated E above E_{hull}	0.13 meV
Predicted Activation Energy	595.7 meV

Notes: All Li are in distorted tetrahedral bonding environments.

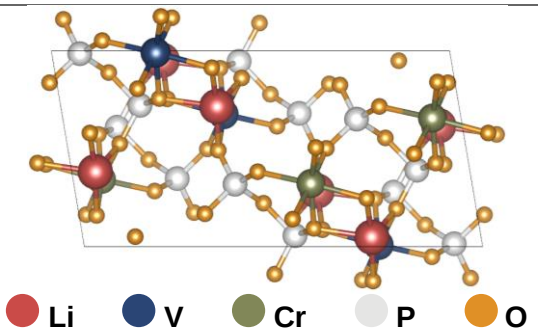

(b-axis view)

c. Unknown-stability compounds (sans Materials Project entry)

There are 18 predictions that have no associated Material's Project entry. These structures lack stability data. Seven of the predicted compounds have already been experimentally examined and are hereafter excluded: Li_2O, Li_2S, $Li_7Y_7Zr_9S_{32}$, $Li_4SnSe_4O_{13}$, Li_2MnBr_4, Li_5AlS_4, $Li_3Fe_2P_3O_{12}$. Another five are currently being excluded because they are used in cathodes: $Li_2Mn_3NiO_8$, $Li_2Mn_3CoO_8$, $Li_5Mn_{16}O_{32}$, $Li_2Mn_{15}AlO_{32}$, $Li_3V_2P_3O_{12}$. The remaining 6 promising structures are discussed below and plotted in order of ascending activation energy in Figure S17.

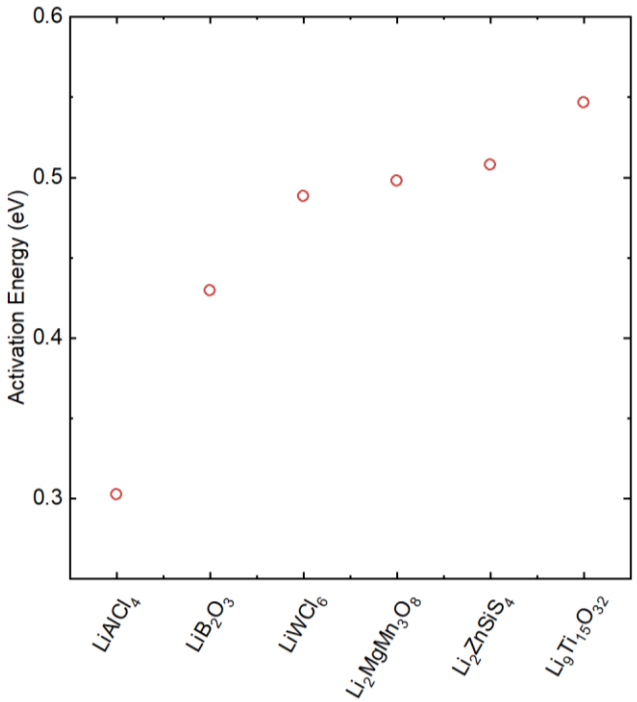

Figure S18. The six promising structures that lack Materials Project data but are predicted to exhibit Li-hopping activation energy below 600 meV.

$LiAlCl_4$

Material's Project ID	NA
ICSD ID	244127
Space Group	$Pmn2_1$ [31]
Calculated Band Gap	NA
Calculated E above E_{hull}	NA
Predicted Activation Energy	302.73 meV

Notes: All Li are in tetrahedral bonding environments. Synthetic method by Prömper et al.[369]

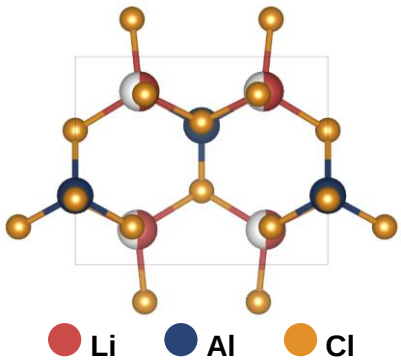

(c-axis view)

LiB_2O_3

Material's Project ID	NA
ICSD ID	183930
Space Group	$I4_1cd$ [110]
Calculated Band Gap	NA
Calculated E above E_{hull}	NA
Predicted Activation Energy	429.69 meV

Notes: All Li are in 5-coordinate bonding environments. Previously studied by Abdel-Khalek et al. in a glass ceramic.[370] Discussed in some detail by Rousse et al.[371]

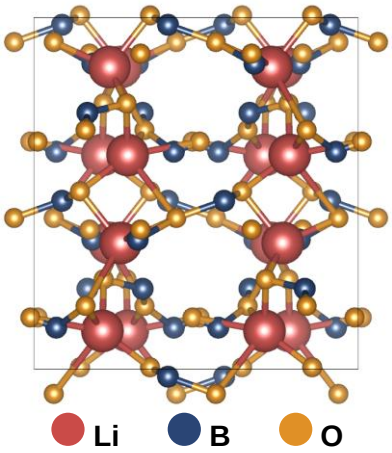

(a-axis view)

$LiWCl_6$

Material's Project ID	NA
ICSD ID	409938
Space Group	$R3H$ [146]
Calculated Band Gap	NA
Calculated E above E_{hull}	NA
Predicted Activation Energy	488.28 meV

Notes: All Li are in octahedral bonding environments.

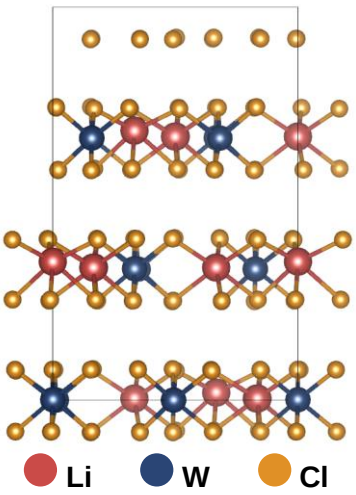

(a-axis view)

$Li_2MgMn_3O_8$

Material's Project ID	NA
ICSD ID	94758
Space Group	$P4_332$ [212]
Calculated Band Gap	NA
Calculated E above E_{hull}	NA
Predicted Activation Energy	498.05 meV

Notes: All Li are in tetrahedral bonding environments. Synthetic method by Branford et al.[372]

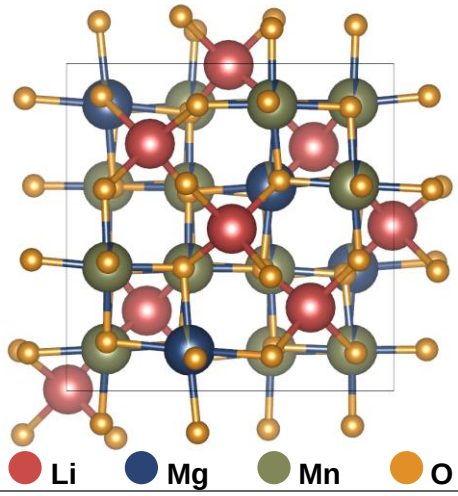

Li_2ZnSiS_4

Material's Project ID	NA
ICSD ID	264457
Space Group	$Pna2_1$ [33]
Calculated Band Gap	NA
Calculated E above E_{hull}	NA
Predicted Activation Energy	507.81 meV

Notes: All Li are in tetrahedral bonding environments. A melt flux synthesis has been developed by Li et al – they examined the material for second-harmonic generation response.[373]

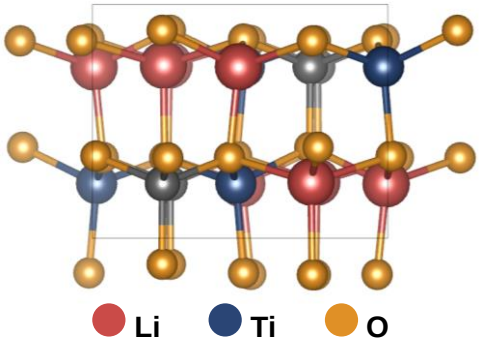

(a-axis view)

$Li_9Ti_{15}O_{32}$

Material's Project ID	NA
ICSD ID	15790
Space Group	$Fd\bar{3}mS$ [227]
Calculated Band Gap	NA
Calculated E above E_{hull}	NA
Predicted Activation Energy	546.88 meV

Notes: Most Li are in tetrahedral bonding environments, with some partial substitution onto the octahedral Ti sites.

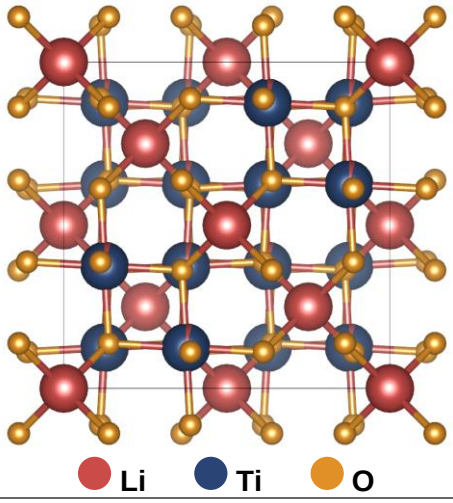

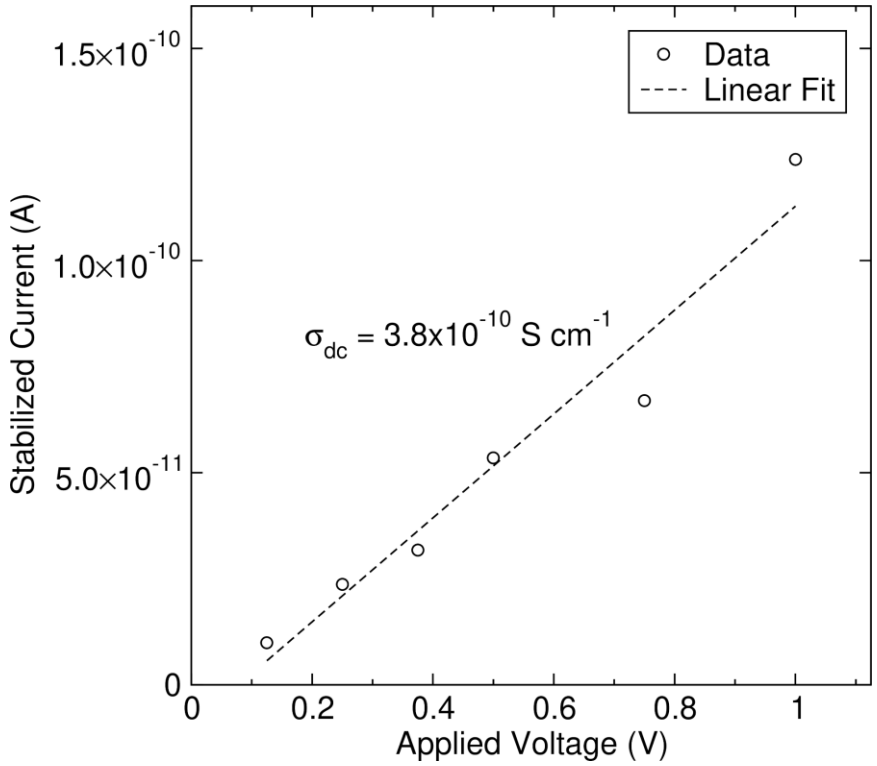

Figure S19. Steady-state current of Au/a-$Li_{2.95}B_{0.95}Si_{0.05}S_3$/Au cell for different voltage polarizations. *Measurements were done at 25°C with applied voltages of 0.125 V, 0.25 V, 0.375 V, 0.5 V and 1.0 V.*

Citations:

1. Ross, S., Welsch, A.-M. & Behrens, H. Lithium conductivity in glasses of the Li_2O–Al_2O_3–SiO_2 system. *Phys. Chem. Chem. Phys.* **17**, 465–474 (2015).
2. Aono, H., Sugimoto, E., Sadaoka, Y., Imanaka, N. & Adachi, G. The electrical properties of ceramic electrolytes for $LiM_xTi_{2-x}(PO_4)_3$ + yLi_2O , M = Ge , Sn , Hf , and Zr systems. *J. Electrochem. Soc.* **140**, 1827 (1993).
3. Mühle, C., Dinnebier, R. E., van Wüllen, L., Schwering, G. & Jansen, M. New insights into the structural and dynamical features of lithium hexaoxometalates Li_7MO_6 (M = Nb, Ta, Sb, Bi). *Inorg. Chem.* **43**, 874–881 (2004).
4. Mizuno, F., Hayashi, A., Tadanaga, K. & Tatsumisago, M. New, highly ion-conductive crystals precipitated from Li_2S–P_2S_5 glasses. *Adv. Mater.* **17**, 918–921 (2005).
5. Yamane, H. *et al.* Crystal structure of a superionic conductor, $Li_7P_3S_{11}$. *Solid State Ion.* **178**, 1163–1167 (2007).
6. Xiao, P. F., Lai, M. O. & Lu, L. Transport and electrochemical properties of high potential tavorite $LiVPO_4F$. *Solid State Ion.* **242**, 10–19 (2013).
7. Hasegawa, T. & Yamane, H. Synthesis and crystal structure analysis of $Li_2NaBP_2O_8$ and $LiNa_2B_5P_2O_{14}$. *J. Solid State Chem.* **225**, 65–71 (2015).
8. Voronin, V. I., Sherstobitova, E. A., Blatov, V. A. & Shekhtman, G. Sh. Lithium-cation conductivity and crystal structure of lithium diphosphate. *J. Solid State Chem.* **211**, 170–175 (2014).
9. Salanne, M., Marrocchelli, D. & Watson, G. W. Cooperative mechanism for the diffusion of Li^+ ions in $LiMgSO_4F$. *J. Phys. Chem. C* **116**, 18618–18625 (2012).
10. Strauss, F. *et al.* Impact of structural polymorphism on ionic conductivity in lithium copper pyroborate $Li_6CuB_4O_{10}$. *Inorg. Chem.* **57**, 11646–11654 (2018).

11. Losilla, E. R., Aranda, M. A. G., Martínez-Lara, M. & Bruque, S. Reversible triclinic-rhombohedral phase transition in $LiHf_2(PO_4)_3$: crystal structures from neutron powder diffraction. *Chem. Mater.* **9**, 1678–1685 (1997).
12. Busche, M. R. *et al.* In situ monitoring of fast li-ion conductor $Li_7P_3S_{11}$ crystallization inside a hot-press setup. *Chem. Mater.* **28**, 6152–6165 (2016).
13. Ohtsuka, H. & Yamaji, A. Preparation and electrical conductivity of LISICON thin films. *Solid State Ion.* **8**, 43–48 (1983).
14. Kanno, R. & Murayama, M. Lithium ionic conductor thio-LISICON: The Li_2S-GeS_2-P_2S_5 system. *J. Electrochem. Soc.* **148**, A742 (2001).
15. Ahn, B. T. & Huggins, R. A. Synthesis and lithium conductivities of Li_2SiS_3 and Li_4SiS_4. *Mater. Res. Bull.* **24**, 889–897 (1989).
16. Deng, Y. *et al.* Structural and mechanistic insights into fast lithium-ion conduction in Li_4SiO_4–Li_3PO_4 solid electrolytes. *J. Am. Chem. Soc.* **137**, 9136–9145 (2015).
17. Khorassani, A. & West, A. R. Li^+ ion conductivity in the system Li_4SiO_4□Li_3VO_4. *J. Solid State Chem.* **53**, 369–375 (1984).
18. Murayama, M. *et al.* Synthesis of new lithium ionic conductor thio-lisicon—lithium silicon sulfides system. *J. Solid State Chem.* **168**, 140–148 (2002).
19. Adachi, G., Imanaka, N. & Aono, H. Fast Li^+ conducting ceramic electrolytes. *Adv. Mater.* **8**, 127–135 (1996).
20. Li, X. *et al.* Water-mediated synthesis of a superionic halide solid electrolyte. *Angew. Chem. Int. Ed.* **58**, 16427–16432 (2019).
21. Dietrich, C. *et al.* Synthesis, structural characterization, and lithium ion conductivity of the lithium thiophosphate $Li_2P_2S_6$. *Inorg. Chem.* **56**, 6681–6687 (2017).
22. Holzmann, T. *et al.* $Li_{0.6}[Li_{0.2}Sn_{0.8}S_2]$ – a layered lithium superionic conductor. *Energy Environ. Sci.* **9**, 2578–2585 (2016).

23. Dolbecq, A. *et al.* Synthesis, X-ray and neutron diffraction characterization, and ionic conduction properties of a new oxothiomolybdate $Li_3[Mo_8S_8O_8(OH)_8\{HWO_5(H_2O)\}]\cdot 18\,H_2O$. *Chem. – Eur. J.* **8**, 349–356 (2002).
24. Huber, S. & Pfitzner, A. $Li_{17}Sb_{13}S_{28}$: A new lithium ion conductor and addition to the phase diagram $Li_2S–Sb_2S_3$. *Chem Eur J* **21**, 13683–13688 (2015).
25. Tomita, Y., Ohki, H., Yamada, K. & Okuda, T. Ionic conductivity and structure of halocomplex salts of group 13 elements. *Solid State Ion.* **136–137**, 351–355 (2000).
26. Asano, T. *et al.* Solid halide electrolytes with high lithium-ion conductivity for application in 4 v class bulk-type all-solid-state batteries. *Adv. Mater.* **30**, 1803075 (2018).
27. Holzmann, T. *et al.* $Li_{0.6}[Li_{0.2}Sn_{0.8}S_2]$ – a layered lithium superionic conductor. *Energy Environ. Sci.* **9**, 2578–2585 (2016).
28. Hockicko, P., Kudelcik, J., Munoz, F. & Munoz-Senovilla, L. Structural and electrical properties of $LiPO_3$ glasses. *Adv. Electr. Electron. Eng.* **13**, 198-205–205 (2015).
29. Rao, S. R., Lingam, C. B., Rajesh, D., Vijayalakshmi, R. P. & Sunandana, C. S. Structural, conductivity and dielectric properties of Li_2SO_4. *Eur. Phys. J. Appl. Phys.* **66**, 30906 (2014).
30. Subban, C. V. *et al.* Search for Li-electrochemical activity and Li-ion conductivity among lithium bismuth oxides. *Solid State Ion.* **283**, 68–74 (2015).
31. Burmakin, E. I., Shehtman, G. S. & Alikin, V. N. Ionic conductivity of $Li_6Ge_2O_7$ and its solid solutions. *Materials Science Forum* vol. 76 107–110 /MSF.76.107 (1991).
32. Weppner, W. & Huggins, R. A. Ionic conductivity of solid and liquid $LiAlCl_4$. *J. Electrochem. Soc.* **124**, 35 (1977).
33. Hellstrom, E. E. & Van Gool, W. Li ion conduction in Li_2ZrO_3, Li_4ZrO_4, and $LiScO_2$. *Solid State Ion.* **2**, 59–64 (1981).
34. Heitjans, P., Tobschall, E. & Wilkening, M. Ion transport and diffusion in nanocrystalline and glassy ceramics. *Eur. Phys. J. Spec. Top.* **161**, 97–108 (2008).

35. Chinnam, P. R., Clymer, R. N., Jalil, A. A., Wunder, S. L. & Zdilla, M. J. Bulk-phase ion conduction in cocrystalline LiCl·N,N-dimethylformamide: a new paradigm for solid electrolytes based upon the pearson hard–soft acid–base concept. *Chem. Mater.* **27**, 5479–5482 (2015).

36. Iqbal, M. *et al.* Lithium ion conduction in doped $LaLiO_2$ system. *Solid State Ion.* **285**, 33–37 (2016).

37. Yin, S.-C., Strobel, P. S., Grondey, H. & Nazar, L. F. $Li_{2.5}V_2(PO_4)_3$: A room-temperature analogue to the fast-ion conducting high-temperature γ-phase of $Li_3V_2(PO_4)_3$. *Chem. Mater.* **16**, 1456–1465 (2004).

38. Saha, S. *et al.* Polymorphism in $Li_4Zn(PO_4)_2$ and stabilization of its structural disorder to improve ionic conductivity. *Chem. Mater.* **30**, 1379–1390 (2018).

39. de Laune, B. P., Bayliss, R. D. & Greaves, C. $LiSbO_2$: synthesis, structure, stability, and lithium-ion conductivity. *Inorg. Chem.* **50**, 7880–7885 (2011).

40. Kim, S.-C., Kwak, H.-J., Yoo, C.-Y., Yun, H. & Kim, S.-J. Synthesis, crystal structure, and ionic conductivity of a new layered metal phosphate, $Li_2Sr_2Al(PO_4)_3$. *J. Solid State Chem.* **243**, 12–17 (2016).

41. Pantyukhina, M. I., Shchelkanova, M. S., Stepanov, A. P. & Buzlukov, A. L. Investigation of ion transport in Li_8ZrO_6 and $Li_6Zr_2O_7$ solid electrolytes. *Bull. Russ. Acad. Sci. Phys.* **74**, 653–655 (2010).

42. Miyazaki, R. & Maekawa, H. Li^+-ion conduction of Li_3AlF_6 mechanically milled with LiCl. *ECS Electrochem. Lett.* **1**, A87 (2012).

43. Brant, J. A. *et al.* Fast lithium ion conduction in Li_2SnS_3: synthesis, physicochemical characterization, and electronic structure. *Chem. Mater.* **27**, 189–196 (2015).

44. Kim, J., Kim, J., Avdeev, M., Yun, H. & Kim, S.-J. $LiTa_2PO_8$: a fast lithium-ion conductor with new framework structure. *J. Mater. Chem. A* **6**, 22478–22482 (2018).

45. Krichen, M., Megdiche, M., Guidara, K. & Gargouri, M. AC conductivity and mechanism of conduction study of lithium barium pyrophosphate $Li_2BaP_2O_7$ using impedance spectroscopy. *Ionics* **21**, 935–948 (2015).

46. Huang, F. Q., Yao, J., Liu, Z., Yang, J. & Ibers, J. A. Synthesis, structure, and ionic conductivity of $Na_5Li_3Ti_2S_8$. *J. Solid State Chem.* **181**, 837–841 (2008).

47. Ettis, H., Naïli, H. & Mhiri, T. The crystal structure, thermal behaviour and ionic conductivity of a novel lithium gadolinium polyphosphate $LiGd(PO_3)_4$. *J. Solid State Chem.* **179**, 3107–3113 (2006).

48. Muller, Ch., Valmalette, J.-C., Soubeyroux, J.-L., Bouree, F. & Gavarri, J.-R. Structural disorder and ionic conductivity in $LiVO_3$: a neutron powder diffraction study from 340 to 890 k. *J. Solid State Chem.* **156**, 379–389 (2001).

49. Kanno, R. *et al.* Synthesis, structure, ionic conductivity, and phase transformation of new double chloride spinel, Li_2CrCl_4. *J. Solid State Chem.* **75**, 41–51 (1988).

50. Schlem, R. *et al.* Lattice dynamical approach for finding the lithium superionic conductor Li_3ErI_6. *ACS Appl. Energy Mater.* **3**, 3684–3691 (2020).

51. Kimura, T. *et al.* Preparation and characterization of lithium ion conductive Li_3SbS_4 glass and glass-ceramic electrolytes. *Solid State Ion.* **333**, 45–49 (2019).

52. Liu, Z. *et al.* Anomalous high ionic conductivity of nanoporous β-Li_3PS_4. *J. Am. Chem. Soc.* **135**, 975–978 (2013).

53. Almond, D. P., Hunter, C. C. & West, A. R. The extraction of ionic conductivities and hopping rates from a.c. conductivity data. *J. Mater. Sci.* **19**, 3236–3248 (1984).

54. Cakmak, G., Nuss, J. & Jansen, M. LiB_6O_9F, the first lithium fluorooxoborate – crystal structure and ionic conductivity. *Z. Für Anorg. Allg. Chem.* **635**, 631–636 (2009).

55. Olivier-Fourcade, J., Maurin, M. & Philippot, E. Modification de la nature de la conductivite electrique par creation de sites vacants dans les phases a caractere semi-conducteur du systeme $Li_2SSb_2S_3$. *Solid State Ion.* **9–10**, 135–137 (1983).

56. Yamane, H., Kikkawa, S. & Koizumi, M. Preparation of lithium silicon nitrides and their lithium ion conductivity. *Solid State Ion.* **25**, 183–191 (1987).

57. Senevirathne, K., Day, C. S., Gross, M. D., Lachgar, A. & Holzwarth, N. A. W. A new crystalline LiPON electrolyte: Synthesis, properties, and electronic structure. *Solid State Ion.* **233**, 95–101 (2013).

58. Seo, I. & Kim, Y. Synthesis and characterization of lithium germanogallium sulfide, $Li_2GeGa_2S_6$. *Solid State Ion.* **261**, 106–110 (2014).

59. Ibarra, J. *et al.* Influence of composition on the structure and conductivity of the fast ionic conductors $La_{2/3-x}Li_{3x}TiO_3$ (0.03≤x≤0.167). *Solid State Ion.* **134**, 219–228 (2000).

60. Belous, A. G., Gavrilenko, O. N., V'yunov, O. I., Kobilyanskaya, S. D. & Trachevskii, V. V. Effect of isovalent substitution on the structure and ionic conductivity of $Li_{0.5-y}Na_yLa_{0.5}\square Nb_2O_6$. *Inorg. Mater.* **47**, 308–312 (2011).

61. Bohnke, O. *et al.* Lithium ion conductivity in new perovskite oxides $[Ag_yLi_{1-y}]_{3x}La_{2/3-x}TiO_3$ (x = 0.09 and 0 ≤ y ≤ 1). *Chem. Mater.* **13**, 1593–1599 (2001).

62. Itoh, M., Inaguma, Y., Jung, W.-H., Chen, L. & Nakamura, T. High lithium ion conductivity in the perovskite-type compounds $Ln_{12}Li_{12}TiO_3$(Ln=La,Pr,Nd,Sm). *Solid State Ion.* **70–71**, 203–207 (1994).

63. Geng, H., Lan, J., Mei, A., Lin, Y. & Nan, C. W. Effect of sintering temperature on microstructure and transport properties of $Li_{3x}La_{2/3-x}TiO_3$ with different lithium contents. *Electrochimica Acta* **56**, 3406–3414 (2011).

64. Raistrick, I. D., Ho, C. & Huggins, R. A. Lithium ion conduction in Li_5A10_4, Li_5GaO_4 and Li_6ZnO_4. *Mater. Res. Bull.* **11**, 953–957 (1976).

65. Saskia Lupart, Gregori, G., Maier, J. & Schnick, W. $Li_{14}Ln_5[Si_{11}N_{19}O_5]O_2F_2$ with Ln = Ce, Nd—representatives of a family of potential lithium ion conductors. *J. Am. Chem. Soc.* **134**, 10132–10137 (2012).

66. Narimatsu, E., Yamamoto, Y., Takeda, T., Nishimura, T. & Hirosaki, N. High lithium conductivity in $Li_{1-2x}Ca_xSi_2N_3$. *J. Mater. Res.* **26**, 1133–1142 (2011).

67. Dissanayake, M. a. K. L. & West, A. R. Structure and conductivity of an Li_4SiO_4–Li_2SO_4 solid solution phase. *J. Mater. Chem.* **1**, 1023–1025 (1991).

68. Ivanov-Shitz, A. K., Kireev, V. V., Mel'nikov, O. K. & Demianets, L. N. Growth and ionic conductivity of γ-Li_3PO_4. *Crystallogr. Rep.* **46**, 864–867 (2001).

69. Kaup, K. *et al.* Correlation of structure and fast ion conductivity in the solid solution series $Li_{1+2x}Zn_{1-x}PS_4$. *Chem. Mater.* **30**, 592–596 (2018).

70. Wang, B., Chakoumakos, B. C., Sales, B. C., Kwak, B. S. & Bates, J. B. Synthesis, crystal structure, and ionic conductivity of a polycrystalline lithium phosphorus oxynitride with the γ-Li_3PO_4 structure. *J. Solid State Chem.* **115**, 313–323 (1995).

71. Kanno, R., Hata, T., Kawamoto, Y. & Irie, M. Synthesis of a new lithium ionic conductor, thio-LISICON–lithium germanium sulfide system. *Solid State Ion.* **130**, 97–104 (2000).

72. Abrahams, I., Bruce, P. G., West, A. R. & David, W. I. F. Structure determination of LISICON solid solutions by powder neutron diffraction. *J. Solid State Chem.* **75**, 390–396 (1988).

73. Burmakin, E. I., Voronin, V. I. & Shekhtman, G. Sh. Crystalline structure and electroconductivity of solid electrolytes $Li_{3.75}Ge_{0.75}V_{0.25}O_4$ and $Li_{3.70}Ge_{0.85}W_{0.15}O_4$. *Russ. J. Electrochem.* **39**, 1124–1129 (2003).

74. Pham, Q. N., Crosnier-Lopez, M.-P., Le Berre, F., Fauth, F. & Fourquet, J.-L. Crystal structure of new Li^+ ion conducting perovskites: $Li_{2x}Ca_{0.5-x}TaO_3$ and $Li_{0.2}[Ca_{1-y}Sr_y]_{0.4}TaO_3$. *Solid State Sci.* **6**, 923–929 (2004).

75. Sebastian, L., Piffard, Y., K. Shukla, A., Taulelle, F. & Gopalakrishnan, J. Synthesis, structure and lithium-ion conductivity of $Li_{2-2x}Mg_{2+x}(MoO_4)_3$ and $Li_3M(MoO_4)_3$ (M III = Cr, Fe). *J. Mater. Chem.* **13**, 1797–1802 (2003).

76. Kaib, T. *et al.* Lithium chalcogenidotetrelates: LiChT—synthesis and characterization of new Li^+ ion conducting Li/Sn/Se compounds. *Chem. Mater.* **25**, 2961–2969 (2013).

77. Roedern, E. *et al.* Solid state synthesis, structural characterization and ionic conductivity of bimetallic alkali-metal yttrium borohydrides $M_Y(BH_4)_4$ (M = Li and Na). *J. Mater. Chem. A* **4**, 8793–8802 (2016).

78. Barpanda, P. *et al.* $LiZnSO_4F$ made in an ionic liquid: a ceramic electrolyte composite for solid-state lithium batteries. *Angew. Chem. Int. Ed.* **50**, 2526–2531 (2011).

79. Murayama, M., Sonoyama, N., Yamada, A. & Kanno, R. Material design of new lithium ionic conductor, thio-LISICON, in the Li_2S–P_2S_5 system. *Solid State Ion.* **170**, 173–180 (2004).

80. Kaib, T. *et al.* New lithium chalcogenidotetrelates, LiChT: synthesis and characterization of the Li^+-conducting tetralithium ortho-sulfidostannate Li_4SnS_4. *Chem. Mater.* **24**, 2211–2219 (2012).

81. Maekawa, H., Iwatani, T., Shen, H., Yamamura, T. & Kawamura, J. Enhanced lithium ion conduction and the size effect on interfacial phase in Li_2ZnI_4–mesoporous alumina composite electrolyte. *Solid State Ion.* **178**, 1637–1641 (2008).

82. Morales, M. & West, A. R. Phase diagram, crystal chemistry and lithium ion conductivity in the perovskite-type system $Pr_{0.5+x}Li_{0.5-3x}TiO_3$. *Solid State Ion.* **91**, 33–43 (1996).

83. Park, K.-H. *et al.* High-voltage superionic halide solid electrolytes for all-solid-state Li-ion batteries. *ACS Energy Lett.* **5**, 533–539 (2020).

84. Kuwano, J. & West, A. R. New Li^+ ion conductors in the system, Li_4GeO_4-Li_3VO_4. *Mater. Res. Bull.* **15**, 1661–1667 (1980).

85. Sahu, G. *et al.* Air-stable, high-conduction solid electrolytes of arsenic-substituted Li_4SnS_4. *Energy Environ. Sci.* **7**, 1053–1058 (2014).

86. Inaguma, Y. *et al.* Effect of substitution and pressure on lithium ion conductivity in perovskites $Ln_{12}Li_{12}TiO_3$ (Ln = La, Pr, Nd AND Sm). *J. Phys. Chem. Solids* **58**, 843–852 (1997).

87. Hodge, I. M., Ingram, M. D. & West, A. R. Ionic conductivity of Li_4SiO_4, Li_4GeO_4, and their solid solutions. *J. Am. Ceram. Soc.* **59**, 360–366 (1976).

88. Schwering, G., Hönnerscheid, A., van Wüllen, L. & Jansen, M. High lithium ionic conductivity in the lithium halide hydrates $Li_{3-n}(OH_n)Cl$ ($0.83 \leq n \leq 2$) and $Li_{3-n}(OH_n)Br$ ($1 \leq n \leq 2$) at ambient temperatures. *ChemPhysChem* **4**, 343–348 (2003).

89. Kanno, R. *et al.* Ionic conductivity and phase transition of the bromide spinels, $Li_{2-2x}M_{1+x}Br_4$ (M = Mg , Mn). *J. Electrochem. Soc.* **133**, 1052 (1986).

90. Kwon, W. J. *et al.* Enhanced Li^+ conduction in perovskite $Li_{3x}La_{2/3-x}\square_{1/3-2x}TiO_3$ solid-electrolytes via microstructural engineering. *J. Mater. Chem. A* **5**, 6257–6262 (2017).

91. Saha, D., Madras, G., Bhattacharyya, A. J. & Guru Row, T. N. Synthesis, structure and ionic conductivity in scheelite type $Li_{0.5}Ce_{0.5-x}Ln_xMoO_4$ (x = 0 and 0.25, Ln = Pr, Sm). *J. Chem. Sci.* **123**, 5–13 (2011).

92. González, C., López, M. L., Gaitán, M., Veiga, M. L. & Pico, C. Relationship between crystal structure and electric properties for lithium-containing spinels. *Mater. Res. Bull.* **29**, 903–910 (1994).

93. Yamane, H., Kikkawa, S. & Koizumi, M. High- and low-temperature phases of lithium boron nitride, Li_3BN_2: Preparation, phase relation, crystal structure, and ionic conductivity. *J. Solid State Chem.* **71**, 1–11 (1987).

94. Kim, C.-S., Hwang, Y.-H., Kim, H. K. & Kim, J. N. Ionic conductivity of crystalline and glassy $Li_2B_4O_7$. *Phys. Chem. Glas.* **44**, 166–169 (2003).

95. Schnick, W. & Luecke, J. Lithium ion conductivity of $LiPN_2$ and Li_7PN_4. *Solid State Ion.* **38**, 271–273 (1990).

96. Inaguma, Y. *et al.* High ionic conductivity in lithium lanthanum titanate. *Solid State Commun.* **86**, 689–693 (1993).

97. Harada, Y., Ishigaki, T., Kawai, H. & Kuwano, J. Lithium ion conductivity of polycrystalline perovskite $La_{0.67-x}Li_{3x}TiO_3$ with ordered and disordered arrangements of the A-site ions. *Solid State Ion.* **108**, 407–413 (1998).

98. Zhang, H., Liu, X., Qi, Y. & Liu, V. On the $La_{2/3-x}Li_{3x}TiO_3/Al_2O_3$ composite solid-electrolyte for Li-ion conduction. *J. Alloys Compd.* **577**, 57–63 (2013).

99. Thangadurai, V. *et al.* X-ray powder diffraction study of $LiLnTiO_4$ (Ln=La, Nd): a lithium-ion conductor. *Materials Science Forum* vols 321–324 965–970 /MSF.321-324.965 (2000).

100. Katsumata, T., Takahata, M., Mochizuki, N. & Inaguma, Y. The relationship between Li ion conductivity and crystal structure for ordered perovskite compounds, $(La_{2/3-1/3p}Li_p)(Mg_{1/2}W_{1/2})O_3$ (p=0.05, 0.11 and 0.14). *Solid State Ion.* **171**, 191–198 (2004).

101. Sedlmaier, S. J. *et al.* Li_4PS_4I: A Li^+ superionic conductor synthesized by a solvent-based soft chemistry approach. *Chem. Mater.* **29**, 1830–1835 (2017).

102. Kato, Y. *et al.* High-power all-solid-state batteries using sulfide superionic conductors. *Nat. Energy* **1**, 1–7 (2016).

103. Takada, K. *et al.* Lithium ion conductive oxysulfide, Li_3PO_4–Li_3PS_4. *Solid State Ion.* **176**, 2355–2359 (2005).

104. Kwon, O. *et al.* Synthesis, structure, and conduction mechanism of the lithium superionic conductor $Li_{10+\delta}Ge_{1+\delta}P_{2-\delta}S_{12}$. *J. Mater. Chem. A* **3**, 438–446 (2015).

105. Hori, S. *et al.* Synthesis, structure, and ionic conductivity of solid solution, $Li_{10+\delta}M_{1+\delta}P_{2-\delta}S_{12}$ (M = Si, Sn). *Faraday Discuss.* **176**, 83–94 (2015).

106. Whiteley, J. M., Woo, J. H., Hu, E., Nam, K.-W. & Lee, S.-H. Empowering the lithium metal battery through a silicon-based superionic conductor. *J. Electrochem. Soc.* **161**, A1812 (2014).

107. Bron, P. *et al.* $Li_{10}SnP_2S_{12}$: an affordable lithium superionic conductor. *J. Am. Chem. Soc.* **135**, 15694–15697 (2013).

108. Krauskopf, T., Culver, S. P. & Zeier, W. G. Bottleneck of diffusion and inductive effects in $Li_{10}Ge_{1-x}Sn_xP_2S_{12}$. *Chem. Mater.* **30**, 1791–1798 (2018).

109. Hori, S. *et al.* Structure–property relationships in lithium superionic conductors having a $Li_{10}GeP_2S_{12}$-type structure. *Acta Crystallogr. Sect. B Struct. Sci. Cryst. Eng. Mater.* **71**, 727–736 (2015).

110. Kamaya, N. *et al.* A lithium superionic conductor. *Nat. Mater.* **10**, 682–686 (2011).

111. Sun, Y., Suzuki, K., Hori, S., Hirayama, M. & Kanno, R. Superionic Conductors: $Li_{10+\delta}[Sn_ySi_{1-y}]_{1+\delta}P_{2-\delta}S_{12}$ with a $Li_{10}GeP_2S_{12}$-type Structure in the Li_3PS_4–Li_4SnS_4–Li_4SiS_4 Quasi-ternary System. *Chem. Mater.* **29**, 5858–5864 (2017).

112. Sun, Y. *et al.* A facile strategy to improve the electrochemical stability of a lithium ion conducting $Li_{10}GeP_2S_{12}$ solid electrolyte. *Solid State Ion.* **301**, 59–63 (2017).

113. Weber, D. A. *et al.* Structural insights and 3D diffusion pathways within the lithium superionic conductor $Li_{10}GeP_2S_{12}$. *Chem. Mater.* **28**, 5905–5915 (2016).

114. Sato, M., Abo, J., Jin, T. & Ohta, M. Structure and ionic conductivity of $MLaNb_2O_7$ (M = K, Na, Li, H). *J. Alloys Compd.* **192**, 81–83 (1993).

115. Bhuvanesh, N. S. P., Crosnier-Lopez, M. P., Bohnke, O., Emery, J. & Fourquet, J. L. Synthesis, crystal structure, and ionic conductivity of novel Ruddlesden−Popper related phases, $Li_4Sr_3Nb_{5.77}Fe_{0.23}O_{19.77}$ and $Li_4Sr_3Nb_6O_{20}$. *Chem. Mater.* **11**, 634–641 (1999).

116. Cordier, G., Gudat, A., Kniep, R. & Rabenau, A. LiCaN and Li_4SrN_2, derivatives of the fluorite and lithium nitride structures. *Angew. Chem. Int. Ed. Engl.* **28**, 1702–1703 (1989).

117. Zhao, G., Muhammad, I., Suzuki, K., Hirayama, M. & Kanno, R. Synthesis, crystal structure, and the ionic conductivity of new lithium ion conductors, *M*-doped $LiScO_2$ (*M* = Zr, Nb, Ta). *Mater. Trans.* **57**, 1370–1373 (2016).

118. Awaka, J. *et al.* Neutron powder diffraction study of tetragonal $Li_7La_3Hf_2O_{12}$ with the garnet-related type structure. *J. Solid State Chem.* **183**, 180–185 (2010).

119. Awaka, J., Kijima, N., Hayakawa, H. & Akimoto, J. Synthesis and structure analysis of tetragonal $Li_7La_3Zr_2O_{12}$ with the garnet-related type structure. *J. Solid State Chem.* **182**, 2046–2052 (2009).

120. Il'ina, E. A. & Pershina, S. V. Composite electrolytes based on tetragonal $Li_7La_3Zr_2O_{12}$ for lithium batteries. in *Solid Electrolytes for Advanced Applications: Garnets and Competitors* (eds. Murugan, R. & Weppner, W.) 167–193 (Springer International Publishing, 2019). doi:10.1007/978-3-030-31581-8_8.

121. Inada, R., Kusakabe, K., Tanaka, T., Kudo, S. & Sakurai, Y. Synthesis and properties of Al-free $Li_{7-x}La_3Zr_{2-x}Ta_xO_{12}$ garnet related oxides. *Solid State Ion.* **262**, 568–572 (2014).

122. Quintana, P. & West, A. R. Conductivity of lithium gallium silicates. *Solid State Ion.* **23**, 179–182 (1987).

123. Mukai, K. & Nunotani, N. Crystal structure and li-ion conductivity of $LiGa_{1-x}Al_xGeO_4$ phenacite compounds with $0 \leq x \leq 1$. *J. Electrochem. Soc.* **163**, A2371 (2016).

124. Arbi, K., Hoelzel, M., Kuhn, A., García-Alvarado, F. & Sanz, J. Structural factors that enhance lithium mobility in fast-ion $Li_{1+x}Ti_{2-x}Al_x(PO_4)_3$ ($0 \leq x \leq 0.4$) conductors investigated by neutron diffraction in the temperature range 100–500 K. *Inorg. Chem.* **52**, 9290–9296 (2013).

125. Mellander, B.-E., Granéli, B. & Roos, J. Ionic conductivity of single crystal $LiNaSO_4$. *Solid State Ion.* **40–41**, 162–164 (1990).

126. Takada, K. *et al.* Lithium ion conduction in lithium magnesium thio-phosphate. *Solid State Ion.* **147**, 23–27 (2002).

127. Hood, Z. D. *et al.* Structural and electrolyte properties of $Li_4P_2S_6$. *Solid State Ion.* **284**, 61–70 (2016).

128. Dietrich, C. *et al.* Local structural investigations, defect formation, and ionic conductivity of the lithium ionic conductor $Li_4P_2S_6$. *Chem. Mater.* **28**, 8764–8773 (2016).

129. Muy, S. *et al.* High-throughput screening of solid-state Li-ion conductors using lattice-dynamics descriptors. *iScience* **16**, 270–282 (2019).

130. Leube, B. T. *et al.* Lithium transport in $Li_{4.4}M_{0.4}M'_{0.6}S_4$ (M = Al^{3+}, Ga^{3+}, and M′ = Ge^{4+}, Sn^{4+}): Combined crystallographic, conductivity, solid state NMR, and computational studies. *Chem. Mater.* **30**, 7183–7200 (2018).

131. Hartwig, P., Weppner, W. & Wichelhaus, W. Fast ionic lithium conduction in solid lithium nitride chloride. *Mater. Res. Bull.* **14**, 493–498 (1979).

132. Kahlaoui, R. *et al.* Cation miscibility and lithium mobility in NASICON $Li_{1+x}Ti_{2-x}Sc_x(PO_4)_3$ ($0 \leq x \leq 0.5$) series: A combined NMR and impedance study. *Inorg. Chem.* **56**, 1216–1224 (2017).

133. Weiss, M., Weber, D. A., Senyshyn, A., Janek, J. & Zeier, W. G. Correlating transport and structural properties in $Li_{1+x}Al_xGe_{2-x}(PO_4)_3$ (LAGP) prepared from aqueous solution. *ACS Appl. Mater. Interfaces* **10**, 10935–10944 (2018).

134. Aono, H., Sugimoto, E., Sadaoka, Y., Imanaka, N. & Adachi, G. Ionic conductivity of solid electrolytes based on lithium titanium phosphate. *J. Electrochem. Soc.* **137**, 1023 (1990).

135. Bounar, N., Benabbas, A., Bouremmad, F., Ropa, P. & Carru, J.-C. Structure, microstructure and ionic conductivity of the solid solution $LiTi_{2-x}Sn_x(PO_4)_3$. *Phys. B Condens. Matter* **407**, 403–407 (2012).

136. Li, Y., Liu, M., Liu, K. & Wang, C.-A. High Li^+ conduction in NASICON-type $Li_{1+x}Y_xZr_{2-x}(PO_4)_3$ at room temperature. *J. Power Sources* **240**, 50–53 (2013).

137. Petit, D., Colomban, Ph., Collin, G. & Boilot, J. P. Fast ion transport in $LiZr_2(PO_4)_3$: Structure and conductivity. *Mater. Res. Bull.* **21**, 365–371 (1986).

138. Kothari, D. H. & Kanchan, D. K. Effect of doping of trivalent cations Ga^{3+}, Sc^{3+}, Y^{3+} in $Li_{1.3}Al_{0.3}Ti_{1.7}(PO_4)_3$ (LATP) system on Li^+ ion conductivity. *Phys. B Condens. Matter* **501**, 90–94 (2016).

139. Aono, H., Sugimoto, E., Sadaaka, Y., Imanaka, N. & Adachi, G. Y. Ionic conductivity of the lithium titanium phosphate ($Li_{1+x}M_xTi_{2-x}(PO_4)_3$, M=Al, Sc, Y, and La) systems. *J. Electrochem. Soc.* **136**, 590 (1989).

140. Xu, H., Wang, S., Wilson, H., Zhao, F. & Manthiram, A. Y-doped NASICON-type $LiZr_2(PO_4)_3$ solid electrolytes for lithium-metal batteries. *Chem. Mater.* **29**, 7206–7212 (2017).

141. Fu, J. Fast Li^+ ion conducting glass-ceramics in the system Li_2O–Al_2O_3–GeO_2–P_2O_5. *Solid State Ion.* **104**, 191–194 (1997).

142. Best, A. S., Forsyth, M. & MacFarlane, D. R. Stoichiometric changes in lithium conducting materials based on $Li_{1+x}Al_xTi_{2-x}(PO_4)_3$: impedance, X-ray and NMR studies. *Solid State Ion.* **136–137**, 339–344 (2000).

143. Arbi, K. *et al.* Lithium mobility in $Li_{1.2}Ti_{1.8}R_{0.2}(PO_4)_3$ compounds (R = Al, Ga, Sc, In) as followed by NMR and impedance spectroscopy. *Chem. Mater.* **16**, 255–262 (2004).

144. Šalkus, T. *et al.* Ionic conductivity of $Li_{1.3}Al_{0.3-x}Sc_xTi_{1.7}(PO_4)_3$ (x=0, 0.1, 0.15, 0.2, 0.3) solid electrolytes prepared by Pechini process. *Solid State Ion.* **225**, 615–619 (2012).

145. Pérez-Estébanez, M., Isasi-Marín, J., Többens, D. M., Rivera-Calzada, A. & León, C. A systematic study of Nasicon-type $Li_{1+x}M_xTi_{2-x}(PO_4)_3$ (M: Cr, Al, Fe) by neutron diffraction and impedance spectroscopy. *Solid State Ion.* **266**, 1–8 (2014).

146. Aono, H., Sugimoto, E., Sadaoka, Y., Imanaka, N. & Adachi, G. Electrical properties and sinterability for lithium germanium phosphate $Li_{1+x}M_xGe_{2-x}(PO_4)_3$, M = Al, Cr, Ga, Fe, Sc, and In systems. *Bull. Chem. Soc. Jpn.* **65**, 2200–2204 (1992).

147. Mugnier, Y., Galez, C., Crettez, J. M., Bourson, P. & Bouillot, J. Dielectric characterization and ionic conductivity of α-$LiIO_3$ crystals related to the growth conditions. *Solid State Commun.* **115**, 619–623 (2000).

148. Yahia, H. B., Shikano, M., Takeuchi, T., Kobayashi, H. & Itoh, M. Crystal structures of the new fluorophosphates $Li_9Mg_3[PO_4]_4F_3$ and $Li_2Mg[PO_4]F$ and ionic conductivities of selected compositions. *J. Mater. Chem. A* **2**, 5858–5869 (2014).

149. Naddari, T., Savariault, J.-M., Feki, H. E., Salles, P. & Salah, A. B. Conductivity and structural investigations in Lacunary $Pb_6Ca_2Li_2(PO_4)_6$ Apatite. *J. Solid State Chem.* **166**, 237–244 (2002).

150. Sato, M., Kono, Y., Ueda, H., Uematsu, K. & Toda, K. Bulk and grain boundary ionic conduction in lithium rare earth-silicates "$LiLnSiO_4$" (Ln = La, Nd, Sm, Eu, Gd, Dy). *Solid State Ion.* **83**, 249–256 (1996).

151. Johnson, R. T., Morosin, B., Knotek, M. L. & Biefeld, R. M. Ionic conductivity in $LiAlSiO_4$. *Phys. Lett. A* **54**, 403–404 (1975).

152. Matsuo, M. *et al.* Synthesis and lithium fast-ion conductivity of a new complex hydride $Li_3(NH_2)_2I$ with double-layered structure. *Chem. Mater.* **22**, 2702–2704 (2010).

153. Aimi, A. *et al.* Synthesis, structure and ionic conductivities of novel Li-ion conductor $A_3Li_xTa_{6-x}Zr_xSi_4O_{26}$ (A=Sr and Ba). *Solid State Ion.* **285**, 19–28 (2016).

154. Alpen, U. v., Rabenau, A. & Talat, G. H. Ionic conductivity in Li_3N single crystals. *Appl. Phys. Lett.* **30**, 621–623 (1977).

155. Lapp, T., Skaarup, S. & Hooper, A. Ionic conductivity of pure and doped Li_3N. *Solid State Ion.* **11**, 97–103 (1983).

156. Röska, B., Akter, I., Hoelzel, M. & Park, S.-H. Na^+/Li^+-ionic conductivity in $Fe_2Na_2K[Li_3Si_{12}O_{30}]$. *J. Solid State Chem.* **264**, 98–107 (2018).

157. Nazri, G. Preparation, structure and ionic conductivity of lithium phosphide. *Solid State Ion.* **34**, 97–102 (1989).

158. Thangadurai, V. & Weppner, W. Effect of sintering on the ionic conductivity of garnet-related structure $Li_5La_3Nb_2O_{12}$ and In- and K-doped $Li_5La_3Nb_2O_{12}$. *J. Solid State Chem.* **179**, 974–984 (2006).

159. Thangadurai, V. & Weppner, W. $Li_6ALa_2Nb_2O_{12}$ (A=Ca, Sr, Ba): A new class of fast lithium ion conductors with garnet-like structure. *J. Am. Ceram. Soc.* **88**, 411–418 (2005).

160. Watelet, H., Picard, J.-P., Besse, J.-P., Baud, G. & Chevalier, R. Structure et proprietes de conduction du compose $K_{0,1}Li_{0,9}SbO_3$. *Solid State Ion.* **2**, 191–194 (1981).

161. Eickhoff, H. *et al.* Lithium phosphidogermanates α- and β-Li_8GeP_4—A novel compound class with mixed Li^+ ionic and electronic conductivity. *Chem. Mater.* **30**, 6440–6448 (2018).

162. Yamane, H., Kikkawa, S. & Koizumi, M. Lithium aluminum nitride, Li_3AlN_2 as a lithium solid electrolyte. *Solid State Ion.* **15**, 51–54 (1985).

163. Kawai, H., Tabuchi, M., Nagata, M., Tukamoto, H. & West, A. R. Crystal chemistry and physical properties of complex lithium spinels $Li_2MM'_3O_8$ (M=Mg, Co, Ni, Zn; M′=Ti, Ge). *J. Mater. Chem.* **8**, 1273–1280 (1998).

164. Shiiba, H., Nakayama, M. & Nogami, M. Ionic conductivity of lithium in spinel-type $Li_{4/3}Ti_{5/3}O_4$–$LiMg_{1/2}Ti_{3/2}O_4$ solid-solution system. *Solid State Ion.* **181**, 994–1001 (2010).

165. Obayashi, H., Gotoh, A. & Nagai, R. Composition dependence of lithium ionic conductivity in lithium nitride-lithium iodide system. *Mater. Res. Bull.* **16**, 581–585 (1981).

166. Cros, C., Hanebali, L., Latie´, L., Villeneuve, G. & Gang, W. Structure, ionic motion and conductivity in some solid-solutions of the $LiClMCl_2$ systems (M=Mg,V,Mn). *Solid State Ion.* **9–10**, 139–147 (1983).

167. Kraft, M. A. *et al.* Influence of lattice polarizability on the ionic conductivity in the lithium superionic argyrodites Li_6PS_5X (X = cl, br, i). *J. Am. Chem. Soc.* **139**, 10909–10918 (2017).

168. Minafra, N., P. Culver, S., Krauskopf, T., Senyshyn, A. & G. Zeier, W. Effect of Si substitution on the structural and transport properties of superionic Li-argyrodites. *J. Mater. Chem. A* **6**, 645–651 (2018).

169. Inoue, Y., Suzuki, K., Matsui, N., Hirayama, M. & Kanno, R. Synthesis and structure of novel lithium-ion conductor $Li_7Ge_3PS_{12}$. *J. Solid State Chem.* **246**, 334–340 (2017).

170. Sakuda, A. *et al.* Mechanochemically prepared Li_2S–P_2S_5–$LiBH_4$ solid electrolytes with an argyrodite structure. *ACS Omega* **3**, 5453–5458 (2018).

171. Boulineau, S., Courty, M., Tarascon, J.-M. & Viallet, V. Mechanochemical synthesis of Li-argyrodite Li_6PS_5X (X=Cl, Br, I) as sulfur-based solid electrolytes for all solid state batteries application. *Solid State Ion.* **221**, 1–5 (2012).

172. Bernges, T., Culver, S. P., Minafra, N., Koerver, R. & Zeier, W. G. Competing structural influences in the Li superionic conducting argyrodites $Li_6PS_{5-x}Se_xBr$ ($0 \le x \le 1$) upon Se substitution. *Inorg. Chem.* **57**, 13920–13928 (2018).

173. Kong, S.-T. *et al.* Li_6PO_5Br and Li_6PO_5Cl: The first lithium-oxide-argyrodites. *Z. Für Anorg. Allg. Chem.* **636**, 1920–1924 (2010).

174. Rao, R. P. & Adams, S. Studies of lithium argyrodite solid electrolytes for all-solid-state batteries. *Phys. Status Solidi A* **208**, 1804–1807 (2011).

175. Kraft, M. A. *et al.* Inducing high ionic conductivity in the lithium superionic argyrodites $Li_{6+x}P_{1-x}Ge_xS_5I$ for all-solid-state batteries. *J. Am. Chem. Soc.* **140**, 16330–16339 (2018).

176. Deiseroth, H.-J. *et al.* Li_7PS_6 and Li_6PS_5X (X: Cl, Br, I): possible three-dimensional diffusion pathways for lithium ions and temperature dependence of the ionic conductivity by impedance measurements. *Z. Für Anorg. Allg. Chem.* **637**, 1287–1294 (2011).

177. Song, Y. B. *et al.* Tailoring solution-processable li argyrodites $Li_{6+x}P_{1-x}M_xS_5I$ (M = Ge, Sn) and their microstructural evolution revealed by cryo-tem for all-solid-state batteries. *Nano Lett.* **20**, 4337–4345 (2020).

178. Ley, M. B. *et al.* $LiCe(BH_4)_3Cl$, a new lithium-ion conductor and hydrogen storage material with isolated tetranuclear anionic clusters. *Chem. Mater.* **24**, 1654–1663 (2012).

179. Jeitschko, W., Bither, T. A. & Bierstedt, P. E. Crystal structure and ionic conductivity of Li boracites. *Acta Crystallogr. B* **33**, 2767–2775 (1977).

180. Wagner, R. *et al.* Fast Li-ion-conducting garnet-related $Li_{7-3x}Fe_xLa_3Zr_2O_{12}$ with uncommon $I\bar{4}3d$ structure. *Chem. Mater.* **28**, 5943–5951 (2016).

181. H. Braga, M., A. Ferreira, J., Stockhausen, V., E. Oliveira, J. & El-Azab, A. Novel Li_3ClO based glasses with superionic properties for lithium batteries. *J. Mater. Chem. A* **2**, 5470–5480 (2014).

182. Stramare, S. & Weppner, W. Structure and conductivity of B-site substituted (Li,La)TiO_3. *Mater. Sci. Eng. B* **113**, 85–90 (2004).

183. Sotomayor, M. E., Várez, A., Bucheli, W., Jimenez, R. & Sanz, J. Structural characterisation and Li conductivity of $Li_{1/2-x}Sr_{2x}La_{1/2-x}TiO_3$ ($0<x<0.5$) perovskites. *Ceram. Int.* **39**, 9619–9626 (2013).

184. Li, Y. *et al.* Fluorine-doped antiperovskite electrolyte for all-solid-state lithium-ion batteries. *Angew. Chem.* **128**, 10119–10122 (2016).

185. J. Miara, L. *et al.* Li-ion conductivity in Li_9S_3N. *J. Mater. Chem. A* **3**, 20338–20344 (2015).

186. Sotomayor, M. E., Levenfeld, B., Varez, A. & Sanz, J. Study of the $La_{1/2+1/2x}Li_{1/2-1/2x}Ti_{1-x}Al_xO_3$ ($0 \leq x \leq 1$) solid solution. A new example of percolative system in fast ion conductors. *J. Alloys Compd.* **720**, 460–465 (2017).

187. Phraewphiphat, T. *et al.* Syntheses, structures, and ionic conductivities of perovskite-structured lithium–strontium–aluminum/gallium–tantalum-oxides. *J. Solid State Chem.* **225**, 431–437 (2015).

188. Chen, C. H. *et al.* Stable lithium-ion conducting perovskite lithium–strontium–tantalum–zirconium–oxide system. *Solid State Ion.* **167**, 263–272 (2004).

189. Huang, B. *et al.* Li-ion conduction and stability of perovskite $Li_{3/8}Sr_{7/16}Hf_{1/4}Ta_{3/4}O_3$. *ACS Appl. Mater. Interfaces* **8**, 14552–14557 (2016).

190. Yu, R., Du, Q.-X., Zou, B.-K., Wen, Z.-Y. & Chen, C.-H. Synthesis and characterization of perovskite-type (Li,Sr)(Zr,Nb)O_3 quaternary solid electrolyte for all-solid-state batteries. *J. Power Sources* **306**, 623–629 (2016).

191. Braga, M. H., Ferreira, J. A., Stockhausen, V., Oliveira, J. E. & El-Azab, A. Novel Li_3ClO based glasses with superionic properties for lithium batteries. *J. Mater. Chem. A* **2**, 5470–5480 (2014).

192. Inaguma, Y. & Itoh, M. Influences of carrier concentration and site percolation on lithium ion conductivity in perovskite-type oxides. *Solid State Ion.* **86–88**, 257–260 (1996).

193. Morata-Orrantia, A., García-Martín, S. & Alario-Franco, M. Á. New $La_{2/3-x}Sr_xLi_xTiO_3$ solid solution: structure, microstructure, and Li^+ conductivity. *Chem. Mater.* **15**, 363–367 (2003).

194. Zhao, Y. & Daemen, L. L. Superionic conductivity in lithium-rich anti-perovskites. *J. Am. Chem. Soc.* **134**, 15042–15047 (2012).

195. Li, S. *et al.* Reaction mechanism studies towards effective fabrication of lithium-rich anti-perovskites Li_3OX (X=Cl, Br). *Solid State Ion.* **284**, 14–19 (2016).

196. Howard, M. A., Clemens, O., Slater, P. R. & Anderson, P. A. Hydrogen absorption and lithium ion conductivity in Li_6NBr_3. *J. Alloys Compd.* **645**, S174–S177 (2015).

197. Liang, C. C. Conduction characteristics of the lithium iodide-aluminum oxide solid electrolytes. *J. Electrochem. Soc.* **120**, 1289 (1973).

198. Lutz, H. D., Steiner, H.-J. & Wickel, Ch. Fast ionic conductivity and crystal structure of spinel-type $Li_{2-x}Mn_{1-x}M_xCl_4$ (M = Ga, In). *Solid State Ion.* **95**, 173–181 (1997).

199. Kanno, R., Takeda, Y. & Yamamoto, O. Ionic conductivity of solid lithium ion conductors with the spinel structure: Li_2MCl_4 (M = Mg, Mn, Fe, Cd). *Mater. Res. Bull.* **16**, 999–1005 (1981).

200. Phraewphiphat, T., Iqbal, M., Suzuki, K., Hirayama, M. & Kanno, R. Synthesis and lithium-ion conductivity of $LiSrB_2O_6F$ (B = Nb^{5+}, Ta^{5+}) with a pyrochlore structure. 粉体および粉末冶金 **65**, 26–33 (2018).

201. Murugan, R., Thangadurai, V. & Weppner, W. Lithium ion conductivity of $Li_{5+x}Ba_xLa_{3-x}Ta_2O_{12}$ (x = 0–2) with garnet-related structure in dependence of the barium content. *Ionics* **13**, 195–203 (2007).

202. Raskovalov, A. A., Il'ina, E. A. & Antonov, B. D. Structure and transport properties of $Li_7La_3Zr_{2-0.75x}Al_xO_{12}$ superionic solid electrolytes. *J. Power Sources* **238**, 48–52 (2013).

203. Murugan, R., Ramakumar, S. & Janani, N. High conductive yttrium doped $Li_7La_3Zr_2O_{12}$ cubic lithium garnet. *Electrochem. Commun.* **13**, 1373–1375 (2011).

204. Wolfenstine, J., Ratchford, J., Rangasamy, E., Sakamoto, J. & Allen, J. L. Synthesis and high Li-ion conductivity of Ga-stabilized cubic $Li_7La_3Zr_2O_{12}$. *Mater. Chem. Phys.* **134**, 571–575 (2012).

205. Li, Y., Tao Han, J.-, An Wang, C.-, Xie, H. & B. Goodenough, J. Optimizing Li^+ conductivity in a garnet framework. *J. Mater. Chem.* **22**, 15357–15361 (2012).

206. Wang, Y. & Lai, W. High ionic conductivity lithium garnet oxides of $Li_{7-x}La_3Zr_{2-x}Ta_xO_{12}$ compositions. *Electrochem. Solid State Lett.* **15**, A68 (2012).

207. Lu, Y., Meng, X., Alonso, J. A., Fernández-Díaz, M. T. & Sun, C. Effects of fluorine doping on structural and electrochemical properties of $Li_{6.25}Ga_{0.25}La_3Zr_2O_{12}$ as electrolytes for solid-state lithium batteries. *ACS Appl. Mater. Interfaces* **11**, 2042–2049 (2019).

208. Wang, D. *et al.* Toward understanding the lithium transport mechanism in garnet-type solid electrolytes: Li^+ ion exchanges and their mobility at octahedral/tetrahedral sites. *Chem. Mater.* **27**, 6650–6659 (2015).

209. Rettenwander, D. *et al.* Synthesis, crystal chemistry, and electrochemical properties of $Li_{7-2x}La_3Zr_{2-x}Mo_xO_{12}$ (x = 0.1–0.4): stabilization of the cubic garnet polymorph via substitution of Zr^{4+} by Mo^{6+}. *Inorg. Chem.* **54**, 10440–10449 (2015).

210. Deviannapoorani, C., Dhivya, L., Ramakumar, S. & Murugan, R. Lithium ion transport properties of high conductive tellurium substituted $Li_7La_3Zr_2O_{12}$ cubic lithium garnets. *J. Power Sources* **240**, 18–25 (2013).

211. He, M., Cui, Z., Chen, C., Li, Y. & Guo, X. Formation of self-limited, stable and conductive interfaces between garnet electrolytes and lithium anodes for reversible lithium cycling in solid-state batteries. *J. Mater. Chem. A* **6**, 11463–11470 (2018).

212. Thangadurai, V., Kaack, H. & Weppner, W. J. F. Novel fast lithium ion conduction in garnet-type $Li_5La_3M_2O_{12}$ (M = Nb, Ta). *J. Am. Ceram. Soc.* **86**, 437–440 (2003).

213. Murugan, R., Weppner, W., Schmid-Beurmann, P. & Thangadurai, V. Structure and lithium ion conductivity of bismuth containing lithium garnets $Li_5La_3Bi_2O_{12}$ and $Li_6SrLa_2Bi_2O_{12}$. *Mater. Sci. Eng. B* **143**, 14–20 (2007).

214. Percival, J., Kendrick, E. & Slater, P. R. Synthesis and characterisation of the garnet-related Li ion conductor, $Li_5Nd_3Sb_2O_{12}$. *Mater. Res. Bull.* **43**, 765–770 (2008).

215. O'Callaghan, M. P., Powell, A. S., Titman, J. J., Chen, G. Z. & Cussen, E. J. Switching on fast lithium ion conductivity in garnets: the structure and transport properties of $Li_{3+x}Nd_3Te_{2-x}Sb_xO_{12}$. *Chem. Mater.* **20**, 2360–2369 (2008).

216. Murugan, R., Weppner, W., Schmid-Beurmann, P. & Thangadurai, V. Structure and lithium ion conductivity of garnet-like $Li_5La_3Sb_2O_{12}$ and $Li_6SrLa_2Sb_2O_{12}$. *Mater. Res. Bull.* **43**, 2579–2591 (2008).

217. Percival, J., Apperley, D. & Slater, P. R. Synthesis and structural characterisation of the Li ion conducting garnet-related systems, $Li_6ALa_2Nb_2O_{12}$ (A=Ca, Sr). *Solid State Ion.* **179**, 1693–1696 (2008).

218. Awaka, J., Kijima, N., Takahashi, Y., Hayakawa, H. & Akimoto, J. Synthesis and crystallographic studies of garnet-related lithium-ion conductors $Li_6CaLa_2Ta_2O_{12}$ and $Li_6BaLa_2Ta_2O_{12}$. *Solid State Ion.* **180**, 602–606 (2009).

219. Allen, J. L., Wolfenstine, J., Rangasamy, E. & Sakamoto, J. Effect of substitution (Ta, Al, Ga) on the conductivity of $Li_7La_3Zr_2O_{12}$. *J. Power Sources* **206**, 315–319 (2012).

220. Janani, N., Deviannapoorani, C., Dhivya, L. & Murugan, R. Influence of sintering additives on densification and Li^+ conductivity of Al doped $Li_7La_3Zr_2O_{12}$ lithium garnet. *RSC Adv.* **4**, 51228–51238 (2014).

221. Buschmann, H. *et al.* Structure and dynamics of the fast lithium ion conductor "$Li_7La_3Zr_2O_{12}$". *Phys. Chem. Chem. Phys.* **13**, 19378–19392 (2011).

222. Kokal, I., Ramanujachary, K. V., Notten, P. H. L. & Hintzen, H. T. Sol–gel synthesis and lithium ion conduction properties of garnet-type $Li_6BaLa_2Ta_2O_{12}$. *Mater. Res. Bull.* **47**, 1932–1935 (2012).

223. A. Howard, M. *et al.* Synthesis, conductivity and structural aspects of $Nd_3Zr_2Li_{7-3x}Al_xO_{12}$. *J. Mater. Chem. A* **1**, 14013–14022 (2013).

224. Matsuda, Y. *et al.* Phase formation of a garnet-type lithium-ion conductor $Li_{7-3x}Al_xLa_3Zr_2O_{12}$. *Solid State Ion.* **277**, 23–29 (2015).

225. Narayanan, S., Ramezanipour, F. & Thangadurai, V. Enhancing Li ion conductivity of garnet-type $Li_5La_3Nb_2O_{12}$ by Y- and Li-codoping: synthesis, structure, chemical stability, and transport properties. *J. Phys. Chem. C* **116**, 20154–20162 (2012).

226. Zeier, W. G., Zhou, S., Lopez-Bermudez, B., Page, K. & Melot, B. C. Dependence of the Li-ion conductivity and activation energies on the crystal structure and ionic radii in $Li_6MLa_2Ta_2O_{12}$. *ACS Appl. Mater. Interfaces* **6**, 10900–10907 (2014).

227. Thangadurai, V. & Weppner, W. $Li_6ALa_2Ta_2O_{12}$ (A = Sr, Ba): Novel garnet-like oxides for fast lithium ion conduction. *Adv. Funct. Mater.* **15**, 107–112 (2005).

228. Thompson, T. *et al.* A tale of two sites: on defining the carrier concentration in garnet-based ionic conductors for advanced Li batteries. *Adv. Energy Mater.* **5**, 1500096 (2015).

229. Shin, D. O. *et al.* Synergistic multi-doping effects on the $Li_7La_3Zr_2O_{12}$ solid electrolyte for fast lithium ion conduction. *Sci. Rep.* **5**, 18053 (2015).

230. Hamao, N., Kataoka, K. & Akimoto, J. Li-ion conductivity and crystal structure of garnet-type $Li_{6.5}La_3M_{1.5}Ta_{0.5}O_{12}$ (*M* = Hf, Sn) oxides. *J. Ceram. Soc. Jpn.* **125**, 272–275 (2017).

231. Abdel-Basset, D. M., Mulmi, S., El-Bana, M. S., Fouad, S. S. & Thangadurai, V. Structure, ionic conductivity, and dielectric properties of Li-rich garnet-type $Li_{5+2x}La_3Ta_{2-x}Sm_xO_{12}$ ($0 \leq x \leq 0.55$) and their chemical stability. *Inorg. Chem.* **56**, 8865–8877 (2017).

232. Shimonishi, Y. *et al.* Synthesis of garnet-type $Li_{7-x}La_3Zr_2O_{12-1/2x}$ and its stability in aqueous solutions. *Solid State Ion.* **183**, 48–53 (2011).

233. Narayanan, S. & Thangadurai, V. Effect of Y substitution for Nb in $Li_5La_3Nb_2O_{12}$ on Li ion conductivity of garnet-type solid electrolytes. *J. Power Sources* **196**, 8085–8090 (2011).

234. Rangasamy, E., Wolfenstine, J. & Sakamoto, J. The role of Al and Li concentration on the formation of cubic garnet solid electrolyte of nominal composition $Li_7La_3Zr_2O_{12}$. *Solid State Ion.* **206**, 28–32 (2012).

235. El Shinawi, H. & Janek, J. Stabilization of cubic lithium-stuffed garnets of the type "$Li_7La_3Zr_2O_{12}$" by addition of gallium. *J. Power Sources* **225**, 13–19 (2013).

236. Howard, M. A. *et al.* Effect of Ga incorporation on the structure and Li ion conductivity of $La_3Zr_2Li_7O_{12}$. *Dalton Trans.* **41**, 12048–12053 (2012).

237. Ramakumar, S., Satyanarayana, L., Manorama, S. V. & Murugan, R. Structure and Li^+ dynamics of Sb-doped $Li_7La_3Zr_2O_{12}$ fast lithium ion conductors. *Phys. Chem. Chem. Phys.* **15**, 11327–11338 (2013).

238. Wang, D. *et al.* The synergistic effects of Al and Te on the structure and Li^+-mobility of garnet-type solid electrolytes. *J. Mater. Chem. A* **2**, 20271–20279 (2014).

239. Tong, X., Thangadurai, V. & Wachsman, E. D. Highly conductive Li garnets by a multielement doping strategy. *Inorg. Chem.* **54**, 3600–3607 (2015).

240. O'Callaghan, M. P., Lynham, D. R., Cussen, E. J. & Chen, G. Z. Structure and ionic-transport properties of lithium-containing garnets $Li_3Ln_3Te_2O_{12}$ (Ln = Y, Pr, Nd, Sm−Lu). *Chem. Mater.* **18**, 4681–4689 (2006).

241. Chen, R.-J. *et al.* Effect of calcining and Al doping on structure and conductivity of $Li_7La_3Zr_2O_{12}$. *Solid State Ion.* **265**, 7–12 (2014).

242. Cussen, E. J., Yip, T. W. S., O'Neill, G. & O'Callaghan, M. P. A comparison of the transport properties of lithium-stuffed garnets and the conventional phases $Li_3Ln_3Te_2O_{12}$. *J. Solid State Chem.* **184**, 470–475 (2011).

243. Arbi, K., Bucheli, W., Jiménez, R. & Sanz, J. High lithium ion conducting solid electrolytes based on NASICON $Li_{1+x}Al_xM_{2-x}(PO_4)_3$ materials (M=Ti, Ge and 0≤x≤0.5). *J. Eur. Ceram. Soc.* **35**, 1477–1484 (2015).

244. Rangasamy, E., Wolfenstine, J., Allen, J. & Sakamoto, J. The effect of 24c-site (A) cation substitution on the tetragonal–cubic phase transition in $Li_{7-x}La_{3-x}A_xZr_2O_{12}$ garnet-based ceramic electrolyte. *J. Power Sources* **230**, 261–266 (2013).

245. Xu, X., Wen, Z., Yang, X. & Chen, L. Dense nanostructured solid electrolyte with high Li-ion conductivity by spark plasma sintering technique. *Mater. Res. Bull.* **43**, 2334–2341 (2008).

246. Hayashi, A., Hama, S., Minami, T. & Tatsumisago, M. Formation of superionic crystals from mechanically milled Li_2S–P_2S_5 glasses. *Electrochem. Commun.* **5**, 111–114 (2003).

247. Minami, K., Hayashi, A., Ujiie, S. & Tatsumisago, M. Electrical and electrochemical properties of glass–ceramic electrolytes in the systems Li_2S–P_2S_5–P_2S_3 and Li_2S–P_2S_5–P_2O_5. *Solid State Ion.* **192**, 122–125 (2011).

248. Fukushima, A., Hayashi, A., Yamamura, H. & Tatsumisago, M. Mechanochemical synthesis of high lithium ion conducting solid electrolytes in a Li_2S-P_2S_5-Li_3N system. *Solid State Ion.* **304**, 85–89 (2017).

249. Ohta, S., Kobayashi, T. & Asaoka, T. High lithium ionic conductivity in the garnet-type oxide $Li_{7-X}La_3(Zr_{2-X}, Nb_X)O_{12}$ (X=0–2). *J. Power Sources* **196**, 3342–3345 (2011).

250. Zaiß, T., Ortner, M., Murugan, R. & Weppner, W. Fast ionic conduction in cubic hafnium garnet $Li_7La_3Hf_2O_{12}$. *Ionics* **16**, 855–858 (2010).

251. Kuhn, A., Duppel, V. & V. Lotsch, B. Tetragonal $Li_{10}GeP_2S_{12}$ and Li_7GePS_8 – exploring the Li ion dynamics in LGPS Li electrolytes. *Energy Environ. Sci.* **6**, 3548–3552 (2013).

252. Kato, Y. *et al.* Synthesis, structure and lithium ionic conductivity of solid solutions of $Li_{10}(Ge_{1-x}M_x)P_2S_{12}$ (M = Si, Sn). *J. Power Sources* **271**, 60–64 (2014).

253. Pradel, A., Pagnier, T. & Ribes, M. Effect of rapid quenching on electrical properties of lithium conductive glasses. *Solid State Ion.* **17**, 147–154 (1985).

254. Bernuy-Lopez, C. *et al.* Atmosphere controlled processing of Ga-substituted garnets for high Li-ion conductivity ceramics. *Chem. Mater.* **26**, 3610–3617 (2014).

255. Ramakumar, S., Satyanarayana, L., V. Manorama, S. & Murugan, R. Structure and Li^+ dynamics of Sb-doped $Li_7La_3Zr_2O_{12}$ fast lithium ion conductors. *Phys. Chem. Chem. Phys.* **15**, 11327–11338 (2013).

256. Gombotz, M., Rettenwander, D. & Wilkening, H. M. R. Lithium-ion transport in nanocrystalline spinel-type $Li[In_xLi_y]Br_4$ as seen by conductivity spectroscopy and NMR. *Front. Chem.* **8**, (2020).

257. Tomita, Y., Matsushita, H., Kobayashi, K., Maeda, Y. & Yamada, K. Substitution effect of ionic conductivity in lithium ion conductor, $Li_3InBr_{6-x}Cl_x$. *Solid State Ion.* **179**, 867–870 (2008).

258. Kanno, R., Takeda, Y., Takada, K. & Yamamoto, O. Ionic conductivity and phase transition of the spinel system $Li_{2-2x}M_{1+x}Cl_4$ (M = Mg , Mn , Cd). *J. Electrochem. Soc.* **131**, 469 (1984).

259. Yin, L., Yuan, H., Kong, L., Lu, Z. & Zhao, Y. Engineering Frenkel defects of anti-perovskite solid-state electrolytes and their applications in all-solid-state lithium-ion batteries. *Chem. Commun.* **56**, 1251–1254 (2020).

260. Hood, Z. D., Wang, H., Samuthira Pandian, A., Keum, J. K. & Liang, C. Li_2OHCl crystalline electrolyte for stable metallic lithium anodes. *J. Am. Chem. Soc.* **138**, 1768–1771 (2016).

261. Bruce, P. G. & West, A. R. Ionic conductivity of LISICON solid solutions, $Li_{2+2x}Zn_{1-x}GeO_4$. *J. Solid State Chem.* **44**, 354–365 (1982).

262. Han, X. *et al.* Negating interfacial impedance in garnet-based solid-state Li metal batteries. *Nat. Mater.* **16**, 572–579 (2017).

263. Inoishi, A., Nishio, A., Yoshioka, Y., Kitajou, A. & Okada, S. A single-phase all-solid-state lithium battery based on $Li_{1.5}Cr_{0.5}Ti_{1.5}(PO_4)_3$ for high rate capability and low temperature operation. *Chem. Commun.* **54**, 3178–3181 (2018).

264. Wu, Z. *et al.* Utmost limits of various solid electrolytes in all-solid-state lithium batteries: A critical review. *Renew. Sustain. Energy Rev.* **109**, 367–385 (2019).

265. Pradel, A. & Ribes, M. Electrical properties of lithium conductive silicon sulfide glasses prepared by twin roller quenching. *Solid State Ion.* **18–19**, 351–355 (1986).

266. Mercier, R., Malugani, J.-P., Fahys, B. & Robert, G. Superionic conduction in Li_2S - P_2S_5 - LiI - glasses. *Solid State Ion.* **5**, 663–666 (1981).

267. Kennedy, J. H. Ionically conductive glasses based on SiS_2. *Mater. Chem. Phys.* **23**, 29–50 (1989).

268. Wada, H., Menetrier, M., Levasseur, A. & Hagenmuller, P. Preparation and ionic conductivity of new B_2S_3-Li_2S-LiI glasses. *Mater. Res. Bull.* **18**, 189–193 (1983).

269. Sahami, S., Shea, S. W. & Kennedy, J. H. Preparation and conductivity measurements of SiS_2-Li_2S-LiBr lithium ion conductive glasses. *J. Electrochem. Soc.* **132**, 985 (1985).

270. Kennedy, J. H., Sahami, S., Shea, S. W. & Zhang, Z. Preparation and conductivity measurements of SiS_2□Li_2S glasses doped with LiBr and LiCl. *Solid State Ion.* **18–19**, 368–371 (1986).

271. Kennedy, J. H. & Yang, Y. A highly conductive Li+-glass system: (1−x) ($0.4SiS_2$ - $0.6Li_2S$) - xLiI. *J. Electrochem. Soc.* **133**, 2437 (1986).

272. Kennedy, J. H. & Yang, Y. Glass-forming region and structure in SiS_2□Li_2S□LiX (X = Br, I). *J. Solid State Chem.* **69**, 252–257 (1987).

273. Kennedy, J. H. & Zhang, Z. Improved stability for the SiS_2-P_2S_5-Li_2S-LiI glass system. *Solid State Ion.* **28–30**, 726–728 (1988).

274. Ribes, M., Barrau, B. & Souquet, J. L. Sulfide glasses: Glass forming region, structure and ionic conduction of glasses in Na_2S-XS_2 (X=Si; Ge), Na_2S-P_2S_5 and Li_2S-GeS_2 systems. *J. Non-Cryst. Solids* **38–39**, 271–276 (1980).

275. Seino, Y., Ota, T., Takada, K., Hayashi, A. & Tatsumisago, M. A sulphide lithium super ion conductor is superior to liquid ion conductors for use in rechargeable batteries. *Energy Environ. Sci.* **7**, 627–631 (2014).

276. Mizuno, F., Hayashi, A., Tadanaga, K. & Tatsumisago, M. High lithium ion conducting glass-ceramics in the system Li_2S–P_2S_5. *Solid State Ion.* **177**, 2721–2725 (2006).

277. Morimoto, H., Yamashita, H., Tatsumisago, M. & Minami, T. Mechanochemical synthesis of new amorphous materials of $60Li_2S{\cdot}40SiS_2$ with high lithium ion conductivity. *J. Am. Ceram. Soc.* **82**, 1352–1354 (1999).

278. Minami, T., Hayashi, A. & Tatsumisago, M. Preparation and characterization of lithium ion-conducting oxysulfide glasses. *Solid State Ion.* **136–137**, 1015–1023 (2000).

279. Hirai, K., Tatsumisago, M. & Minami, T. Thermal and electrical properties of rapidly quenched glasses in the systems Li_2S-SiS_2-Li_xMO_y (Li_xMO_y = Li_4SiO_4, Li_2SO_4). *Solid State Ion.* **78**, 269–273 (1995).

280. Abrahams, I. & Hadzifejzovic, E. Lithium ion conductivity and thermal behaviour of glasses and crystallised glasses in the system Li_2O–Al_2O_3–TiO_2–P_2O_5. *Solid State Ion.* **134**, 249–257 (2000).

281. Hayashi, A., Yamashita, H., Tatsumisago, M. & Minami, T. Characterization of Li_2S–SiS_2–Li_xMO_y (M=Si, P, Ge) amorphous solid electrolytes prepared by melt-quenching and mechanical milling. *Solid State Ion.* **148**, 381–389 (2002).

282. Hayashi, A., Hama, S., Morimoto, H., Tatsumisago, M. & Minami, T. High lithium ion conductivity of glass–ceramics derived from mechanically milled glassy powders. *Chem. Lett.* **30**, 872–873 (2001).

283. Mizuno, F., Hayashi, A., Tadanaga, K. & Tatsumisago, M. New lithium-ion conducting crystal obtained by crystallization of the Li_2S – P_2S_5 glasses. *Electrochem. Solid State Lett.* **8**, A603 (2005).

284. Hayashi, A., Komiya, R., Tatsumisago, M. & Minami, T. Characterization of Li_2S–SiS_2–Li_3MO_3 (M=B, Al, Ga and In) oxysulfide glasses and their application to solid state lithium secondary batteries. *Solid State Ion.* **152–153**, 285–290 (2002).

285. Hayashi, A., Ishikawa, Y., Hama, S., Minami, T. & Tatsumisago, M. Fast lithium-ion conducting glass-ceramics in the system Li_2S-SiS_2-P_2S_5. *Electrochem. Solid State Lett.* **6**, A47 (2003).

286. Iio, K., Hayashi, A., Morimoto, H., Tatsumisago, M. & Minami, T. Mechanochemical synthesis of high lithium ion conducting materials in the system Li_3N−SiS_2. *Chem. Mater.* **14**, 2444–2449 (2002).

287. Machida, N., Yamamoto, H. & Shigematsu, T. A new amorphous lithium-ion conductor in the system Li_2S–P_2S_3. *Chem. Lett.* **33**, 30–31 (2003).

288. Sakamoto, R., Tatsumisago, M. & Minami, T. Preparation of fast lithium ion conducting glasses in the system Li_2S−SiS_2−Li_3N. *J. Phys. Chem. B* **103**, 4029–4031 (1999).

289. Abdel-Baki, M., Salem, A. M., Abdel-Wahab, F. A. & El-Diasty, F. Bond character, optical properties and ionic conductivity of $Li_2O/B_2O_3/SiO_2/Al_2O_3$ glass: Effect of structural substitution of Li_2O for LiCl. *J. Non-Cryst. Solids* **354**, 4527–4533 (2008).

290. Machida, N., Yoneda, Y. & Shigematsu, T. Mechano-chemical synthesis of lithium ion conducting materials in the system Li_2O-Li_2S-P_2S_5. *J. Jpn. Soc. Powder Powder Metall.* **51**, 91–97 (2004).

291. Hayashi, A. *et al.* Thermal and electrical properties of rapidly quenched Li_2S-SiS_2-Li_2O-P_2O_5 oxysulfide glasses. *Solid State Ion.* **113–115**, 733–738 (1998).

292. Zhang, Y., Chen, K., Shen, Y., Lin, Y. & Nan, C.-W. Synergistic effect of processing and composition x on conductivity of xLi_2S-$(100-x)P_2S_5$ electrolytes. *Solid State Ion.* **305**, 1–6 (2017).

293. 有紀米田, 信也町田 & 利彦重松. メカニカルミリング法による LiI-Li_2S-SiS_2 系非晶質材料の作製とリチウムイオン伝導特性. 粉体および粉末冶金 **49**, 799–806 (2002).

294. Hayashi, A., Hirai, K., Tatsumisago, M., Takahashi, M. & Minami, T. Preparation of $Li_6Si_2S_7$-$Li_6B_4X_9$ (X = S, O) glasses by rapid quenching and their lithium ion conductivities. *Solid State Ion.* **86–88**, 539–542 (1996).

295. Yersak, T. A., Salvador, J. R., Pieczonka, N. P. W. & Cai, M. Dense, melt cast sulfide glass electrolyte separators for Li metal batteries. *J. Electrochem. Soc.* **166**, A1535 (2019).

296. Dietrich, C. *et al.* Lithium ion conductivity in Li_2S–P_2S_5 glasses – building units and local structure evolution during the crystallization of superionic conductors Li_3PS_4, $Li_7P_3S_{11}$ and $Li_4P_2S_7$. *J. Mater. Chem. A* **5**, 18111–18119 (2017).

297. Yamauchi, A., Sakuda, A., Hayashi, A. & Tatsumisago, M. Preparation and ionic conductivities of $(100-x)(0.75Li_2S{\cdot}0.25P_2S_5){\cdot}xLiBH_4$ glass electrolytes. *J. Power Sources* **244**, 707–710 (2013).

298. Xu, R., Xia, X., Wang, X., Xia, Y. & Tu, J. Tailored Li_2S–P_2S_5 glass-ceramic electrolyte by MoS_2 doping, possessing high ionic conductivity for all-solid-state lithium-sulfur batteries. *J. Mater. Chem. A* **5**, 2829–2834 (2017).

299. Xu, R. *et al.* All-solid-state lithium–sulfur batteries based on a newly designed $Li_7P_{2.9}Mn_{0.1}S_{10.7}I_{0.3}$ superionic conductor. *J. Mater. Chem. A* **5**, 6310–6317 (2017).

300. Zhou, P., Wang, J., Cheng, F., Li, F. & Chen, J. A solid lithium superionic conductor $Li_{11}AlP_2S_{12}$ with a thio-LISICON analogous structure. *Chem. Commun.* **52**, 6091–6094 (2016).

301. Hood, Z. D. *et al.* The “filler effect”: A study of solid oxide fillers with β-Li_3PS_4 for lithium conducting electrolytes. *Solid State Ion.* **283**, 75–80 (2015).

302. Rangasamy, E. *et al.* A high conductivity oxide–sulfide composite lithium superionic conductor. *J. Mater. Chem. A* **2**, 4111–4116 (2014).

303. Trevey, J. E., Jung, Y. S. & Lee, S.-H. Preparation of Li_2S–$GeSe_2$–P_2S_5 electrolytes by a single step ball milling for all-solid-state lithium secondary batteries. *J. Power Sources* **195**, 4984–4989 (2010).

304. Trevey, J. E., Gilsdorf, J. R., Miller, S. W. & Lee, S.-H. Li_2S–Li_2O–P_2S_5 solid electrolyte for all-solid-state lithium batteries. *Solid State Ion.* **214**, 25–30 (2012).

305. Hayashi, A., Muramatsu, H., Ohtomo, T., Hama, S. & Tatsumisago, M. Improvement of chemical stability of Li_3PS_4 glass electrolytes by adding M_xO_y (M = Fe, Zn, and Bi) nanoparticles. *J. Mater. Chem. A* **1**, 6320–6326 (2013).

306. Huang, B. *et al.* Li_3PO_4-doped $Li_7P_3S_{11}$ glass-ceramic electrolytes with enhanced lithium ion conductivities and application in all-solid-state batteries. *J. Power Sources* **284**, 206–211 (2015).

307. Lu, P. *et al.* Study on (100-x)(70Li_2S-30P_2S_5)-xLi_2ZrO_3 glass-ceramic electrolyte for all-solid-state lithium-ion batteries. *J. Power Sources* **356**, 163–171 (2017).

308. Bates, J. B. *et al.* Fabrication and characterization of amorphous lithium electrolyte thin films and rechargeable thin-film batteries. *J. Power Sources* **43**, 103–110 (1993).

309. Fleutot, B., Pecquenard, B., Martinez, H., Letellier, M. & Levasseur, A. Investigation of the local structure of LiPON thin films to better understand the role of nitrogen on their performance. *Solid State Ion.* **186**, 29–36 (2011).

310. Suzuki, N., Shirai, S., Takahashi, N., Inaba, T. & Shiga, T. A lithium phosphorous oxynitride (LiPON) film sputtered from unsintered Li_3PO_4 powder target. *Solid State Ion.* **191**, 49–54 (2011).

311. Ménétrier, M., Estournès, C., Levasseur, A. & Rao, K. J. Ionic conduction in B_2S_3-Li_2S-LiI glasses. *Solid State Ion.* **53–56**, 1208–1213 (1992).

312. Takada, K., Aotani, N. & Kondo, S. Electrochemical behaviors of Li^+ ion conductor, Li_3PO_4-Li_2S-SiS_2. *J. Power Sources* **43**, 135–141 (1993).

313. Minami, K., Hayashi, A. & Tatsumisago, M. Crystallization process for superionic $Li_7P_3S_{11}$ glass–ceramic electrolytes. *J. Am. Ceram. Soc.* **94**, 1779–1783 (2011).

314. Schlaikjer, C. R. & Liang, C. C. Ionic conduction in calcium doped polycrystalline lithium iodide. *J. Electrochem. Soc.* **118**, 1447 (1971).

315. Poulsen, F. W., Andersen, N. H., Kindl, B. & Schoonman, J. Properties of LiI—Alumina composite electrolytes. *Solid State Ion.* **9–10**, 119–122 (1983).

316. Aono, H., Sugimoto, E., Sadaoka, Y., Imanaka, N. & Adachi, G. Electrical property and sinterability of $LiTi_2(PO_4)_3$ mixed with lithium salt (Li_3PO_4 or Li_3BO_3). *Solid State Ion.* **47**, 257–264 (1991).

317. Aono, H., Sugimoto, E., Sadaoka, Y., Imanaka, N. & Adachi, G. Ionic conductivity of $LiTi_2(PO_4)_3$ mixed with lithium salts. *Chem. Lett.* **19**, 331–334 (1990).

318. He, L. X. & Yoo, H. I. Effects of B-site ion (M) substitution on the ionic conductivity of $(Li_{3x}La_{2/3-x})_{1+y/2}(MyTi_{1-y})O_3$ (M=Al, Cr). *Electrochimica Acta* **48**, 1357–1366 (2003).

319. Inaguma, Y., Chen, L., Itoh, M. & Nakamura, T. Candidate compounds with perovskite structure for high lithium ionic conductivity. *Solid State Ion.* **70–71**, 196–202 (1994).

320. Chung, H.-T., Kim, J.-G. & Kim, H.-G. Dependence of the lithium ionic conductivity on the B-site ion substitution in $(Li_{0.5}La_{0.5})Ti_{1-x}M_xO_3$ (M=Sn, Zr, Mn, Ge). *Solid State Ion.* **107**, 153–160 (1998).

321. Thangadurai, V. & Weppner, W. Effect of B-site substitution of $(Li,La)TiO_3$ perovskites by di-, tri-, tetra- and hexavalent metal ions on the lithium ion conductivity. *Ionics* **6**, 70–77 (2000).

322. Morata-Orrantia, A., García-Martín, S., Morán, E. & Alario-Franco, M. Á. A New $La_{2/3}Li_xTi_{1-x}Al_xO_3$ solid solution: structure, microstructure, and Li^+ conductivity. *Chem. Mater.* **14**, 2871–2875 (2002).

323. Kawai, H. & Kuwano, J. Lithium ion conductivity of A-site deficient perovskite solid solution $La_{0.67-x}Li_{3x}TiO_3$. *J. Electrochem. Soc.* **141**, L78 (1994).

324. Zhang, Y., Chen, K., Shen, Y., Lin, Y. & Nan, C.-W. Enhanced lithium-ion conductivity in a $LiZr_2(PO_4)_3$ solid electrolyte by Al doping. *Ceram. Int.* **43**, S598–S602 (2017).

325. Chowdari, B. V. R., Radhakrishnan, K., Thomas, K. A. & Subba Rao, G. V. Ionic conductivity studies on $Li_{1-x}M_{2-x}M'_xP_3O_{12}$ (H = Hf, Zr; M′ = Ti, Nb). *Mater. Res. Bull.* **24**, 221–229 (1989).

326. Ado, K., Saito, Y., Asai, T., Kageyama, H. & Nakamura, O. Li^+-ion conductivity of $Li_{1+x}M_xTi_{2-x}(PO_4)_3$ (M: Sc^{3+}, Y^{3+}). *Solid State Ion.* **53–56**, 723–727 (1992).

327. Xiong, L. *et al.* LiF assisted synthesis of $LiTi_2(PO_4)_3$ solid electrolyte with enhanced ionic conductivity. *Solid State Ion.* **309**, 22–26 (2017).

328. Fu, J. Superionic conductivity of glass-ceramics in the system Li_2O-Al_2O_3-TiO_2-P_2O_5. *Solid State Ion.* **96**, 195–200 (1997).

329. Dhivya, L. & Murugan, R. Effect of simultaneous substitution of Y and Ta on the stabilization of cubic phase, microstructure, and Li^+ conductivity of $Li_7La_3Zr_2O_{12}$ lithium garnet. *ACS Appl. Mater. Interfaces* **6**, 17606–17615 (2014).

330. Liu, Z., Huang, F., Yang, J., Wang, B. & Sun, J. New lithium ion conductor, thio-LISICON lithium zirconium sulfide system. *Solid State Ion.* **179**, 1714–1716 (2008).

331. Chen, H. & Adams, S. Bond softness sensitive bond-valence parameters for crystal structure plausibility tests. *IUCrJ* **4**, 614–625 (2017).

332. Adams, S. Practical considerations in determining bond valence parameters. in *Bond Valences* (eds. Brown, I. D. & Poeppelmeier, K. R.) 91–128 (Springer, 2014). doi:10.1007/430_2013_96.

333. He, B. *et al.* A highly efficient and informative method to identify ion transport networks in fast ion conductors. *Acta Mater.* **203**, 116490 (2021).

334. Henkelman, G., Uberuaga, B. P. & Jónsson, H. A climbing image nudged elastic band method for finding saddle points and minimum energy paths. *J. Chem. Phys.* **113**, 9901–9904 (2000).

335. Henkelman, G. & Jónsson, H. Improved tangent estimate in the nudged elastic band method for finding minimum energy paths and saddle points. *J. Chem. Phys.* **113**, 9978–9985 (2000).

336. Giannozzi, P. *et al.* QUANTUM ESPRESSO: a modular and open-source software project for quantum simulations of materials. *J. Phys. Condens. Matter* **21**, 395502 (2009).

337. Giannozzi, P. *et al.* Advanced capabilities for materials modelling with Quantum ESPRESSO. *J. Phys. Condens. Matter* **29**, 465901 (2017).

338. Perdew, J. P., Burke, K. & Ernzerhof, M. Generalized gradient approximation made simple. *Phys. Rev. Lett.* **77**, 3865–3868 (1996).

339. Dal Corso, A. Pseudopotentials periodic table: From H to Pu. *Comput. Mater. Sci.* **95**, 337–350 (2014).

340. Xu, X. *et al.* Lithium reaction mechanism and high rate capability of VS_4 –graphene nanocomposite as an anode material for lithium batteries. *J. Mater. Chem. A* **2**, 10847–10853 (2014).

341. Britto, S. *et al.* Multiple redox modes in the reversible lithiation of high-capacity, Peierls-distorted vanadium sulfide. *J. Am. Chem. Soc.* **137**, 8499–8508 (2015).

342. Lian, R. *et al.* Nucleation and conversion transformations of the transition metal polysulfide VS_4 in lithium-ion batteries. *ACS Appl. Mater. Interfaces* **11**, 22307–22313 (2019).

343. Geller, S. Refinement of the crystal structure of cryolithionite, $\{Na_3\}[Al_2](Li_3)F_{12}$. *Am. Mineral.* **56**, 18–23 (1971).

344. Xiao, R., Li, H. & Chen, L. Candidate structures for inorganic lithium solid-state electrolytes identified by high-throughput bond-valence calculations. *J. Materiomics* **1**, 325–332 (2015).

345. Liu, Z., Sun, Y., Singh, D. J. & Zhang, L. Switchable out-of-plane polarization in 2D $LiAlTe_2$. *Adv. Electron. Mater.* **5**, 1900089 (2019).

346. Ma, C.-G. & Brik, M. G. First principles studies of the structural, electronic and optical properties of $LiInSe_2$ and $LiInTe_2$ chalcopyrite crystals. *Solid State Commun.* **203**, 69–74 (2015).

347. Augustine, A. M., Sudarsanan, V., Patra, L., Kavitha, M. & Ravindran, P. Li-rich $Li_6MnxFe_{(1-x)}S_4$ as cathode material for Li-ion battery. *AIP Conf. Proc.* **2115**, 030623 (2019).

348. Isaenko, L. *et al.* $LiGaTe_2$: A new highly nonlinear chalcopyrite optical crystal for the mid-IR. *Cryst. Growth Des.* **5**, 1325–1329 (2005).

349. Bianchini, F., Fjellvåg, H. & Vajeeston, P. A first-principle investigation of the Li diffusion mechanism in the super-ionic conductor lithium orthothioborate Li_3BS_3 structure. *Mater. Lett.* **219**, 186–189 (2018).

350. Suzuki, N. *et al.* Theoretical and experimental studies of KLi_6TaO_6 as a Li-ion solid electrolyte. *Inorg. Chem.* **60**, 10371–10379 (2021).

351. Kawasaki, Y. *et al.* Synthesis and electrochemical properties of Li_3CuS_2 as a positive electrode material for all-solid-state batteries. *ACS Appl. Energy Mater.* **4**, 20–24 (2021).

352. Huang, F. Q., Yang, Y., Flaschenriem, C. & Ibers, J. A. Syntheses and structures of LiAuS and Li_3AuS_2. *Inorg. Chem.* **40**, 1397–1398 (2001).

353. Kahle, L., Marcolongo, A. & Marzari, N. High-throughput computational screening for solid-state Li-ion conductors. *Energy Environ. Sci.* **13**, 928–948 (2020).

354. Muy, S. *et al.* High-throughput screening of solid-state li-ion conductors using lattice-dynamics descriptors. *iScience* **16**, 270–282 (2019).

355. Li, X. *et al.* Progress and perspectives on halide lithium conductors for all-solid-state lithium batteries. *Energy Environ. Sci.* **13**, 1429–1461 (2020).

356. Sendek, A. D. *et al.* Machine learning-assisted discovery of many new solid Li-ion conducting materials. *ArXiv180802470 Cond-Mat Physicsphysics* (2018).

357. Kim, Y., Martin, S. W., Ok, K. M. & Halasyamani, P. S. Synthesis of the thioborate crystal $Zn_xBa_2B_2S_{5+x}$ (x ≈ 0.2) for second order nonlinear optical applications. *Chem. Mater.* **17**, 2046–2051 (2005).

358. Wang, Y. *et al.* Design principles for solid-state lithium superionic conductors. *Nat. Mater.* **14**, 1026–1031 (2015).

359. Li, P. & Liu, Z.-H. Hydrothermal synthesis, characterization, and thermodynamic properties of a new lithium borate, $Li_3B_5O_8(OH)_2$. *J. Chem. Eng. Data* **55**, 2682–2686 (2010).

360. Snydacker, D. H., Hegde, V. I. & Wolverton, C. Electrochemically stable coating materials for Li, Na, and Mg metal anodes in durable high energy batteries. *J. Electrochem. Soc.* **164**, A3582 (2017).

361. Sakuda, A. *et al.* Amorphous metal polysulfides: electrode materials with unique insertion/extraction reactions. *J. Am. Chem. Soc.* **139**, 8796–8799 (2017).

362. He, X. *et al.* Crystal structural framework of lithium super-ionic conductors. *Adv. Energy Mater.* **9**, 1902078 (2019).

363. D. Richards, W., Wang, Y., J. Miara, L., Chul Kim, J. & Ceder, G. Design of $Li_{1+2x}Zn_{1-x}PS_4$, a new lithium ion conductor. *Energy Environ. Sci.* **9**, 3272–3278 (2016).

364. Chen, E. M. & Poudeu, P. F. P. Thermal and electrochemical behavior of $Cu_{4-x}Li_xS_2$ (x=1, 2, 3) phases. *J. Solid State Chem.* **232**, 8–13 (2015).

365. Devlin, K. P. *et al.* Polymorphism and second harmonic generation in a novel diamond-like semiconductor: Li_2MnSnS_4. *J. Solid State Chem.* **231**, 256–266 (2015).

366. Steiner, H. J. & Lutz, H. D. Li_2BeCl_4 and Na_2BeCl_4: Two olivine-type chlorides. *J. Solid State Chem.* **100**, 179–181 (1992).

367. Rao, K. K., Yao, Y. & Grabow, L. C. Accelerated modeling of lithium diffusion in solid state electrolytes using artificial neural networks. *Adv. Theory Simul.* **3**, 2000097 (2020).

368. Körbel, S., L. Marques, M. A. & Botti, S. Stability and electronic properties of new inorganic perovskites from high-throughput ab initio calculations. *J. Mater. Chem. C* **4**, 3157–3167 (2016).

369. Prömper, S. W. & Frank, W. Lithium tetra-chlorido-aluminate, $LiAlCl_4$: a new polymorph (oP12, $Pmn2_1$) with Li^+ in tetra-hedral inter-stices. *Acta Crystallogr. Sect. E Crystallogr. Commun.* **73**, 1426–1429 (2017).

370. Abdel-Khalek, E. K., Mohamed, E. A., Salem, S. M., Ebrahim, F. M. & Kashif, I. Study of glass-nanocomposite and glass–ceramic containing ferroelectric phase. *Mater. Chem. Phys.* **133**, 69–77 (2012).

371. Rousse, G., Baptiste, B. & Lelong, G. Crystal structures of $Li_6B_4O_9$ and $Li_3B_{11}O_{18}$ and application of the dimensional reduction formalism to lithium borates. *Inorg. Chem.* **53**, 6034–6041 (2014).

372. Branford, W., Green, M. A. & Neumann, D. A. Structure and ferromagnetism in Mn^{4+} spinels: $AM_{0.5}Mn_{1.5}O_4$ (A = Li, Cu; M = Ni, Mg). *Chem. Mater.* **14**, 1649–1656 (2002).

373. Li, G., Chu, Y. & Zhou, Z. From $AgGaS_2$ to Li_2ZnSiS_4: realizing impressive high laser damage threshold together with large second-harmonic generation response. *Chem. Mater.* **30**, 602–606 (2018).